

---

Doctoral Dissertations

Student Theses and Dissertations

---

Fall 1985

## An analysis of mill sound levels to aid in the control and understanding of the grinding process

Scott Douglas Morrison

Follow this and additional works at: [https://scholarsmine.mst.edu/doctoral\\_dissertations](https://scholarsmine.mst.edu/doctoral_dissertations)



Part of the [Metallurgy Commons](#)

Department: **Materials Science and Engineering**

---

### Recommended Citation

Morrison, Scott Douglas, "An analysis of mill sound levels to aid in the control and understanding of the grinding process" (1985). *Doctoral Dissertations*. 535.

[https://scholarsmine.mst.edu/doctoral\\_dissertations/535](https://scholarsmine.mst.edu/doctoral_dissertations/535)

This thesis is brought to you by Scholars' Mine, a service of the Missouri S&T Library and Learning Resources. This work is protected by U. S. Copyright Law. Unauthorized use including reproduction for redistribution requires the permission of the copyright holder. For more information, please contact [scholarsmine@mst.edu](mailto:scholarsmine@mst.edu).

AN ANALYSIS OF MILL SOUND LEVELS  
TO AID IN THE CONTROL AND  
UNDERSTANDING OF THE GRINDING PROCESS

BY

SCOTT DOUGLAS MORRISON, 1956-

A DISSERTATION

Presented to the Faculty of the Graduate School of the

UNIVERSITY OF MISSOURI-ROLLA

In Partial Fulfillment of the Requirements for the Degree

DOCTOR OF PHILOSOPHY

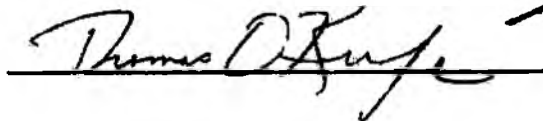

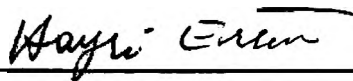
in

METALLURGICAL ENGINEERING

1985



Advisor



## ABSTRACT

An experimental study has been made to evaluate the relationships between grinding parameters and the directional sound levels emitted from the collision of the grinding media with the mill wall for a laboratory batch ball mill.

Discrete frequency and single frequency band sound pressure level measurements were performed to investigate the changes in sound levels with grind time. It was demonstrated that the reduction in sound levels with grind time observed for a narrow sized feed can be used to indicate optimum breakage rates, overall time-based particle size distribution, and ore character.

The relationships established with the discrete frequency and single frequency band monitoring have determined that mill sound levels could be used as an on-line production parameter for a batch mill and as a laboratory indicator of relative grindability.

Multiple frequency band sound power level measurements during the wet grinding of feed materials, having a distribution of particle sizes, has shown that mill sound levels can indicate the actual effective pulp viscosity in the mill and hence permit the identification of the dynamic rheological regime existing within the mill. The results show that the production of fine particles is not directly related to the sound levels. However, rheological

transitions from dilatant to pseudoplastic, to pseudoplastic with yield rheology, as identified by the sound levels, are reflected in the fine particle production. It also was shown that mill sound will reflect mill pulp rheology with and without the presence of a grinding additive and for the case where the additive is or is not effective.

## ACKNOWLEDGEMENTS

The author would like to express his deepest appreciation for the excellent guidance, instruction, and fellowship given by Dr. J. L. Watson of the Department of Metallurgical Engineering, without which this thesis would not have been possible.

The author would like to acknowledge the assistance and instruction given by Dr. A. E. Morris and Dr. T. J. O'Keefe of the Department of Metallurgical Engineering and Dr. H. Erten of the Department of Mining Engineering throughout the course of study and research.

A special debt of gratitude is owed to Dr. A. Cummings of the Department of Mechanical Engineering for his assistance with the fundamental aspects of sound and their relation to this study, and to the Department of Mechanical Engineering for the use of sound measuring equipment.

The author would like to acknowledge and thank the Department of Metallurgical Engineering and the Arco Foundation for their generous financial and administrative support.

The support given by the U.S.B.M. Rolla Research Center for particle size analysis is greatly appreciated.

Finally the author would like to thank his wife Brigitte for her constant support during his program at the University of Missouri-Rolla.

## TABLE OF CONTENTS

|  | Page |
|--|------|
| ABSTRACT.....                              | ii   |
| ACKNOWLEDGEMENTS.....                      | iv   |
| LIST OF ILLUSTRATIONS.....                 | viii |
| LIST OF TABLES.....                        | xii  |
| LIST OF SYMBOLS.....                       | xiii |
| I. INTRODUCTION.....                       | 1    |
| A. GRINDING.....                           | 1    |
| B. PROJECT STATEMENT.....                  | 11   |
| II. LITERATURE REVIEW.....                 | 13   |
| A. GENERAL GRINDING STUDIES AND REVIEW     |      |
| ARTICLES.....                              | 13   |
| A1. Introduction.....                      | 13   |
| A2. Laboratory Batch Grinding Studies....  | 15   |
| B. ACOUSTICS.....                          | 22   |
| B1. Fundamental Considerations.....        | 22   |
| B2. Laboratory Studies of Grinding         |      |
| Mill Noise.....                            | 28   |
| C. USE OF SOUND MEASUREMENTS IN INDUSTRIAL |      |
| GRINDING OPERATIONS.....                   | 38   |
| III. EXPERIMENTAL PROCEDURES.....          | 47   |
| A. SAMPLE PREPARATION.....                 | 47   |
| B. GRINDING CONDITIONS.....                | 50   |
| C. DATA ACQUISITION AND SOUND MEASURING    |      |
| SYSTEMS.....                               | 51   |

## TABLE OF CONTENTS (CONTINUED)

|  | Page |
|--|------|
| D. SAMPLE ANALYSIS.....                        | 60   |
| E. SOUND DATA ANALYSIS.....                    | 61   |
| IV. RESULTS AND DISCUSSION.....                | 65   |
| A. NARROW FREQUENCY BAND ANALYSIS RESULTS..... | 65   |
| A1. Angular Directivity Testing Results..      | 66   |
| A2. Discrete Frequency Analysis Results..      | 70   |
| B. SINGLE FREQUENCY BAND ANALYSIS RESULTS..... | 72   |
| B1. Breakage Rate and Noise Energy             |      |
| Optimization Results.....                      | 73   |
| B2. Particle Size and Noise Energy             |      |
| Variation Results.....                         | 82   |
| B2a. Single Frequency Band                     |      |
| Testing.....                                   | 82   |
| B2b. Particle Damping Tests.....               | 84   |
| B2c. Discrete Frequency                        |      |
| Analysis.....                                  | 89   |
| B3. Ore Character and Noise Energy             |      |
| Variation Results.....                         | 93   |
| C. MULTIPLE FREQUENCY BAND ANALYSIS RESULTS... | 107  |
| C1. Pulp Viscosity and Grinding                |      |
| Additive Results.....                          | 109  |
| C1a. Magnetite Ore.....                        | 109  |
| C1b. Molybdenite Ore.....                      | 121  |

## TABLE OF CONTENTS (CONTINUED)

|   | Page |
|---|------|
| C2. Ore Character and Noise Energy        |      |
| Variation Results.....                    | 128  |
| V. CONCLUSIONS.....                       | 139  |
| VI. RECOMMENDATIONS FOR FURTHER WORK..... | 142  |
| A. LABORATORY GRINDING.....               | 142  |
| B. INDUSTRIAL TESTING.....                | 143  |
| BIBLIOGRAPHY.....                         | 144  |
| VITA.....                                 | 149  |
| APPENDICES.....                           | 150  |
| A. DATA AQUISITION PROGRAMS.....          | 150  |
| A1. Single Frequency Band Analysis.....   | 150  |
| A2. Multiple Frequency Band Analysis..... | 155  |
| B. SOUND DATA ANALYSIS PROGRAMS.....      | 159  |
| B1. Absorbed Noise Energy.....            | 159  |
| B2. Cumulative Frequency Analysis.....    | 161  |
| C. SCREEN SIZE ANALYSIS PROGRAM.....      | 165  |
| D. MILL CHARGE DETERMINATION PROGRAM..... | 168  |



## LIST OF ILLUSTRATIONS

| Figure   | Page |
|--|------|
| 1. Flowsheet of Typical Grinding Circuit from the Missouri Lead Belt <sup>4</sup> .....  | 5    |
| 2. Motion of a Charge in a Ball Mill <sup>3</sup> .....  | 6    |
| 3. Illustration of an Early Mechanical Size Reduction Device <sup>14</sup> .....   | 14   |
| 4. Radiated Noise Spectra with 50kg Ball load, 50mm Ball Size, and Operating at 60 RPM <sup>54</sup>   |      |
| a. Without added Damping   |      |
| b. With Damping Layer loosely wrapped  |      |
| c. With Damping Layer bonded   |      |
| d. Background Noise.....   | 29   |
| 5. Average Power Spectrum <sup>2</sup>   |      |
| a. Quartz  |      |
| b. Chrysocolla.....  | 31   |
| 6. Example of Sound Power Level with Grind Time  |      |
| a. Sound Power Level with Grind Time, and Baseline used for Absorbed Noise Energy Calculation.   |      |
| b. Cross-Hatched Area used for Absorbed Noise Energy.....  | 33   |
| 7. Mill Sound Variation with Grind Time and Mill Speed for a 2 kg Feed <sup>12</sup> .....   | 35   |
| 8. Absorbed Noise Energy Variation with Fineness of Grind for Dolomite <sup>12</sup> .....   | 36   |
| 9. Percent Absorbed Noise Energy plotted as a function of Fineness of Grind for various Dolomite Feed Charge Weights and Mill Speed <sup>12</sup> .....                                      | 37   |
| 10. Percent Absorbed Noise energy plotted as a function of Fineness of Grind for a 0.5 kg Dolomite Feed Charge found with various sized 2 kg Ball Charges and Mill Speed <sup>12</sup> ..... | 40   |
| 11. Sound Pressure Level Variations with Grind Time for the Wet Grinding of Four Feed Materials at 75 RPM <sup>12</sup> .....  | 41   |
| 12. Percent Absorbed Noise Energy plotted as a function of Fineness of Grind for 1 kg of each of Four Different Charge Materials ground at 65 and 75 RPM <sup>12</sup> .....                 | 43   |

## LIST OF ILLUSTRATIONS (CONTINUED)

| Figure  | Page |
|---|------|
| 13. Flowsheet of Feed Sample Preparation Techniques for the Production of -1.6 mm and -3.3+1.6 mm Feed Sizes.....                                       | 49   |
| 14. Schematic Diagram of Sound Measuring, Data Acquisition, and Computer Systems used for Multiple and Single Frequency Band Monitoring.....            | 53   |
| 15. Schematic Diagram of the Microphone Placement Positions for Angular Directivity Testing.....  | 55   |
| 16. Schematic Diagram of Microphone and Accelerometer Placement for Particle Dampening Tests.....   | 57   |
| 17. Example of Sound Level Variation with Grind Time with Reference Baselines to Calculate ANE and DANE.....  | 63   |
| 18. Angular Directivity Test Results at 7800 Hz.....  | 67   |
| 19. Angular Directivity Test Results at 4500 Hz.....  | 68   |
| 20. Angular Directivity Test Results at 3600 Hz.....  | 69   |
| 21. Sound Frequency Spectrum of Ball Mill Operating under Standard Conditions with No Charge.....   | 71   |
| 22. First Order Breakage Kinetics Plot.....   | 74   |
| 23. Absorbed Noise Energy and Breakage Rate Variation with Mill Speed for Dolomite.....   | 76   |
| 24. Absorbed Noise Energy Relationships with Breakage Rate for Dolomite (conditions as in Figure 23)....  | 77   |
| 25. Absorbed Noise Energy and Breakage Rate Variations with Ball Load for Dolomite.....   | 78   |
| 26. Absorbed Noise Energy Relationships with Breakage Rate for Dolomite (conditions as in Figure 25)....  | 80   |
| 27. Absorbed Noise Energy and Breakage Variation with Feed Size for Dolomite.....   | 81   |
| 28. Sound Level and Size Variations with Grind Time for Dolomite.....   | 83   |
| 29. Sound Pressure and Acceleration Frequency Spectra for the Collision of a 2.5 cm Ball on the Mill filled with 125 Balls with No Ore Layer Present... | 86   |

## LIST OF ILLUSTRATIONS (CONTINUED)

| Figure  | Page |
|---|------|
| 30. Sound Pressure and Acceleration Frequency Spectra for the Collision of a 2.5 cm Ball on the Mill filled with 125 Balls with a Layer of -417+295 Micron Particles Present..... | 87   |
| 31. Acceleration Variation Relationships with Particle Size for 1.5 kHz.....  | 90   |
| 32. Acceleration Variation Relationships with Particle Size for 2.3 kHz.....  | 91   |
| 33. Acceleration Variation Relationships with Particle Size for 3.25 kHz.....   | 92   |
| 34. Sound Pressure Variation with Grind Time for various Discrete Frequencies.....  | 95   |
| 35. Sound Pressure Variation with Grind Time for various Discrete Frequencies.....  | 96   |
| 36. Sound Power Variation with Grind Time for Dry Grinding.....   | 98   |
| 37. Rosin-Rammler Size Distribution Plots for Dry Grinding.....   | 99   |
| 38. Sound Power Variation with Grind Time for Wet Grinding.....   | 104  |
| 39. Product Size Distributions for Wet Grinding.....  | 105  |
| 40. Sound Power Variation with Grind Time for a Magnetite Ore.....  | 112  |
| 41. Sound Power Variation as a function of Grind Time and Percent Solids for Magnetite Ore...   | 114  |
| 42. Absorbed Noise Energy Relationships with Pulp Density for a Magnetite with and without a Grinding Additive (NA = No Additive A = Additive).                                   | 115  |
| 43. Sound Power Variations with Grind Time for a Magnetite Ore with and without a Grinding Additive.....  | 118  |
| 44. Sound Power Variations with Grind Time for a Magnetite Ore with and without a Grinding Additive at High Pulp Densities.....   | 119  |

## LIST OF ILLUSTRATIONS (CONTINUED)

| Figure  | Page |
|---|------|
| 45. Sound Power Variations with Grind Time for a Molybdenite Ore.....   | 122  |
| 46. Sound Power Variation as a function of Grind Time and Percent Solids for a Molybdenite Ore.....                             | 123  |
| 47. Absorbed Noise Energy Relationships with Pulp Density for a Molybdenite Ore with and without a Grinding Additive.....       | 124  |
| 48. Sound Power Variation with Grind Time for a Molybdenite Ore with and without a Grinding Additive at Low Pulp Densities..... | 127  |
| 49. Sound Power Variation with Grind Time for Magnetite, Traprock, and Artificial Mixtures.....                                 | 131  |
| 50. Absorbed Noise Energy Variations for Time Increments with Magnetite/Traprock Mixtures.....                                  | 136  |
| 51. Logarithmic Relationships between DANE, K, and Grindability with the Magnetite/Traprock Mixtures.                           | 138  |

## LIST OF TABLES

| Table   | Page |
|---|------|
| I. Distribution of Energy in a Ball Mill <sup>2</sup> .....   | 2    |
| II. Comparison of 1-Octave and 1/3-Octave Bands <sup>48</sup> ....  | 24   |
| III. Effect of Ball Size on Mill Sound Levels <sup>12</sup> .....   | 39   |
| IV. Variation of Wet Mill Grinding Sound Energies<br>with Feed Type <sup>12</sup> .....   | 42   |
| V. Ball Charge Quantities for a Molybdenite Ore.....  | 52   |
| VI. Discrete Frequency Acceleration Values for the<br>Collision of a 2.5 cm Ball through a Layer of<br>various Sized Particles..... | 88   |
| VII. Discrete Frequency Sound Pressure Values<br>with Grind Time.....   | 94   |
| VIII. Comparison of Sound and Size Parameters for Dry<br>Grinding.....  | 101  |
| IX. Comparison of Sound and Size Parameters for Wet<br>Grinding.....  | 106  |
| X. Example of Reproducibility of Sound And Size Data<br>for Magnetite Ore.....  | 108  |
| XI. Size Distribution of Magnetite and Molybdenite<br>Feed Ores.....  | 110  |
| XII. Fine Particle Production for Magnetite Ore with<br>Pulp Density<br>a. Without Additive<br>b. With Additive.....                | 117  |
| XIII. Fine Particle Production with Pulp Density for<br>Molybdenite ore<br>a. Without Additive<br>b. With Additive.....             | 125  |
| XIV. Grinding Conditions and Physical Properties of<br>Magnetite and Traprock Feed Materials and Mixture<br>Ratios.....             | 129  |
| XV. Fine Particle Production with Grind Time for<br>Magnetite, Traprock, and Mixture Ratios.....                                    | 133  |
| XVI. Absorbed Noise Energy Values for Time Increments<br>with Magnetite, Traprock, and Mixture Ratios.....                          | 135  |

## LIST OF SYMBOLS

|                |  |
|----------------|--|
| A              | - Vibration Acceleration (m / (sec x sec) )            |
| A <sub>o</sub> | - Reference Vibration Acceleration (m / (sec x sec) )  |
| AL             | - Acceleration Level (dB)                              |
| ANE            | - Absorbed Noise Energy (mw-min)                       |
| b              | - Discrete Breakage Function                           |
| B              | - Breakage Matrix                                      |
| CA             | - Cumulative Average Sound Power                       |
| cc             | - Cubic Centimeter                                     |
| cm             | - Centimeter   |
| D              | - Mill Diameter (m)                                    |
| DANE           | - Delta Absorbed Noise Energy                          |
| d              | - Ball Diameter (m)                                    |
| dB             | - Decibel  |
| F              | - Feed Size Distribution Matrix                        |
| G              | - Grind Parameter                                      |
| g              | - gram   |
| Hz             | - Hertz (cycles / sec)                                 |
| I              | - Sound Intensity (watts / (m x m) )                   |
| IL             | - Sound Intensity Level (dB)                           |
| I <sub>m</sub> | - Identity Matrix                                      |
| I <sub>o</sub> | - Reference Sound Intensity (watts / (m x m) )         |
| K              | - Specific Breakage Rate Constant (min <sup>-1</sup> ) |
| kg             | - Kilogram   |
| kHz            | - Kilohertz (thousands of cycles / sec)                |

## LIST OF SYMBOLS (CONTINUED)

|     |   |
|-----|---|
| kwh | - Kilowatt Hour                               |
| M   | - Rosin Rammler Mean                          |
| Ma  | - Ore Charge Wt.                              |
| m   | - Meter                                       |
| min | - Minute                                      |
| mm  | - Millimeter                                  |
| mw  | - Milliwatt                                   |
| N   | - Rosin-Rammler Slope                         |
| Nc  | - Critical Speed (RPM)                        |
| n   | - Number of Breakage Events                   |
| P   | - Sound Pressure (Pascals)                    |
| Po  | - Reference Sound Pressure (Pascals)          |
| Ps  | - Product Size Distribution Matrix            |
| PWL | - Sound Power Level (dB)                      |
| Q   | - Directivity Factor                          |
| R   | - Acoustical Room Constant                    |
| RPM | - Revolutions per Minute                      |
| r   | - Distance from Source to SPL Measurement (m) |
| S   | - Selection Matrix                            |
| SPL | - Sound Pressure Level (dB)                   |
| t   | - time  |
| V   | - Vibration Velocity (m / sec)                |
| Vo  | - Reference Vibration Velocity (m / sec)      |
| VL  | - Vibration Velocity Level (dB)               |
| W   | - Mass Fraction                               |

## LIST OF SYMBOLS (CONTINUED)

- Wp - Sound Power (watt)  
Wpo - Reference Sound Power (watt)  
Wr - Weight Percent Retained  
Wt - Weight  
X - Screen Size  
Xi - General Greakage Matrix



## I. INTRODUCTION

### A. GRINDING

Before most mined ore can be considered a useful product or amenable to further treatment it must be subjected to a size reduction process. The present practice generally consists of the unit operations of crushing and grinding in series with an integrated classification system to produce the required particle size distribution. The combination of crushing and grinding is termed comminution.

The importance of comminution is illustrated when examining the tonnages involved, the capital and operating costs, energy consumption, and efficiency. In the mineral field alone the average annual tonnage<sup>1</sup> of ores which were processed by crushing and grinding in the 1970's was approximately  $2500 \times 10^6$ . When considering that the capital and operating costs of crushing and grinding can amount to 50% or more of the total<sup>2</sup>, which equates to several dollars per tonne, this is a major expense in the production of mineral commodities. From an energy and efficiency standpoint the energy consumption at U.S. ore beneficiation plants exceeds 100 billion kwh per year of which approximately 50% is used for grinding alone. The distribution of energy for grinding<sup>2</sup> is presented in Table I. As can be seen only an extremely small portion of the total energy input to a mill is used for the production

Table I. Distribution of Energy in a Ball Mill<sup>2</sup>

| <u>Energy Distribution</u>            | <u>Energy Consumption %</u> |
|---------------------------------------|-----------------------------|
| Bolt Friction                         | 4.3                         |
| Gear Losses                           | 8.0                         |
| Heat Absorbed by Air Circulation      | 33.1                        |
| Heat Losses Through Mill Shell        | 6.4                         |
| Heat Absorbed by Product              | 47.1                        |
| Theoretical Energy for Size Reduction | <u>0.6</u>                  |
| Total                                 | 100.0                       |

of new surfaces. With the above economic and efficiency considerations the grinding process is an extremely expensive and energy intensive process.

Crushing is the first mechanical stage in the process of comminution and is generally performed in stages. The feed top size to this series of operations can be as large as 1.5 m and the product from 0.5-2 cm. The run-of-mine ore is reduced in the primary crushing stage to 10-20 cm or a size suitable for transport and/or feeding to the secondary crushers. The primary crushers are operated in open circuit with or without heavy duty grizzly or scalping screens. Secondary crushing is used to reduce the particle size of the ore to a suitable size for grinding. It is also operated in open circuit with or without a screening operation. Cone crushers are the major apparatus used in secondary crushing. Tertiary crushing can be implemented if there is a need for further particle size reduction prior to the grinding process. The breakage of ore particles in the crushing process is predominately achieved by compressive forces<sup>3</sup> generated by the action of the jaw, gyratory, or cone crushing machines.

Grinding is the last stage in the process of comminution with a product particle size of typically less than 1 mm. It is performed in rotating cylindrical vessels containing an appropriate volumetric loading of a grinding medium such as steel balls or rods, hard rocks, or the ore itself. Depending on the end use of the ground material

this process can be performed dry or in a water suspension. A typical industrial practice for the grinding of lead and zinc ore from the Missouri Lead Belt involves rod and ball mills with a cyclone classification system<sup>4</sup>. An example of this type of system can be seen in Figure 1 where the feed from the crushing circuit is fed to a rod mill. The product from the rod mill is fed to a bank of cyclone classifiers, the oversize is fed to the ball mill and the undersize to the flotation process. The product from the ball mill is returned to the cyclones.

The breakage of ore particles in the grinding process is achieved by a combination of compressive and shearing forces generated by the intimate contact of the grinding medium and the feed material in the rotating vessel. The forces generated and the resultant product character are dictated to a large extent by the mode of operation of the mill. The speed of the mill is the determining factor in establishing the modes of operation. Grinding mills are operated at a percentage of the critical speed ( $N_c$ ), which is the speed at which centrifuging occurs. This is defined mathematically by the equation:

$$N_c = 42.3 / (D-d)^{0.5} \quad (1)$$

where  $D$  is the diameter of the mill in meters and  $d$  is the diameter of the ball in meters, and  $N_c$  is expressed in RPM. Equation (1) is derived from a force balance of the motion of the charge in the rotating vessel. Figure 2 shows the motion of a charge in a grinding mill. The rotation and

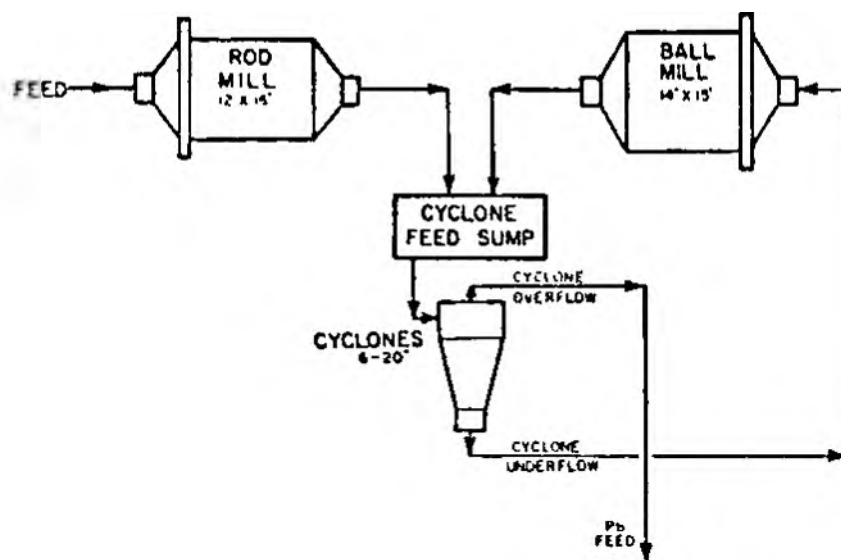


Figure 1. Flowsheet of Typical Grinding Circuit from the Missouri Lead Belt<sup>4</sup>

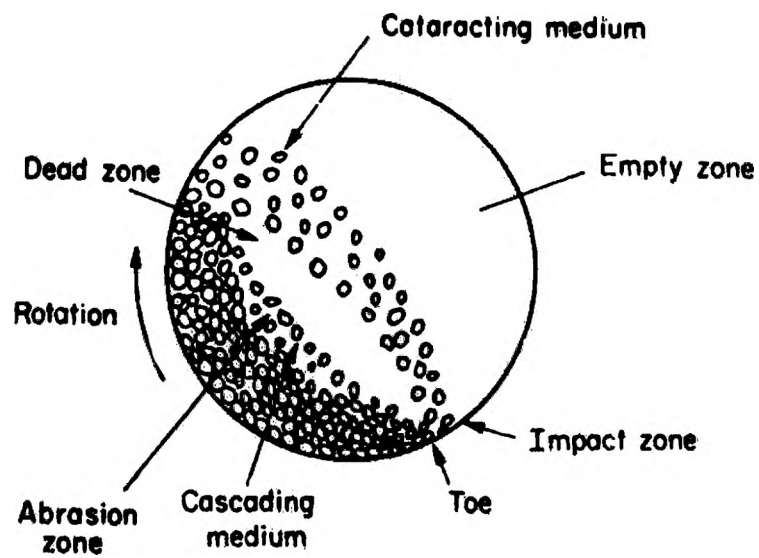


Figure 2. Motion of a Charge in a Ball Mill<sup>3</sup>

friction of the mill shell lift the grinding medium along the rising side of the mill until a position of dynamic equilibrium is reached. It then cascades and cataracts down the free surface of the medium, around a dead zone where little movement occurs, to the toe of the charge<sup>3</sup>. When the mill is operated at 70-85%  $N_c$  this level of speed produces a cataracting mode of operation which leads to coarser grinding. At these speeds the medium are projected clear of the charge in a parabolic path before landing on the toe of the charge. The resultant forces are predominately compressive. At 50-70%  $N_c$  the medium tend to roll down to the toe of the charge and this leads to finer grinding and increased slimes production. This mode of operation essentially produces abrasive or shearing forces. In industrial practice<sup>5</sup> the mill is operated at a range of about 65-82%  $N_c$ .

The charge volume of a grinding mill is the percentage of the mill interior filled with grinding medium and includes the void spaces between the medium. Both the volume of the charge and size of the individual medium control several important factors in the grinding process. The charge volume affects the power drawn by the mill and is a maximum at approximately 50% charge volume. In operating terms unless grate discharge methods are used, less than 50% charge volume must be used so that the medium are not rejected to the discharge. For overflow discharge ball mills this must actually be less than 45%. The

practical operating range is from 30-50% for industrial mills<sup>5</sup>. The charge volume also affects the void spaces between the balls which can be filled with the material to be ground and therefore can affect throughput. The void spacing should be filled to maximize both the grinding medium effects and throughput. The selection of grinding medium size is also a crucial factor in determining throughput and operation of the mill. As the relative size of the medium decreases, the surface area for grinding increases, giving a higher capacity. On the other hand, as the medium size increases, the forces generated between the grinding surfaces increases so that larger particles can be broken.

The grinding stage is a particularly crucial stage in mineral concentration because it must be operated continuously, as opposed to the crushing operations that can be stopped periodically when there is sufficient inventory. In addition there is limited surge capacity in the grinding circuit. There are many variables in the grinding process that have to be extremely well controlled in order to enable the downstream processes of mineral recovery to be operated efficiently. These include pulp density, percentages of fine or coarse particles, and flow rates. Considering the above process variables, and others such as natural variability in ore hardness, the grinding process is very complex and hence difficult to quantify and control.



There are several means by which grinding has been quantified. The most commonly used technique in the laboratory and industrially is particle size distribution. On an industrial scale the examination of the production of a certain size of material from the final classification system is often used as a sales parameter, and also as an input variable for automatic control systems.

Another technique to evaluate the grinding process is the grindability of an ore. This is achieved by a standardized laboratory technique for determining the production of a certain size of material under controlled grinding conditions. The values obtained from this test can aid in the design of grinding processes. Additionally the rate at which particles are broken from the top size to the sizes below can be used as a measure of the relative hardness of ores. Evaluation of the rate of breakage from all sizes within a feed distribution is used as the basis for the kinetic modelling and simulation of the grinding process. As can be expected these rates will depend on the type of ore being ground and the type of equipment used.

The control of the grinding process involves sophisticated schemes that basically incorporate three components; instrumentation, control hardware, and control strategies. These components allow measurement and control of direct process variables in efforts to increase the efficiency of the process and have made significant increases in plant throughput and operating cost

savings<sup>6</sup>. Although the present control strategies have been successful in improving the control of the grinding process, there are limitations due to lack of sufficient information about controller-variable responses to manipulated changes, interaction between variables, and the effect of harsh operating environments on instrumentation. The problems with control are magnified when taking into consideration the difficulties with mathematical descriptions of the grinding process and problems with signal processing from sensors. Additionally, equipment associated problems can cause deviation from the expected dynamic response of the system. Such effects can be caused by wear of the grinding ball and mill liner, cyclone coatings, pumps, valves, and impellers. Another important factor for grinding operations are ore changes, which can contribute several unmeasured variables in the process. Several properties which are either difficult or impossible to measure on stream are ore hardness, slurry viscosity, and ore density<sup>6</sup>.

As mentioned earlier less than 1% of the energy input to a mill is actually used in particle size reduction. Most of the remainder is consumed in gear transmission losses and frictional heat generation. A very small percentage is emitted as sound waves from the collision of the grinding medium against the mill shell and itself. These sound emissions have been used to a limited extent as an indirect measure of grinding mill operational conditions. Their use

in control strategies has been primarily to indicate mill loading conditions and as a feedback mechanism to control feed rates<sup>7-11</sup>.

## B. PROJECT STATEMENT

The obvious remedy to overcome some of the inefficiencies of the grinding process would be to increase the effectiveness of control by the use of an indirect, remote, non-invasive technique to measure the critical optimizing variables of the process. This would alleviate the problems of direct measured variable interactions, and, if the difficult to measure variables could be detected, the increased efficiency and hence cost savings could be substantial.

One possible indirect technique which has been used with some degree of success in industry<sup>7-11</sup> and studied in the laboratory<sup>1,12-13</sup> is the measurement of noise levels. In order to examine the extent to which the measurement of noise levels, as an indirect process variable, could benefit in the control and understanding of the grinding process, a three-part laboratory scale study was undertaken. One part examined narrow frequency band sound levels to determine the resonant frequencies of the mill shell from ball/liner collisions, and the directivity of the emitted sound levels. A second part examined sound levels in a single frequency band during the grinding

process to quantify the degree to which the process variables of mill ball loading, mill speed, particle size distributions, and ore character could be related to sound energy levels. The final part examined sound levels in multiple frequency bands during the grinding process to examine the degree to which the process variables of pulp density and viscosity, grinding additives, production of certain sized particles, and ore character could be correlated with sound energy levels.

## II. LITERATURE REVIEW

### A. GENERAL GRINDING STUDIES AND REVIEW ARTICLES

#### A1. Introduction

One of the earliest known mentions of a mechanical size reduction process with specific reference to minerals is found in "De Re Metallica", written by G. Agricola in about 1556. A thorough description of what today would be termed a stamp mill can be found and is reproduced here in Figure 3. As can be seen, the major force generated in the process is compressive, produced from the dropping of the heads of the stamps. To date there has been a drastic change in the equipment used to perform the size reduction process but little change has been made in the actual breakage mechanism<sup>14</sup>. A detailed review of the development of the process of size reduction from the time of Agricola would be beyond the scope of this review, so the remainder of this section will concentrate on current technological advancements relative to the subject matter of this study.

Size reduction, or the process of comminution is an important step in the recovery of most minerals in that it may be used to<sup>5</sup>:

1. Produce particles of the required shape and size;
2. Liberate valuable minerals from gangue so they can



A—MORTAR. B—UPRIGHT POSTS. C—CROSS-BEAMS. D—STAMPS. E—THEIR HEADS  
 F—AXLE (CAM-SHAFT). G—TOOTH OF THE STAMP (TAPPET). H—TEETH OF AXLE (CAMs).

Figure 3. Illustration of an Early Mechanical Size Reduction Device<sup>14</sup>

be concentrated;

3. Increase the surface area available for chemical reaction.

## A2. Laboratory Batch Grinding Studies

As mentioned earlier the grinding process is expensive. This has stimulated research efforts on grinding to establish energy size-reduction relationships in an effort to reduce the expense. There are numerous early publications<sup>16-19</sup> on which are based the principles of energy-size reduction relationships. These studies were concerned with the relationship between energy consumed by a grinding mill and the amount of size reduction that was achieved. Size reduction was studied as a function of:

1. The amount of new surface area of particles produced;
2. The volume of material broken;
3. The diameter of the product particles.

On an experimental basis it was observed that the decrease in size was proportional to the energy expended per unit weight of particles, and that the energy required to bring about the same relative size change was inversely proportional to some function of the particle size<sup>15</sup>.

These relationships have been interpreted somewhat differently by Bond<sup>17</sup>, Kick<sup>20</sup>, and Rittinger<sup>21</sup>

but have been used successfully in mathematical descriptions of the grinding process and the design of grinding equipment.

Because the ratio of energy loss to energy used in the production of new surfaces is an extremely large value, there are limitations in trying to qualitatively describe the grinding process from an energy input standpoint. The relationships between the feed to, and the product from the grinding process are the parameters that are being studied by various researchers in order to quantify the process, and constitute the major current research efforts in grinding. The process variables that exist within the mill such as charge volume and particle size distribution, pulp density and viscosity, mill speed, and mill ball size and distribution are the factors that are under investigation<sup>15</sup> to establish quantitatively the relation between mill feed and product. Some of the current research efforts<sup>27</sup> in grinding involve manipulating the above process variables in an effort to ascertain what effects are generated, and what additional components can be incorporated into theoretically developed mathematical models, and subsequent implementation in control strategies.

Two models have been developed for the grinding process, namely the kinetic and matrix models. In batch grinding all the material remains in the mill for the required time. Plug flow through a continuous mill is in



fact equivalent to batch grinding, with the average residence time equal to the grind time<sup>5</sup>. A kinetic model can be used for both batch and continuous operation to describe the grinding process. The model assumes that a part of the material in any size fraction is disappearing because of breakage, while other material is entering the size fraction as a result of breakage of particles in larger size fractions<sup>22</sup>. Thus for the top size fraction:

$$dW_1/dt_1 = -K_1W_1 \quad (2)$$

for the second size fraction;

$$dW_2/dt = -K_2W_2 + b_1K_1W_1 \quad (3)$$

for the third size fraction;

$$dW_3/dt = -K_3W_3 + bK_2W_2 + b_2K_1W_1 \quad (4)$$

and in general;

$$dW_i/dt = -K_iW_i + \sum_{j=1}^{j=i-1} b(i-j)K_jW_j \quad (5)$$

where  $W$  is the mass fraction in size  $i$  at time  $t$ ,  $K$  is the specific breakage rate constant for size  $i$ , and  $b$  is the discrete breakage function for particles being broken from size  $i$  to size  $j$ . The data necessary to utilize this model are generally derived from batch grinding experiments. A certain sized sample is ground for a series of small time intervals and the material remaining in the original size is measured and the values of  $K$  and  $W$  can be determined. The breakage function can be calculated mathematically if

the material breaks according to the Rosin-Rammler distribution, or measured quantitatively by the use of radioactive tracers<sup>23</sup>.

The matrix model<sup>15,24-25</sup> employs matrix algebra to describe a succession of breakage events, the feed to each event being the product from the preceding event and thus the time component comes from stages of grinding. From a mass balance of a breakage process it can be shown that:

$$P_s = X_i^n F \quad (6)$$

where  $P_s$  and  $F$  are  $N \times 1$  matrices of feed and product size distributions with  $N$  being the number of size intervals, and  $n$  the number of breakage events. The  $X_i$  matrix is composed of two components, namely the material left unbroken in a size, plus the material appearing from breakage of coarser sizes. The proportion of  $X_i$  which refers to those particles in the feed which are actually broken is represented by the symbol  $S$ . If the remaining portion can be represented by the term  $(I_m - S)$ , then the proportion of particles which are broken is  $B \times S \times F$  where  $B$  is the breakage matrix and  $I_m$  is the identity matrix. The remainder of the particles which will pass through unbroken is equal to  $(I_m - S) \times F$ . The overall equation becomes<sup>15</sup>:

$$P_s = B S F + (I_m - S) F \text{ or } P_s = (B S + I_m - S) F \quad (7)$$

Both of the models described above have been shown to be capable of simulating breakage in a wide variety of size reduction operations<sup>26-29</sup> These models are of limited application to the design of new size reduction

circuits<sup>30-32</sup>. Thus further studies are underway to quantify the effects of poorly known process variables<sup>32-34</sup>. There is an extensive amount of literature describing how these models are being used to simulate industrial circuits and assess their performance<sup>34-36</sup>. Current research is aimed at evaluating these models in terms of their susceptibility to various control mechanisms<sup>37</sup> and to highlight the areas where further modifications are necessary.

The research into the effects of the process variables of ball load and distribution, mill speed, and the nature of mill contents on the parameters of the above mentioned models is extensive<sup>33-40</sup>, and the highlights of this work deserve summarization. One of the most intensively studied model parameters is the grinding rate constant (K), of the kinetic grinding model. This review will limit itself to a summary of the efforts made to quantify the effects of process variables on this parameter. Herbst and Fuerstenau<sup>38</sup> have shown the relationships between mill speed, ball loading, and the breakage rate constant. Using mill conditions of constant ball void filling they found that K peaked at approximately 75% of critical speed with a ball loading of 23%, and at 60% critical speed with 18% ball loading. Austin<sup>39</sup> analyzed the relationship between ball size distribution, mill diameter and breakage rate constant. This study found that the maximum value of K can be related by:

$$K(\max) = D^n d^2 \quad (8)$$

where  $D$  is the mill diameter in meters,  $d$  the ball diameter in meters, and  $n$  has a value of 0.1-0.2. In addition it was found that the specific rate of breakage of a given particle size increases with decreasing ball size, because in a given mill there are more fracture events due to the greater number of balls. This holds true only if the balls have sufficient energy to maintain fracture. If this is not the case then the breakage rate decreases. For a mixture of ball sizes, the breakage rate is the weighted average of the individual sizes. In their study of the amount of ore charge in the mill, Kelsall et. al.<sup>40</sup> found that the breakage rate constant remains constant as the void space between the media fills. Thus the absolute rate of breakage is given by the product of  $K$  and the hold-up in the mill. When the void space overfills, the breakage rate decreases in proportion to the amount of ore charge ( $Ma$ ) present, so that the product  $K \times Ma$  remains approximately constant.

The nature of the mill contents has a profound effect on breakage rates. There are several publications<sup>41-43</sup> detailing the effects of particle size distribution of the feed on breakage rates. The general conclusion is that a coarser average diameter feed leads to higher breakage rates until a maximum is attained after which a decrease is observed.

It is well documented that under standard operation conditions, the pulp density has a major effect upon

grinding efficiency, so there has been considerable research<sup>44-46</sup> into pulp density and viscosity relationships with mill performance. It is generally accepted that an optimum pulp density exists at which size reduction is optimized. Below this pulp density the probability of a particle being broken will fall due to decreasing numbers of particles. At higher pulp densities the pulp viscosity will increase and particle agglomeration and impact cushioning will occur.

Klimpel et. al.<sup>47</sup> have performed the bulk of the research into the effects of grinding additives on mill performance. This work has lead to the characterization of mineral-water slurries in rheological terms. The pulp rheology research concludes that some ores demonstrate viscosity regimes ranging from dilatant to pseudoplastic with yield. In this case, the optimum viscous regime to perform grinding is in the pseudoplastic range of pulp densities. In this viscous regime, if chemical additives are introduced, the slurry rheological characteristics will be altered. An increase in net production of a certain size and increased throughput may then occur under these conditions, due to the effect of the additive on the pulp viscosity in the pseudoplastic regime.

The laboratory evaluation of the crucial parameters of the grinding process discussed above have been aimed at providing a more thorough understanding of this complex process. Many of them have been implemented in control

strategies as direct measured variables and have aided in increasing the efficiency of the process.

The preceding discussion has detailed some of the fundamental and applied aspects of grinding. This process is extremely energy and capital intensive, and difficult to quantify and control. The most recent advances in grinding technology have been made in the area of process control and simulation using sophisticated measuring and computer systems. A novel approach that has been implemented in several industrial grinding operations, has been the use of sound levels as a control parameter. The following section will detail some of the fundamentals of acoustics and review what advances have been made in the laboratory and industrially with this concept.

## B. ACOUSTICS

### B1. Fundamental Considerations

The scientific discipline of acoustics and noise measurements is presented in numerous textbooks and journals<sup>48-50</sup>. Considering that acoustics was the major tool used in this study a brief discussion of the main principles involved is appropriate.

Air-borne sound is a variation in normal atmospheric pressure. For a simple tone, the number of times per second that the pressure changes through a complete cycle is the

frequency of the sound<sup>52</sup>. The most commonly used devices for measuring sound levels are the 1, 1/3, and 1/10 octave band analyzers. These devices receive their name from the fact that they are capable of separating the noise signal spectrum into frequency bands that can be 1, 1/3, or 1/10 octaves in width. A 1 octave band has a center frequency that is  $2^{0.5}$  times the lower cutoff frequency and an upper cutoff frequency that is twice the lower cutoff frequency. A 1/3 or 1/10 octave band splits the octave into three or ten parts. A list of the upper, lower and center frequencies of the 1 and 1/3 octave bands is shown in Table II<sup>48</sup>.

Because of the very wide range of sound power, intensity, and pressure encountered in an acoustical environment, it is customary to use the logarithmic scale known as the decibel scale to describe these quantities, i.e. to relate the quantity logarithmically to some standard reference. The decibel (dB) is a dimensionless unit for expressing the ratio of two parameters, which can be acoustical, mechanical, or electrical. The number of decibels is 10 times the logarithm to the base 10 of the power ratio. One bel is equal to 10 decibels. Thus sound power level (PWL) is defined as<sup>48-49,52</sup>:

$$\text{PWL} = 10 \log(W_p/W_{p0}) \text{ dB} \quad \text{re } W_0 \text{ watts} \quad (9)$$

where  $W_p$  is power in watts,  $W_{p0}$  is the reference power also in watts, and re = refers to the reference power  $W_{p0}$ . For standard power reference  $W_{p0} = 10^{-12}$  watt, therefore,

Table II. Comparison of 1-Octave and 1/3-Octave Bands<sup>48</sup>

| 1-Octave                    |                       |                             | 1/3-Octave                  |                       |                             |
|-----------------------------|-----------------------|-----------------------------|-----------------------------|-----------------------|-----------------------------|
| Lower Cutoff Frequency (Hz) | Center Frequency (Hz) | Upper Cutoff Frequency (Hz) | Lower Cutoff Frequency (Hz) | Center Frequency (Hz) | Upper Cutoff Frequency (Hz) |
| 11                          | 16                    | 22                          | 14.1                        | 16                    | 17.8                        |
|                             |                       |                             | 17.8                        | 20                    | 22.4                        |
|                             |                       |                             | 22.4                        | 25                    | 28.2                        |
| 22                          | 31.5                  | 44                          | 28.2                        | 31.5                  | 35.5                        |
|                             |                       |                             | 35.5                        | 40                    | 44.7                        |
|                             |                       |                             | 44.7                        | 50                    | 56.2                        |
| 44                          | 63                    | 88                          | 56.2                        | 63                    | 70.8                        |
|                             |                       |                             | 70.8                        | 80                    | 89.1                        |
|                             |                       |                             | 89.1                        | 100                   | 112                         |
| 88                          | 125                   | 177                         | 112                         | 125                   | 141                         |
|                             |                       |                             | 141                         | 160                   | 178                         |
|                             |                       |                             | 178                         | 200                   | 224                         |
| 177                         | 250                   | 355                         | 224                         | 250                   | 282                         |
|                             |                       |                             | 282                         | 315                   | 355                         |
|                             |                       |                             | 355                         | 400                   | 447                         |
| 355                         | 500                   | 710                         | 447                         | 500                   | 562                         |
|                             |                       |                             | 562                         | 630                   | 708                         |
|                             |                       |                             | 708                         | 800                   | 891                         |
| 710                         | 1000                  | 1420                        | 891                         | 1000                  | 1122                        |
|                             |                       |                             | 1122                        | 1250                  | 1413                        |
|                             |                       |                             | 1413                        | 1600                  | 1778                        |
| 1420                        | 2000                  | 2840                        | 1778                        | 2000                  | 2239                        |
|                             |                       |                             | 2239                        | 2500                  | 2818                        |
|                             |                       |                             | 2818                        | 3150                  | 3548                        |
| 2840                        | 4000                  | 5680                        | 3548                        | 4000                  | 4467                        |
|                             |                       |                             | 4467                        | 5000                  | 5623                        |
|                             |                       |                             | 5623                        | 6300                  | 7079                        |
| 5680                        | 8000                  | 11360                       | 7079                        | 8000                  | 8913                        |
|                             |                       |                             | 8913                        | 10000                 | 11220                       |
|                             |                       |                             | 11220                       | 12220                 | 14130                       |
| 11360                       | 16000                 | 22720                       | 14130                       | 16000                 | 17780                       |
|                             |                       |                             | 17780                       | 20000                 | 22390                       |



$$\text{PWL} = (10\log W_o + 120) \text{ dB.} \quad (10)$$

Sound intensity level (IL) is similarly defined as:

$$\text{IL} = 10\log(I/I_o) \text{ dB re } I_o \text{ watts/m}^2 \quad (11)$$

where the standard sound intensity reference

$I_o = 10^{-12}$  watts/m<sup>2</sup>, therefore,

$$\text{IL} = (10\log I + 120) \text{ dB.} \quad (12)$$

Sound pressure level (SPL) is thus defined as:

$$\text{SPL} = 20\log(P/P_o) \text{ dB re } P_o \text{ N/m}^2 \quad (13)$$

where  $P$  is the acoustic pressure in N/m<sup>2</sup>,  $P_o$  is the

reference acoustic pressure having a value of  $2(10)^{-5}$

N/m<sup>2</sup> or 0.0002 microbar, which is approximately the

lowest level sound detectable to the human ear, therefore,

$$\text{SPL} = (20\log P + 94) \text{ dB} \quad (14)$$

A conversion from the measured sound pressure levels (SPL) in decibels to sound power levels (PWL) in decibels for room acoustics can be made by the use of the following:

$$\text{PWL} = \text{SPL} - [10\log(Q/4(3.14)r^2 + 4/R) - 10] \text{ dB} \quad (15)$$

where  $Q$  is a dimensionless directivity factor,  $r$  the

distance from the source to the point of SPL measurement,

and  $R$  is a room constant. Once this conversion has been

made the actual sound power in watts can be determined by

the use of equation (9). If the bracketed portion of

equation (15) is neglected then there is an equality

between PWL and SPL in decibels. The sound power levels for

the experimental work to be presented in later section were

determined using this equality (bracketed portion

neglected) and equation (9) and are therefore not true

sound powers but a modified value which incorporates a constant representing a portion of equation (15).

An example of the practical application of equation (11) is given as follows for the determination of the acoustic intensity level 10 m from a source which radiates 1 watt of acoustic power, using the reference intensity of  $10^{-12}$  watts<sup>53</sup>.

First calculate the sound intensity at 10m from the source:

$$\text{Power radiated } W = (\text{intensity})(\text{surface area}) = I(4(3.14)r^2)$$

(assuming spherical sound wave propagation.)

$$\text{Then } I = W/A = 1/(4(3.14)(100)) = 0.00079 \text{ watt/m}^2, \text{ thus}$$

$$IL = 10\log(0.00079/10^{-12}) = 89\text{dB re } 10^{-12} \text{ watt/m}^2$$

The nature of the sound wave propagation must be considered when studying noise levels. In actual practice, most noise sources do not have uniform spherical radiation. Consequently the sound is not radiating uniformly in all directions, either because the shape of the sound source is not spherical or because the amplitude and time phases of the vibration of different parts of the source are not uniform, or both<sup>52</sup>. The use of sound pressure/power contours, which measure the directivity of the noise source are a means by which an accurate determination of sound radiation characteristics, and proper microphone positioning can be made<sup>49</sup>.

Sound pressure levels in dB are a useful parameter to describe sound waves quantitatively and are measured by such sound measuring devices as octave band analyzers.

However for describing the noise emission characteristics of a source, it is not a satisfactory quantity in itself as it is dependent on the distance between the source and the monitoring device as well as the environment in which the measurements are made. In contrast the specification of sound power level as a sound characteristic enables the analysis of the emitted noise to be essentially independent of the environment in which the data are obtained<sup>48</sup>.

A very common source of noise is vibration. Audible noise can be created by the transmission of solid-borne audio-frequency vibration to air. Thus the measurement of vibration is an indirect measurement of noise. Similarly to acoustics the velocity of a vibration may be expressed in dB form as;

$$VL = 20\log(V/V_0) \text{ dB re } V_0 \text{ m/sec} \quad (16)$$

where  $V_0 = 10^{-8}$  m/sec is the standard velocity reference. Vibrational acceleration may be expressed in dB form as;

$$AL = 20\log(A/A_0) \text{ dB re } A_0 \text{ m/sec}^2 \quad (17)$$

where  $A_0 = 10^{-5}$  m/sec<sup>2</sup> is the standard acceleration reference<sup>48-49,52</sup>. Vibrational measuring systems may be entirely mechanical or a mixture of mechanical and electrical or optical devices. The most commonly used device for vibration measurements is a piezoelectric accelerometer, in which a piezoelectric element is deflected by its own inertia when it is subjected to vibration. The voltage emitted is proportional to

acceleration.

## B2. Laboratory Studies of Grinding Mill Noise

Several types of noise measurements have been made on a laboratory scale grinding mills. Reddy et. al.<sup>54</sup> studied the sound emitted from a 1/10 scale compartmentalized cement grinding mill to determine the frequency spectra for a particular speed, ball load and size, with and without the application of an asbestos rubber damping sheet around the mill shell. The frequency response to these conditions can be seen in Figure 4. The resultant radiated noise spectra reveals that the highest noise levels lie in the frequency range of 0.5-8.0 kHz. The addition of a damping layer does not change the frequency spectrum significantly but does alter the noise levels.

The second type of noise measurement made on size reduction equipment in the laboratory was of a more fundamental type. Harrington et. al.<sup>2</sup> studied the acoustic emission properties of quartz and chrysocolla in a cone crusher. They have proposed that since the energy associated with rock fracture is related to fracture sonority, it should be possible to use this sound to measure the actual energy expended. Because of the large amount of extraneous noise in the crushing and grinding environment the authors developed a pattern recognition analysis technique to differentiate between the acoustic

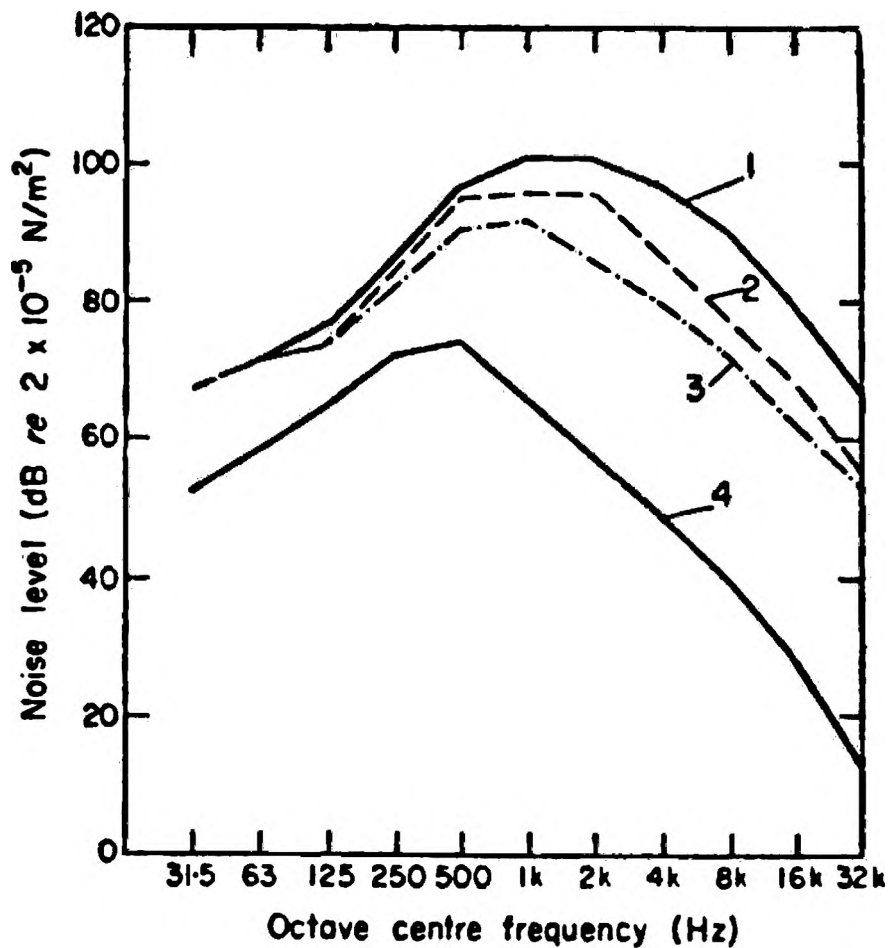


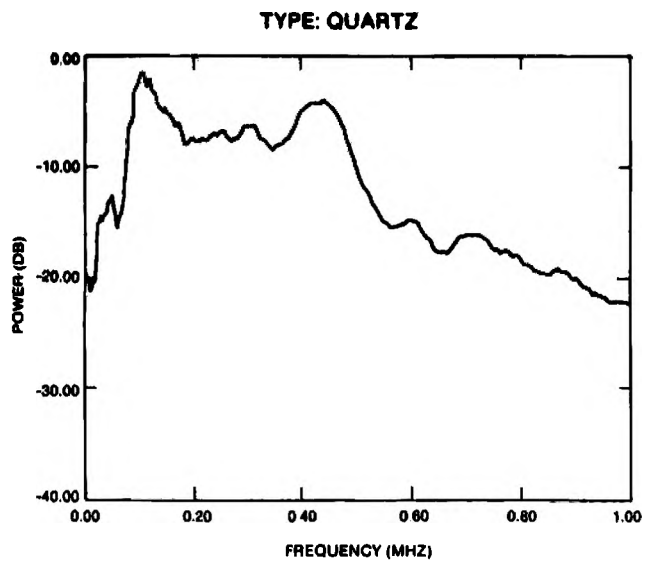
Figure 4. Radiated Noise Spectra with 50 kg Ball load, 50 mm Ball Size, and Operating at 60 RPM<sup>54</sup>

1. Without added Damping
2. With Damping Layer loosely wrapped
3. With Damping Layer bonded
4. Background Noise

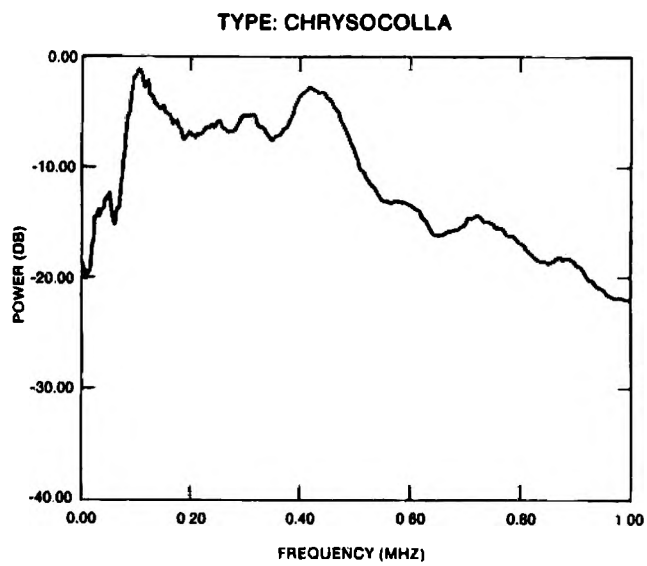
emission signals of the two types of minerals and two extraneous noises, a metal tap and a plastic tap. The normalized spectra for these signals can be seen in Figure 5. By utilizing various features of these waveforms, a system of pattern recognition was developed to make this differentiation. The results of this work lend empirical support to the theoretical proposition that acoustic emission produced by rock fracture can be differentiated from some non-fracture acoustic emission that might be found in a milling environment.

A third type of laboratory study performed to relate sound levels to grinding parameters was performed by Watson<sup>12</sup>. The results of this work will be discussed in detail as they are the basis of the research for this thesis. The noise generated by a 20x20 cm batch laboratory ball mill was studied to quantify the noise-generating mechanism and determine the effects of the mill parameters of ball size and load, mill speed, and ore type and feed size on the sound and particle production levels.

The noise generating mechanism was caused primarily by impact between the steel balls and the mill shell or what is referred to as ball/liner collisions. This hypothesis was substantiated by Watson and Cummings<sup>58</sup> who demonstrated that when the mill was lined with rubber the emitted noise was substantially reduced. Hence, ball/ball collisions do not significantly contribute to the overall sound levels.



a.



b.

Figure 5. Average Power Spectrum<sup>2</sup>

a. Quartz

b. Chrysocolla

It was found that if a particulate charge was introduced into the mill, the sound pressure levels initially decreased with grind time to a certain level and would then increase. This sequence of sound pressure level variations can be seen in Figure 6(a) and is attributed to the particulate character of the charge at a given time. It is theorized that above a certain size, particles will be able to block the collisions generated by ball/liner collisions. Initially these particles will be broken into several more particles still of sufficient size to block the collisions and hence the sound level decreases with time. At a certain point in time the size of the particles in the mill will be of a size insufficient to substantially block the ball/liner collision and the sound levels will increase. Thus the breakage of coarse particles will reduce the noise and the production of fine particles will cause the increase in noise levels.

An energy parameter representing the reduction in sound power levels (using a reference power of  $10^{-12}$  watts) derived from sound pressure levels was proposed by Watson<sup>12</sup> as an indicator of the grinding process from the standpoint of coarse breakage and material type. This energy parameter was arbitrarily chosen to evaluate relationships between sound and grinding. It is established by summing the area beneath the constant plot of the ball/liner sound power levels without a charge and the reducing noise levels with time curve resulting from the



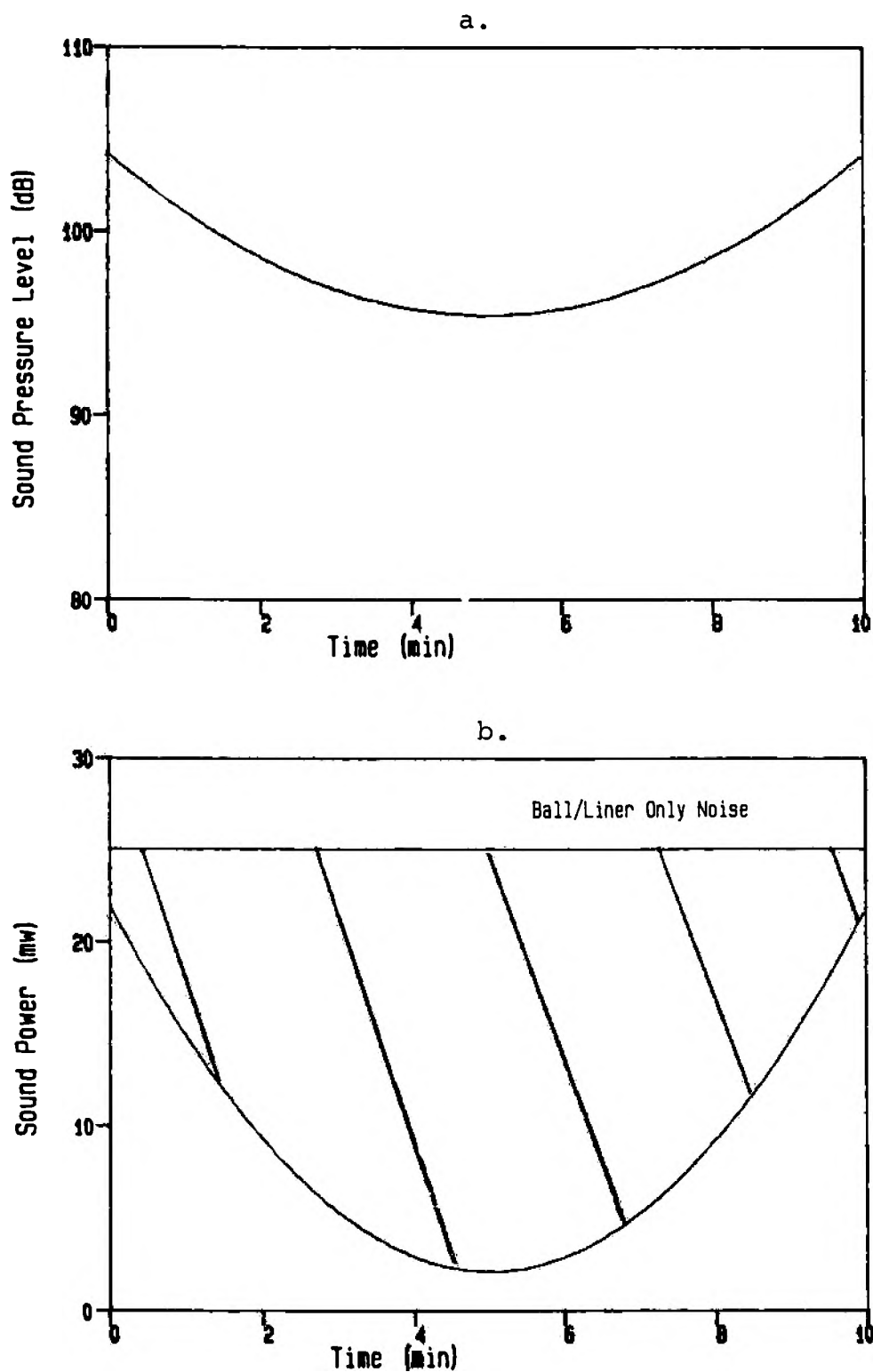


Figure 6. Example of Sound Power with Grind Time<sup>12</sup>

- a. Sound Power with Grind Time, and Baseline used for Absorbed Noise Energy calculation.
- b. Cross-Hatched Area used for Absorbed Noise Energy

introduction of ore particles. The cross hatched area in Figure 6(b) is given as an example of this evaluation. This "absorbed noise energy" parameter having units of milliwatt-min is used as the calculated value or as a percentage of the total available sound energy level (ie the area under the ball/liner plot).

Initial tests using a General Radio Real Time Multiple Frequency Band Analyzer were performed by Watson to establish an appropriate frequency range for further mill noise investigation. The upper frequency range (>2 kHz) was found to be indicative of the ball/liner collisions. From this, the frequency band 8 kHz was chosen to be monitored by a General Radio Precision Sound Level Meter linked to an Apple computer via an Isaac data acquisition system. Typical sound level variations with grind time and mill speed with a 2 kg charge are reproduced in Figure 7 to illustrate the initial rapidly decreasing sound levels with grind time resulting from coarse particle breakage. Figure 8 illustrates the relationship between absorbed noise energy values and the production of material less than 0.59 mm with both mill speed and charge variations, and the same relationship for the % absorbed noise can be seen in Figure 9 which demonstrates that there was an overall relationship between the % absorbed noise energy and fineness of grind. The results indicate that both mill speed and charge weight have an effect on the absorbed noise energy and that with increasing speed and charge weight the absorbed noise

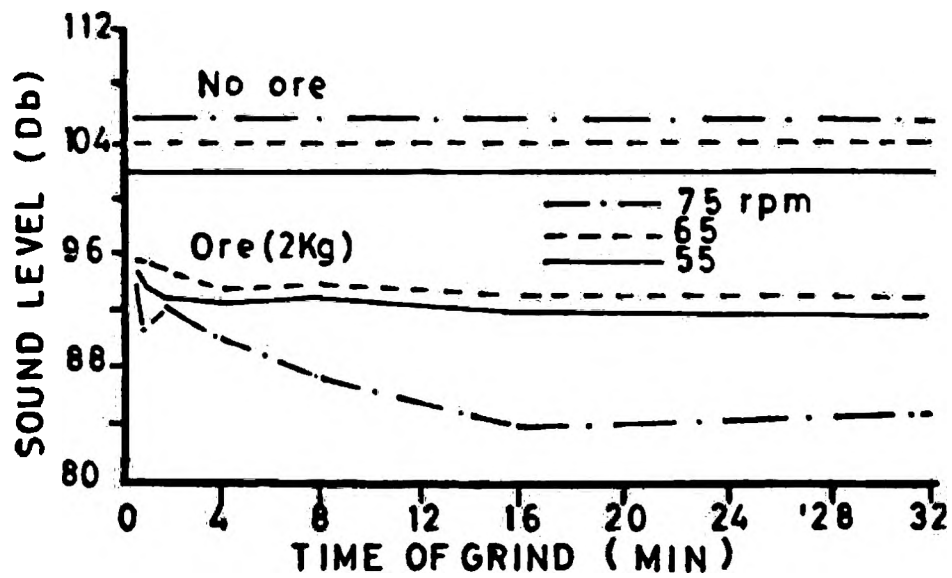


Figure 7. Mill Sound Variation with Grind Time and Mill Speed for a 2 kg Feed<sup>12</sup>

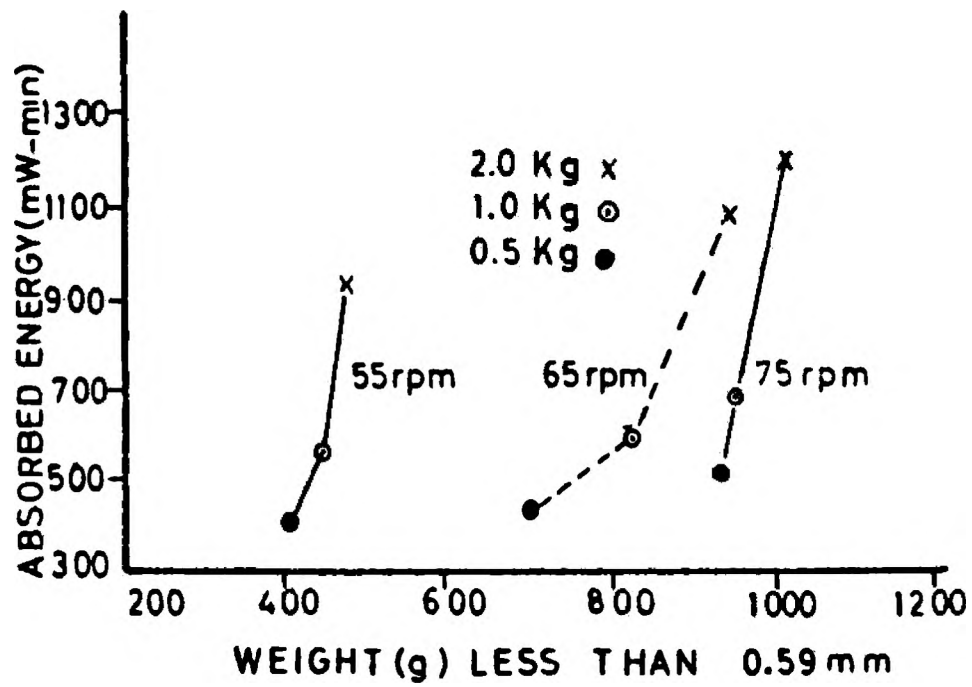


Figure 8. Absorbed Noise Energy Variation with Fineness of Grind for Dolomite<sup>12</sup>

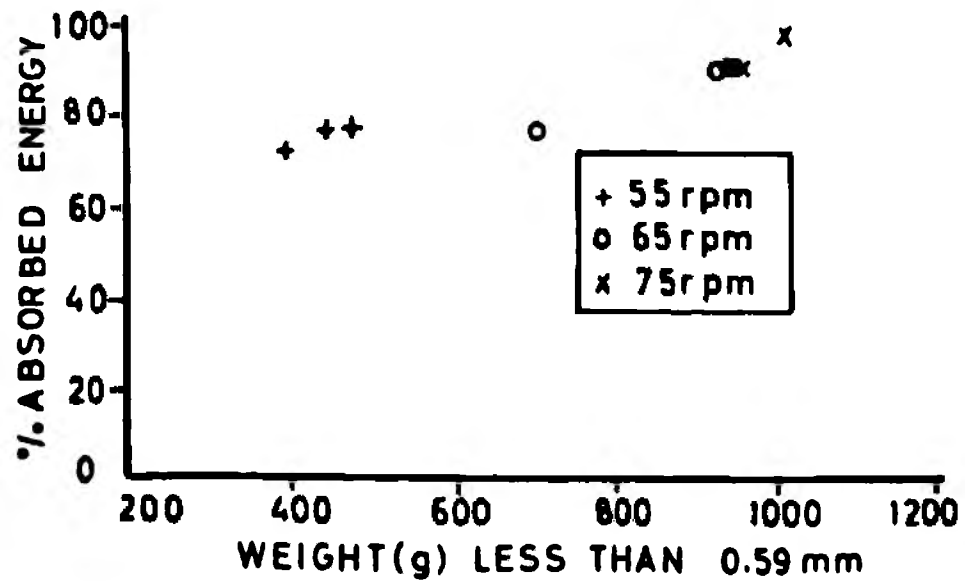


Figure 9. Percent Absorbed Noise Energy plotted as a function of Fineness of Grind for various Dolomite Feed Charge Weights and Mill Speed<sup>12</sup>

energy will reflect an increase in production of  $-0.59$  mm particles. Table III summarizes the results of 12 tests that were performed in order to establish the effects of ball size on similar test parameters. These results are plotted in Figure 10 and again a loose overall relationship is illustrated.

In a separate program Watson<sup>12</sup> investigated the effects of feed character on sound levels for four materials subjected to wet grinding. The resultant sound power levels with grind time are reproduced in Figure 11 and illustrate that a difference between materials under similar grinding conditions can be detected by the sound level changes. The sound and grinding parameters for these tests are shown in Table IV and a similar plot to Figure 10 can be seen in Figure 12. Again a relationship between coarse grinding and absorbed noise energy was found, in this case indicating the differences in material characteristics.

A later publication by Watson and Morrison<sup>13</sup> is an extension of the above described work by Watson<sup>12</sup> and constitutes the basic theme of this thesis. This as well as an additional paper by Watson and Morrison<sup>55</sup> describes research to be presented in this thesis and will not be discussed in this section.

### C. USE OF SOUND MEASUREMENTS IN INDUSTRIAL GRINDING OPERATIONS

Table III. Effect of Ball Size on Mill Sound Levels<sup>12</sup>

Test Parameters

2 kg of Balls  
 500 g -6.6+4.3 mm Dolomite  
 32 Minute Grind  
 Size A = -12.7+6.3 mm  
 Size B = -19.0+12.7 mm  
 Size C = -25.4+19.0 mm  
 Size D = +25.4 mm

| RPM | Ball Size | Absorbed Sound Energy (mw min) | % Absorbed Sound Energy | -0.59 mm Material (g) |
|-----|-----------|--------------------------------|-------------------------|-----------------------|
| 55  | A         | 298                            | 94.2                    | 110                   |
|     | B         | 557                            | 95.2                    | 196                   |
|     | C         | 653                            | 96.6                    | 315                   |
|     | D         | 442                            | 97.7                    | 391                   |
| 65  | A         | 403                            | 95.2                    | 142                   |
|     | B         | 733                            | 96.2                    | 237                   |
|     | C         | 768                            | 97.3                    | 380                   |
|     | D         | 569                            | 97.8                    | 447                   |
| 75  | A         | 531                            | 94.3                    | 221                   |
|     | B         | 966                            | 97.2                    | 314                   |
|     | C         | 1162                           | 98.0                    | 426                   |
|     | D         | 803                            | 96.6                    | 445                   |

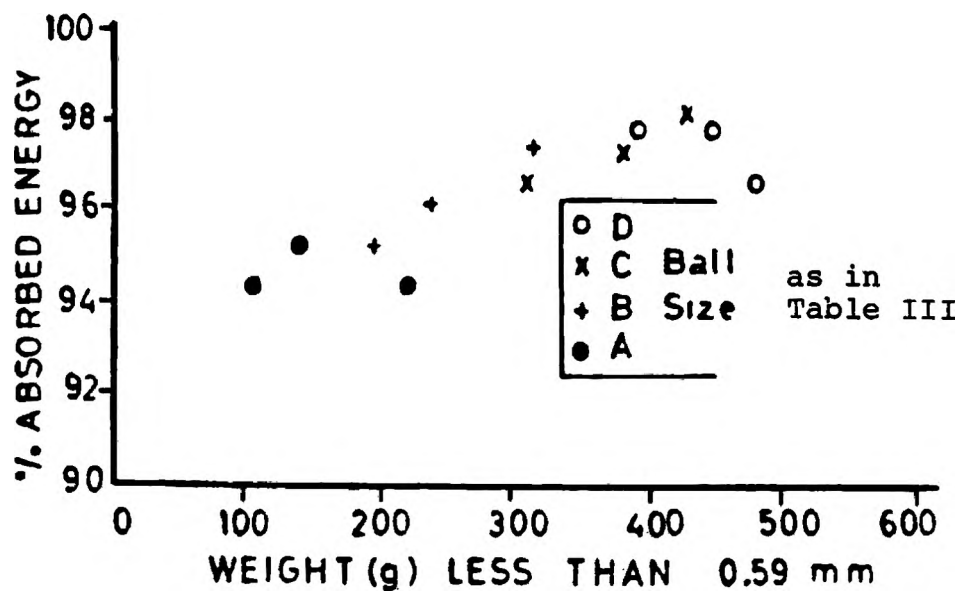


Figure 10. Percent Absorbed Noise energy plotted as a function of Fineness of Grind for a 0.5 kg Dolomite Feed Charge found with various sized 2 kg Ball Charges and Mill Speed<sup>12</sup>



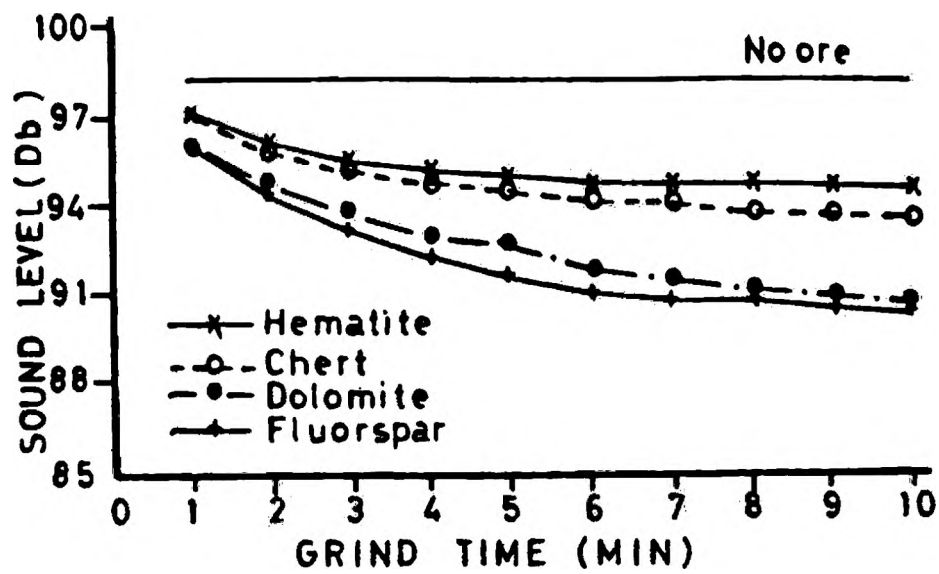


Figure 11. Sound Pressure Level Variations with Grind Time for the Wet Grinding of Four Feed Materials at 75 RPM<sup>12</sup>

Table IV. Variation of Wet Mill Grinding Sound Energies  
with Feed Type<sup>12</sup>

Test Parameters

9.9 kg of Balls  
1 kg of Ore  
10 Minute Grind  
C = Chert  
F = Flourspar  
D = Dolomite  
H = Hematite

| <u>RPM</u> | <u>Ore Type</u> | <u>Absorbed Sound<br/>Energy (mw min)</u> | <u>% Absorbed<br/>Sound Energy</u> | <u>-0.59 mm<br/>Material (g)</u> | <u>Work<br/>Index<br/>(kwh/ton)</u> |
|------------|-----------------|---|------------------------------------|----------------------------------|-------------------------------------|
| 65         | C               | 10.6                                      | 33                                 | 123                              | 13.6                                |
|            | F               | 19.3                                      | 58                                 | 412                              | 8.9                                 |
|            | D               | 17.6                                      | 53                                 | 306                              | 11.3                                |
|            | H               | 9.5                                       | 28                                 | 209                              | 17.0                                |
| 75         | C               | 28.4                                      | 44                                 | 113                              |                                     |
|            | F               | 41.9                                      | 65                                 | 449                              |                                     |
|            | D               | 40.5                                      | 63                                 | 300                              |                                     |
|            | H               | 27.3                                      | 42                                 | 209                              |                                     |

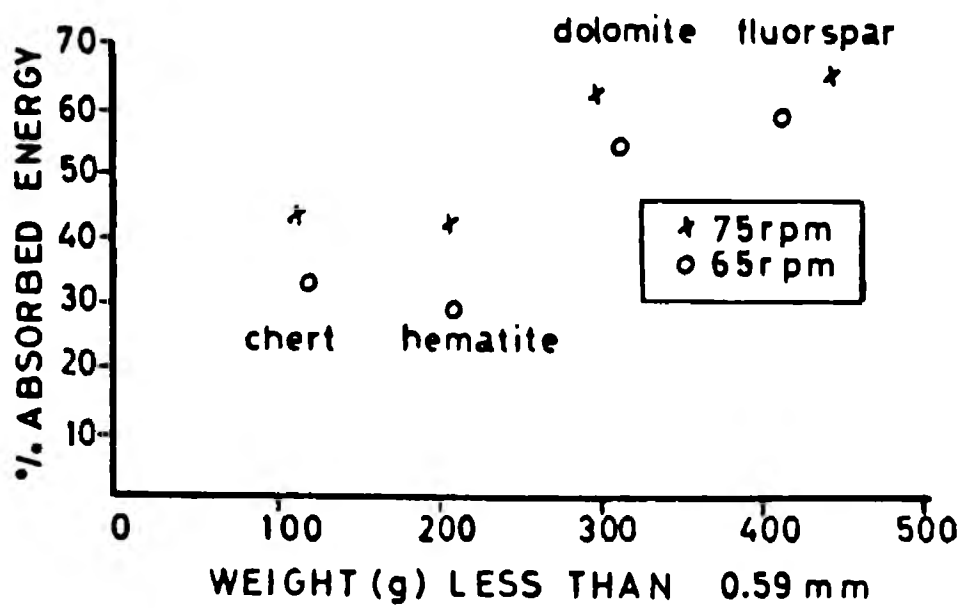


Figure 12. Percent Absorbed Noise Energy plotted as a function of Fineness of Grind for 1 kg of each of Four Different Charge Materials ground at 65 and 75 RPM<sup>12</sup>

There has been little published information on the use of sound measurements in industrial grinding operations and what literature is available on installed systems contains very little detail on the fundamental aspects of system development.

The use of sound measurements to control the grinding process is first cited in the literature with the advent of the "Hardinge Electric Ear". This was a radio-electric device adapted to translate differences in mill sound automatically to changes in feed rates<sup>11</sup>. This control strategy was successfully implemented at a variety of locations<sup>56</sup> and is still in use today at industrial mineral grinding operations.

There have been a several adaptations in the use of this sound based grinding control system. One of these control systems was developed at the concentration plant of the Vuonos mine in Finland<sup>7</sup>. In this case the controlled variable is the noise and the manipulated variables are the components of the feed to the semi-autogenous mills. The emitted noise levels were evaluated on a frequency spectrum basis to identify which part of the spectrum represented the collision of the media with the mill liner. It was found that the state of the mill was best reflected by the 1500-2500 Hz frequency range.

The feed components to the mill at this location are

fine ore, lump ore, and water. A change in the fine ore feed when all other components were held constant had a considerable and rapid effect on the noise levels. When the fine ore was increased the noise levels dropped rapidly. The change in lump ore feed had a much slower and smaller effect than the fine ore and in an opposite direction. The effect of increasing water, and thus decreasing pulp density, on the noise levels of the mill was similar to that found with lump ore but the gain in noise levels was higher. Increasing the water allowed the medium to penetrate the ore more freely and hence increase the noise. These observations were then incorporated into a computer control algorithm for establishing a certain base grinding efficiency and then feeding the maximum amount of fine ore. It is claimed that in the course of long term testing that the noise control system increased the throughput of the mills by 10-15% with a marginal reduction in production of -200 mesh material.

A further system was installed in Canada at the East Malartic mine concentration plant<sup>12</sup>. It employed a sound level control strategy that used the measurement of a narrow frequency range of sound from the mills. The sound level was maintained at a constant level by varying the feed rate. The authors claimed that this control system provided a significant reduction in the variability of the fineness of grind and the variability of the screen analysis of all the products of the grinding circuit.

Another system used in the Soviet Union<sup>9</sup> for the grinding of limestone and nephelite implemented a sound based control strategy to control pulp density. The researchers found a linear relationship between sound frequency at a certain location within the mill and moisture content of the pulp.

The domestic cement industry has found increased use of sound based control systems<sup>8</sup>. It has been shown that the part of the emitted sound spectrum that best indicates the qualitative and quantitative changes in the feed material lies around 3.0 kHz. This frequency band is separated using high band pass filters and used as a feedback variable to control feed rate and loading conditions.

The preceding review of the recent advancements made in utilizing sound levels as a control parameter shows that this tool has potential as an indirect non-invasive technique to better understand and quantify the complex process of grinding. The following section will detail the experimental procedures undertaken in an effort to further identify whether sound levels can reveal useful data about the critical operating parameters of a batch ball mill and hopefully provide a mechanism for implementing improved control of continuous mills.

### III. EXPERIMENTAL PROCEDURES

#### A. SAMPLE PREPARATION

The procedures used in grinding charge preparation are listed below in outline form.

1. The raw materials used in this study were magnetite and molybdenum ore, quartz, olivine, dolomite, trap rock, and coal. The following is a listing of the source and nature of these materials.

a. Magnetite ore Samples were obtained from the stockpiled product of the secondary crushing and screening operation of the Pea Ridge Iron Ore Co. near Sullivan MO. The ore was nominally 5.0 cm in diameter.

b. Molybdenite ore Samples were obtained from the Climax Molybdenum mine of Amax Inc. in Climax CO. The ore was the feed to the rod mill and contained a distribution of particles from 2.5 cm down.

c. Quartz Samples were obtained from the Connecticut Silica Co. Inc. in Leyard CN.. This material was shipped to U.M.R. as their product "#2 Stone" and was nominally 1.3 cm in diameter.

d. Olivine Samples were obtained from a stockpile at the Pea Ridge Iron Ore Co. Inc. near Sullivan Mo. where it is used as an additive to the iron ore pelletization process. This material was nominally 5.0 cm

in diameter.

e. Dolomite Samples were obtained from freshly blasted faces of the U.M.R. experimental mine in Rolla, MO.. The ore was hand picked to ensure the purest material was obtained as extremely variable hardness materials are present in the mine. The nominal top size of this material was 10 cm.

f. Coal Samples were obtained from the stockpile at the U.M.R. power plant in Rolla, MO.. The coal is processed by washing and comes from a variety of Missouri locations. The nominal top size of this material was 2.5 cm.

g. Trap Rock Samples were obtained from stockpiles at the Pea Ridge Iron Ore Co. Inc. where it is mined and processed by crushing and screening and sold as road ballast. The nominal top size of this material 1.3 cm.

2. All raw materials contained a certain percentage of moisture and were dried in a steam oven at 80 degrees C for 24 hours.

3. Upon completion of drying the ore materials were subjected to size reduction and classification to obtain the required particle size distribution for experimental feedstock. An example for the production of  $-3.3+1.6$  mm and  $-1.6$  mm magnetite ore is given in Figure 13. All ore materials were prepared in sufficient quantity to allow a series of experiments to be completed.

4. When crushing and screening were completed all



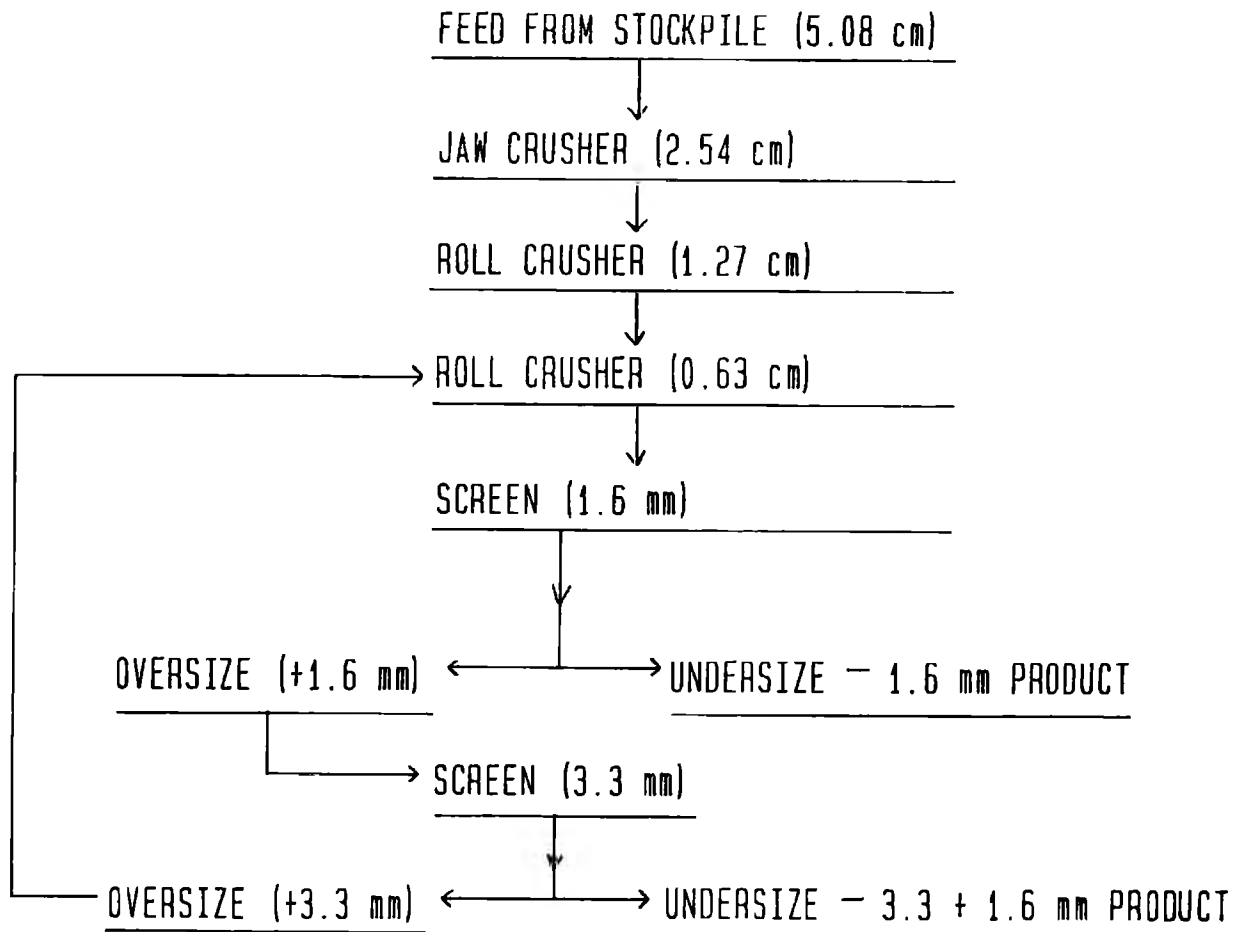


Figure 13. Flowsheet of Feed Sample Preparation Techniques for the Production of -1.6 mm and -3.3+1.6 mm Feed Sizes

sample materials were thoroughly mixed and sampled. A screen analysis was then performed to establish the feed size distribution. For certain experiments pure magnetite ore was utilized and this was obtained by separating the prepared magnetite ore with a retractable hand magnet.

#### B. GRINDING CONDITIONS

A 20X20 cm steel laboratory mill containing 5-20 kg. of approximately 2.5 cm cast steel balls was utilized for the majority of the test work. The mill had a volume of 6283 cc and the standard charge of 125 2.5 cm balls weighing 10 kg occupied 1073 cc with a void volume of 1000 cc. Thus the mill ball loading was 17.1% by volume. The mill was operated at speeds of 55-80 rpm (58-85% critical). Unless otherwise mentioned a charge of 125 balls and 1000 cc of ore or pulp will be referred to as the standard mill conditions, which gave 33% total occupied volume. The typical charge size distributions were -6.6+3.3 mm and -3.3+1.6 mm, but some tests investigated grinding and sound relationships using a feed size down to -104 microns, and others used a distribution of particles from -1.6 mm down. Most experimental charges were based on volumetric loadings. If the test was performed on a dry basis the charge was measured in a 1 liter graduated cylinder and the weight recorded. On a wet basis, using varying pulp densities, the charge weights and water volume for a

constant volumetric loading were calculated using a computer program which is included as Appendix D. A sample output can be seen in Table V. For wet grinding tests using a grinding additive, 1.25 kg/tonne of Dow Chemical Co Inc. Grinding Aid # GA-4274 was added using a calibrated pipette. The mill, balls, and charge were rotated on a Norton # P-2084-A05 Jar Mill which was enclosed in a plywood box having the dimensions 82 X 60 X 120 cm.

### C. DATA ACQUISITION AND SOUND MEASURING SYSTEMS

The data acquisition systems used for the experimental work with single and multiple frequency band sound monitoring systems can be seen in Figure 14. For the purpose of clarity the discussion of the sound measuring systems used for this study will be presented in the same sequence as the Results and Discussion Section is ordered.

#### 1. Narrow Frequency Analysis Systems

##### a. Angular Directivity Tests

The system used for these tests consisted of a General Radio # 1564 Sound and Vibration Analyzer coupled with a General Radio #1521-B Graphic Level Recorder. This system was used to perform angular directivity measurements on the emitted sound levels of the mill. This system enabled the

Table V. Ball Charge Quantities for a Molybdenite Ore

Material = Molybdenite Ore  
 Density (g/cc) = 3.35  
 Mill Void Volume (cc) = 1000

| <u>% Solids<br/>by Wt.</u> | <u>%Solids<br/>by Volume</u> | <u>Ore Charge<br/>(g)</u> | <u>Water Charge<br/>(cc)</u> |
|----------------------------|------------------------------|---------------------------|------------------------------|
| 60                         | 30                           | 1036                      | 690                          |
| 62                         | 32                           | 1097                      | 672                          |
| 64                         | 34                           | 1161                      | 653                          |
| 66                         | 36                           | 1229                      | 633                          |
| 68                         | 38                           | 1300                      | 611                          |
| 70                         | 41                           | 1375                      | 589                          |

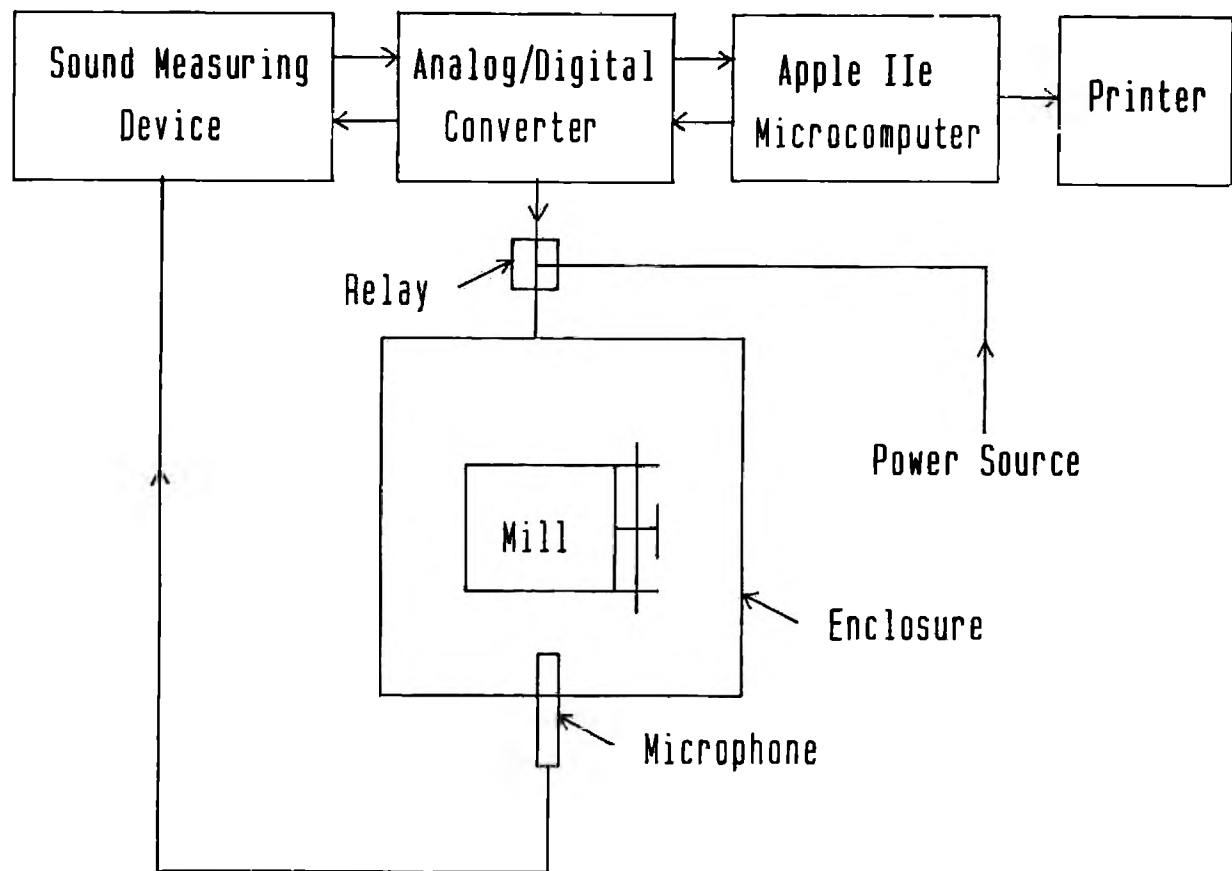


Figure 14. Schematic Diagram of Sound Measuring, Data Acquisition, and Computer Systems used for Multiple and Single Frequency Band Monitoring

monitoring of 1/10 octave bands from 21.5 Hz-20 kHz and the relative sound pressure levels in decibels. A 2.5 cm General Radio # 1560-9570 Ceramic microphone with a General Radio # 1560-P40 Preamplifier was placed at a distance of 1 meter from the mill shell centered at the horizontal axis and moved radially around the mill in 10 degree increments for 180 degrees. This positioning sequence can be seen in Figure 15. This experimental work was performed outdoors because directivity measurements are affected by enclosures. The graphic level recorder was set at a writing speed of 2.5 cm per minute and the analyzer was mechanically driven at a proportional rate through the entire frequency spectrum. Once the frequency spectrum was established the analyzer was preset at a selected frequency and the strip chart recorder actuated to determine the intensity levels of each frequency at the various positions around the mill. These values were then plotted on polar coordinate paper to enable estimations of the angular directivity of the emitted sound, which aided in the evaluation of proper microphone positioning in subsequent testing.

#### b. Discrete Frequency Tests

The second system used for narrow frequency analysis was a Spectral Dynamics S.D. Dynamic Analyzer II. This was used with a B&K #4133 1.3 cm condenser microphone coupled

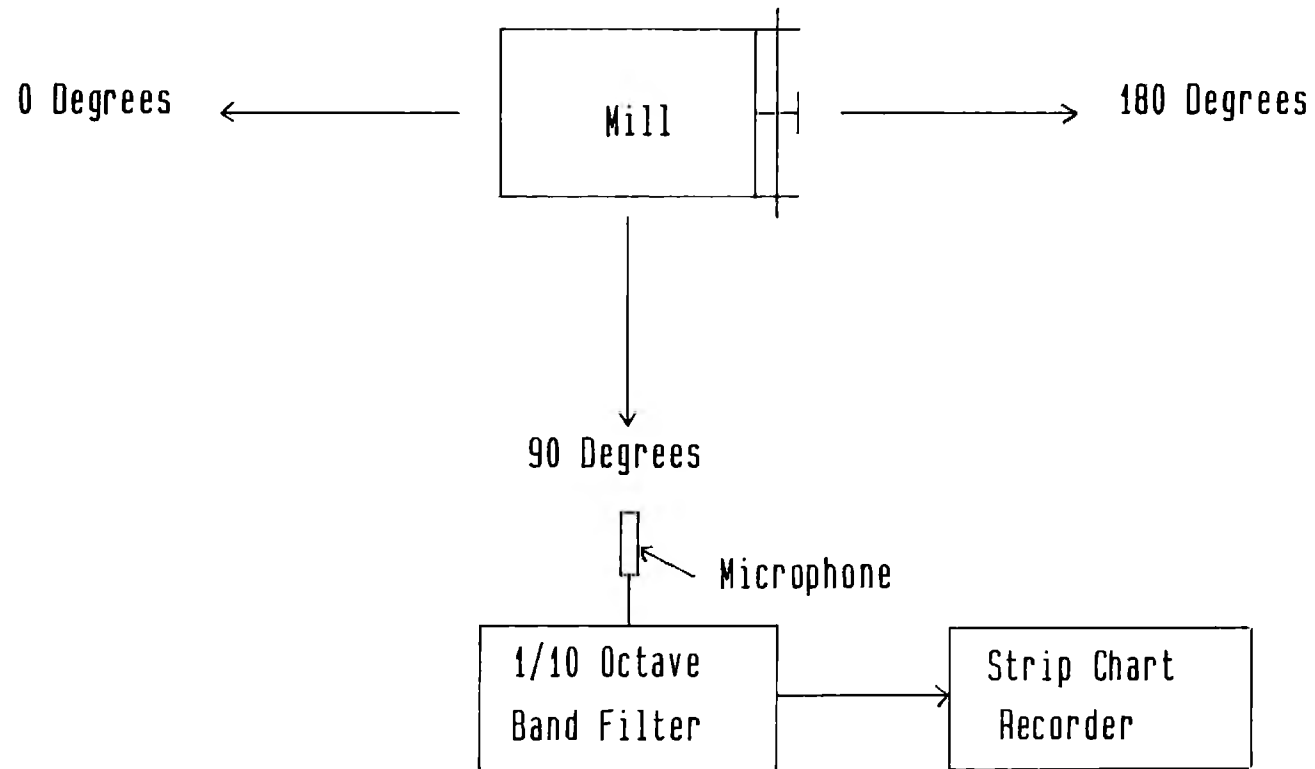


Figure 15. Schematic Diagram of the Microphone Placement Positions for Angular Directivity Testing

with a B&K # 2619 Preamplifier, and #2609 measuring amplifier placed 80 cm from the mill shell, centered at the horizontal axis. This system was used to establish the resonant frequencies of the mill shell operating under standard conditions with no ore charge by measuring a transient sound signal and converting this into a discrete frequency spectra by fast Fourier transforms incorporated in the system computer hardware. Additionally it provided frequency spectra on a continual basis by averaging the transient signals over a preset sampling interval. The output from this system was displayed graphically using an integrated Hewlett-Packard # 7470-A plotter.

### c. Particle Damping Tests

A similar system to that used for the discrete frequency testing was used to establish the vibrational characteristics of the mill shell due to a single 2.5 cm ball collision on the top of the mill shell. In addition the damping effects of a layer approximately 2 cm deep of a two sieve series of dolomite particles from 1.6 mm to -53 microns was determined. A B&K # 4374 piezoelectric accelerometer was attached to the mill shell in the location detailed in Figure 16. The transient vibrational signal as well as the acoustic signal from the collision was then captured by the Dynamic Analyzer in the same fashion as for the resonant frequency determination, and



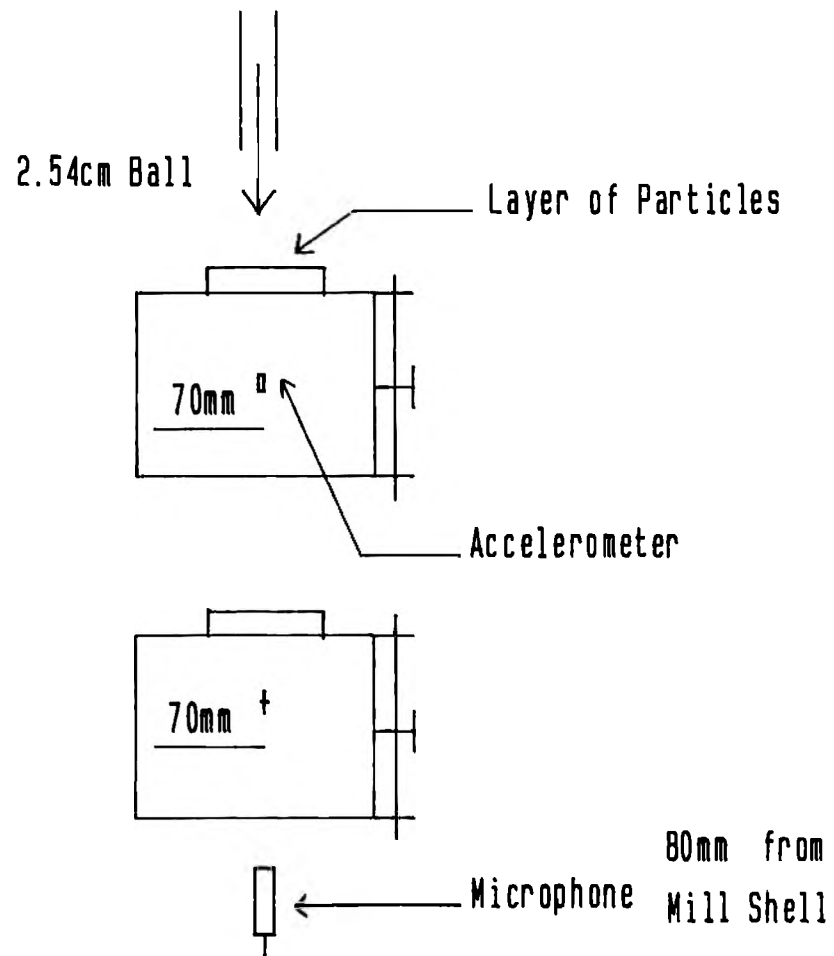


Figure 16. Schematic Diagram of Microphone and Accelerometer Placement for Particle Damping Tests

the spectrum plotted.

## 2. Single Frequency Band Tests

For the single frequency band experimental work a General Radio Precision Sound Level Meter and Analyzer #1982 was used, which allowed the monitoring of single frequency bands on a 1/3 octave basis from 31.5 Hz-16 kHz. The microphone used was a General Radio #1962 1.3 cm electret condenser microphone. Four decibel ranges were available for use which were 30-80, 50-100, 70-120, and 90-140 with four associated weighting filters, A, B, C, and flat. For all experimental work the microphone was placed 25.4 cm from the center of the horizontal axis of the mill within the wooden enclosure. The decibel range of 70-120 and frequency band of 8 kHz and corresponding weighting filter C was used for all sound measurements. The d.c. output of the sound level meter ranged from 0-3 volts, which corresponded linearly with sound pressure readings, was input to an Isaac # 91A data acquisition system. This system was linked to an Apple IIe microcomputer, and using a Basic computer program (appendix A1), enabled 13 sound pressure level samples to be taken at the preset frequency each second with a 10 second average being logged four times each minute. Additionally the sound pressure level (dB re 0.0002 Microbar) was converted to sound power values (milliwatts re  $10^{-12}$  watts) and tabulated at one minute

averages for the length of the grind time. Prior to each experimental series the data acquisition system was calibrated using a B&K Sound Level Calibrator # 4230 with an acoustic output of 94 dB at 1000 Hz, and a General Radio # 1562-A Sound Level Calibrator with an acoustic output of 114 dB at the frequencies 125, 250, 500, 1000, and 2000 Hz. The Basic computer program also incorporated a signal on a real time basis, to be output via the Isaac system through a solid state relay, to turn the mill on and off at the preset grinding time.

### 3. Multiple Frequency Band Tests

For the Multiple frequency band measurements a General Radio # 1925 Multifilter and #1926 Multichannel R.M.S. Detector were used which allowed continual monitoring of the 30 frequency bands on a 1/3 octave basis from 25 Hz-20 kHz. A General Radio # 1560-P40 Preamplifier and General Radio # 1560-9570 2.5 cm ceramic microphone was placed 25.4 cm from the mill shell in the same configuration as the single frequency system.

The R.M.S. detector enabled the monitoring of the frequency bands continually by integrating the input signal over a preset time interval and storing it remotely from the Isaac and computer system. The integration period used with this system was 16 seconds, during which a total of 1024 samples of the frequency spectrum were taken for an

average sampling rate of 32/second and an average sample spacing of 32.2 microseconds.

The analog output of the R.M.S. detector consisted of two channels. One channel (y axis) generated a 0-1 volt signal which corresponded linearly with decibels and the other channel (x axis) generated a 0-1 volt signal which corresponded to the 30 frequency band channels from the Multifilter. An output rate of 8 channels per second was chosen for input to the Isaac system, which equates to approximately 3.75 seconds to generate an entire frequency spectrum.

A computer program (appendix A2) was written to accept the output from the real time analysis so that 3 integrated samples of the spectrum were obtained per minute for the length of the experiment. Upon completion of each test using this system the sound data in a digital form were stored on magnetic discs for subsequent data manipulation. This required two dimensional arrays storing 30 channels of sound data, each element representing the sound intensity levels in the frequency band for any given 16 second integration period. This system also incorporated the relay system for turning the mill on and off at the beginning and end of the experimental grind.

#### D. SAMPLE ANALYSIS

At the end of an experiment, the sample and grinding

media were removed from the mill and separated using a 1.27 cm screen. If grinding was performed on a wet basis the mill was washed with water to remove all particles and the media cleaned in a similar fashion. The sample was then filtered to remove excess water and dried in a steam oven at 80 degrees C.. This was done either at the end of the established grind time or in increments to ascertain kinetic or time based particle size distribution data.

All samples were then thoroughly mixed and reduced in mass to an appropriate size for screening by riffle reduction or incremental division. The product size distributions were then determined using two and root two series screens in conjunction with a Rotap screen shaker. To determine the values for percentage less than 100 microns, samples were analyzed by wet screening. A cyclosizer was used for the determination of particle size distributions for less than 75 microns. The determination of ore specific gravity in g/cc was done using a Beckman # 930 Air Comparison Pycnometer.

The measurement of the relative grindability in grams/revolution (g/rev) at a certain mesh size, was performed using a 20x20 cm laboratory mill with 125 2.5 cm cast steel balls operated at 62 rpm. The procedure is an adaptation of the Bond Grindability Test<sup>57</sup>.

#### E. SOUND DATA ANALYSIS

The measured sound pressure levels from the systems discussed above were manipulated in various ways. The computer generated values for sound power values for the single frequency band sound monitoring were portrayed graphically, an example of which can be seen in Figure 17. Additionally the sound power was integrated over the grind time using the reference base line of the sound power emitted by the mill and balls to calculate the sound energy absorbed by grinding of the ore. This value with units of milliwatt-minutes has been termed ANE (absorbed noise energy). A second noise energy parameter was calculated similarly to ANE but used an artificial baseline that was closer in absolute value to the actual maximum achieved during the experimental grind. This value termed DANE (delta absorbed noise energy), was in certain instances better able to reflect the quantitative relationships between sound levels and grinding parameters. An example of the baselines used for these two noise energy parameters in reference to typical sound power measurement for a 10 minute grind is shown in Figure 17 with the resultant noise energy values for ANE and DANE.

The data stored on magnetic discs for the multiple frequency sound monitoring experimental work was manipulated subsequent to a series of tests by the use of the computer program in Appendix B2. This program converted the digital values of the spectrum generated by the analog output of the RMS Detector first to sound pressure levels

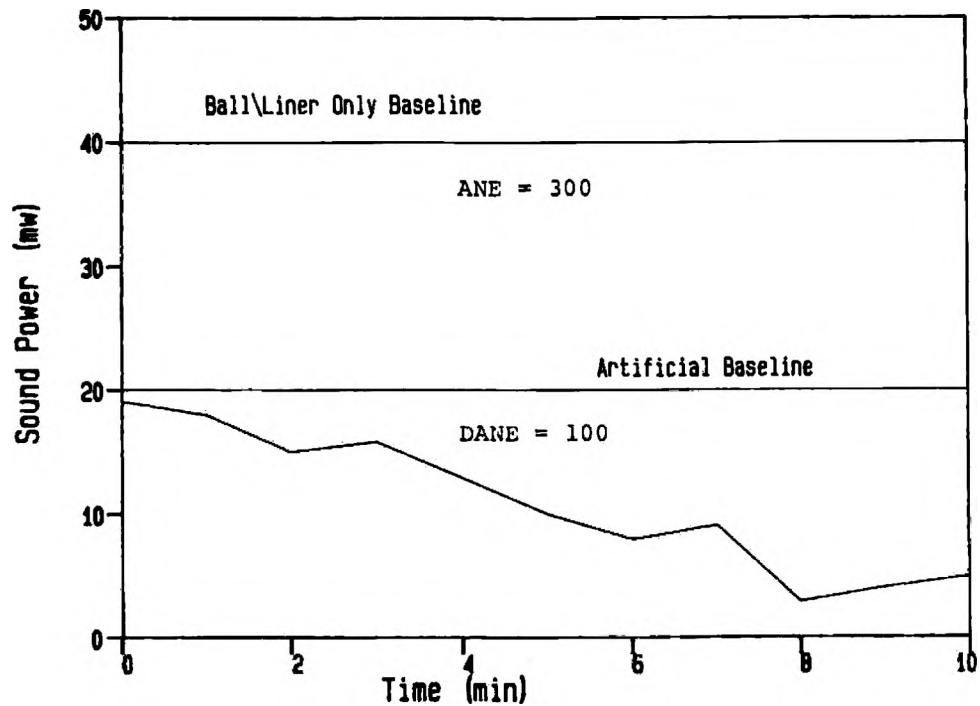


Figure 17. Example of Sound Level Variation with Grind Time with Reference Baselines to Calculate ANE and DANE

(dB) and then to sound powers (milliwatts). Finally a single overall cumulative average (CA) sound power value was calculated from the frequency range of 2-8 kHz.



#### IV. RESULTS AND DISCUSSION

For the sake of clarity the experimental results and discussion are combined and will be presented in three sections. This is done because of the large number of figures and tables used to illustrate the relationships between noise levels and grinding parameters.

The first section (A) deals with experimental work undertaken to provide acoustic detail for the investigations and to supplement the results obtained with single and multiple frequency band analysis which are presented in the subsequent two sections (B and C). Section A is subdivided into three parts. The first part and a portion of the second part discuss results that stand alone. The second section (B) on single frequency band monitoring is also subdivided into three parts to present the work of the publication by Watson and Morrison<sup>13</sup> as well as supporting results from narrow frequency band monitoring. The third section (C) on multiple frequency monitoring is subdivided into two parts. The first presents the results by Watson and Morrison<sup>55</sup> and the second part discusses the final experimental work performed to study the relationships between artificial ore mixtures, grinding parameters and noise levels.

##### A. NARROW FREQUENCY BAND ANALYSIS RESULTS

### A1. Angular Directivity Test Results

The results of the angular directivity tests at 7.8, 4.5, and 3.6 kHz respectively are presented in Figures 18-20. These tests were performed by the equipment detailed in section C part 1a of the Experimental Procedures. The graphs show the sound pressure levels of the mill operating under standard conditions with no ore charge as a function of the angle of noise measurement from the source.

The polar coordinate plots seen in Figures 18-20 illustrate the lobate character of the sound pressure levels emitted from the mill. For all three frequencies plotted there are three lobes present, which reflect the geometric configuration of the mill. The center lobe displays the highest relative intensity level. As the angle of measurement moves in either direction from the position perpendicular to the mill there is a decrease of intensity until the secondary lobes appear. These lobes represent sections of the mill where the structural response to ball/liner collisions is at a maximum. In relation to the geometry of the mill the lobes appear to reflect the ends and cylindrical portion.

These tests were performed in an effort to justify the microphone placement position, and from Figures 18-20 it is apparent that the area with the highest emitted sound is in the position perpendicular to the long axis of the mill and this is the position used for all testing.

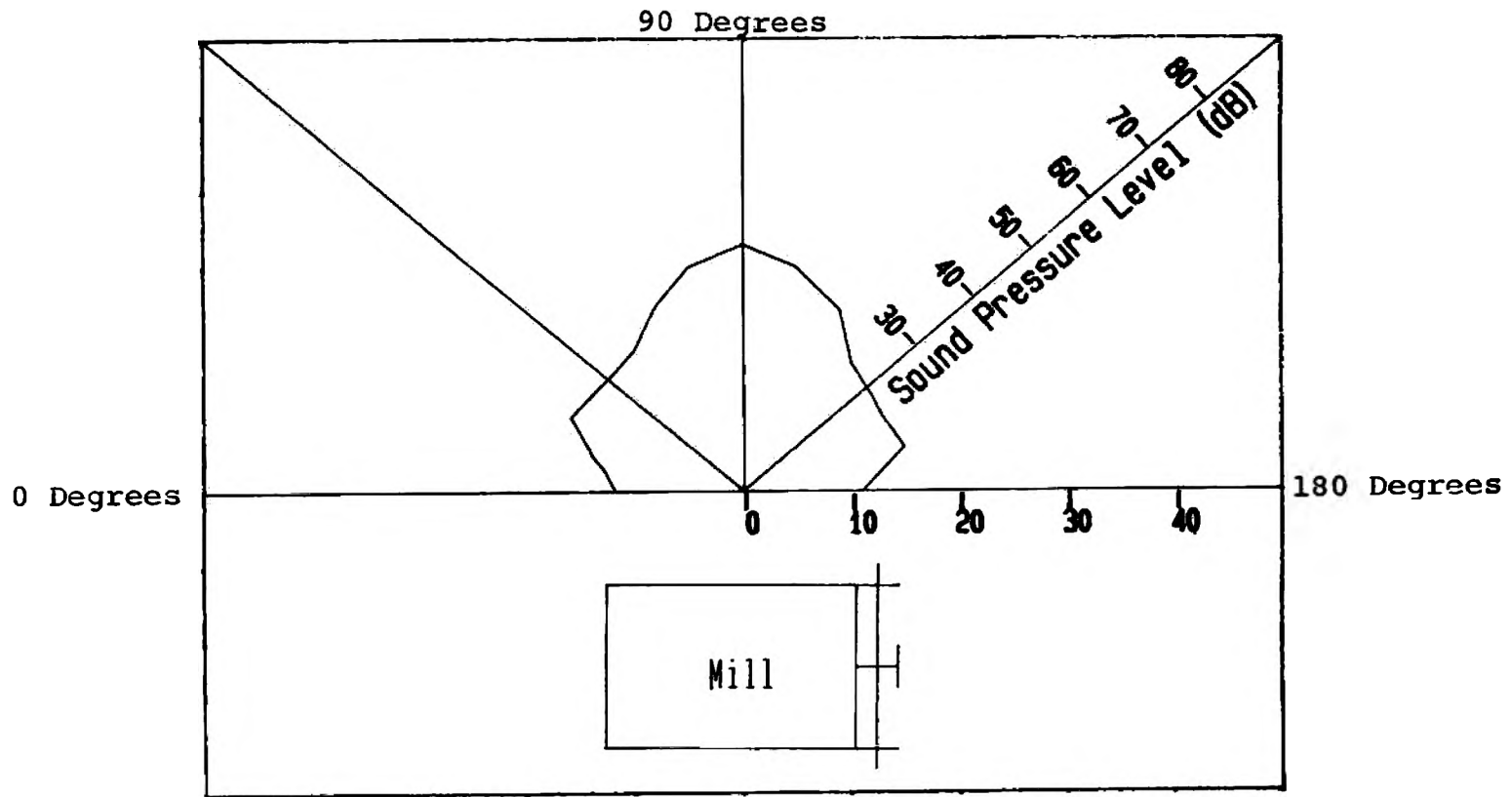


Figure 18. Angular Directivity Test Results at 7800 Hz

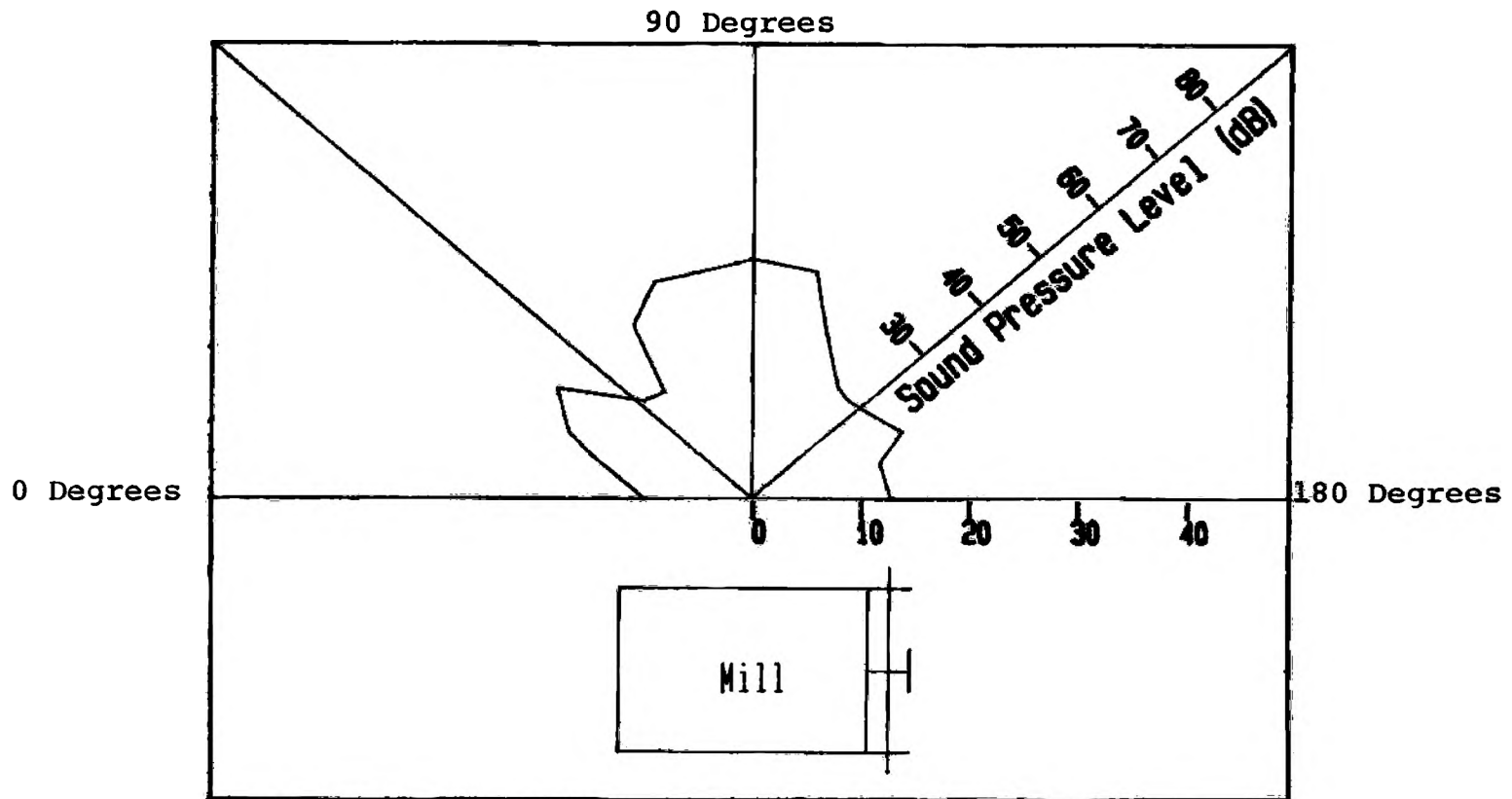


Figure 19. Angular Directivity Test Results at 4500 Hz

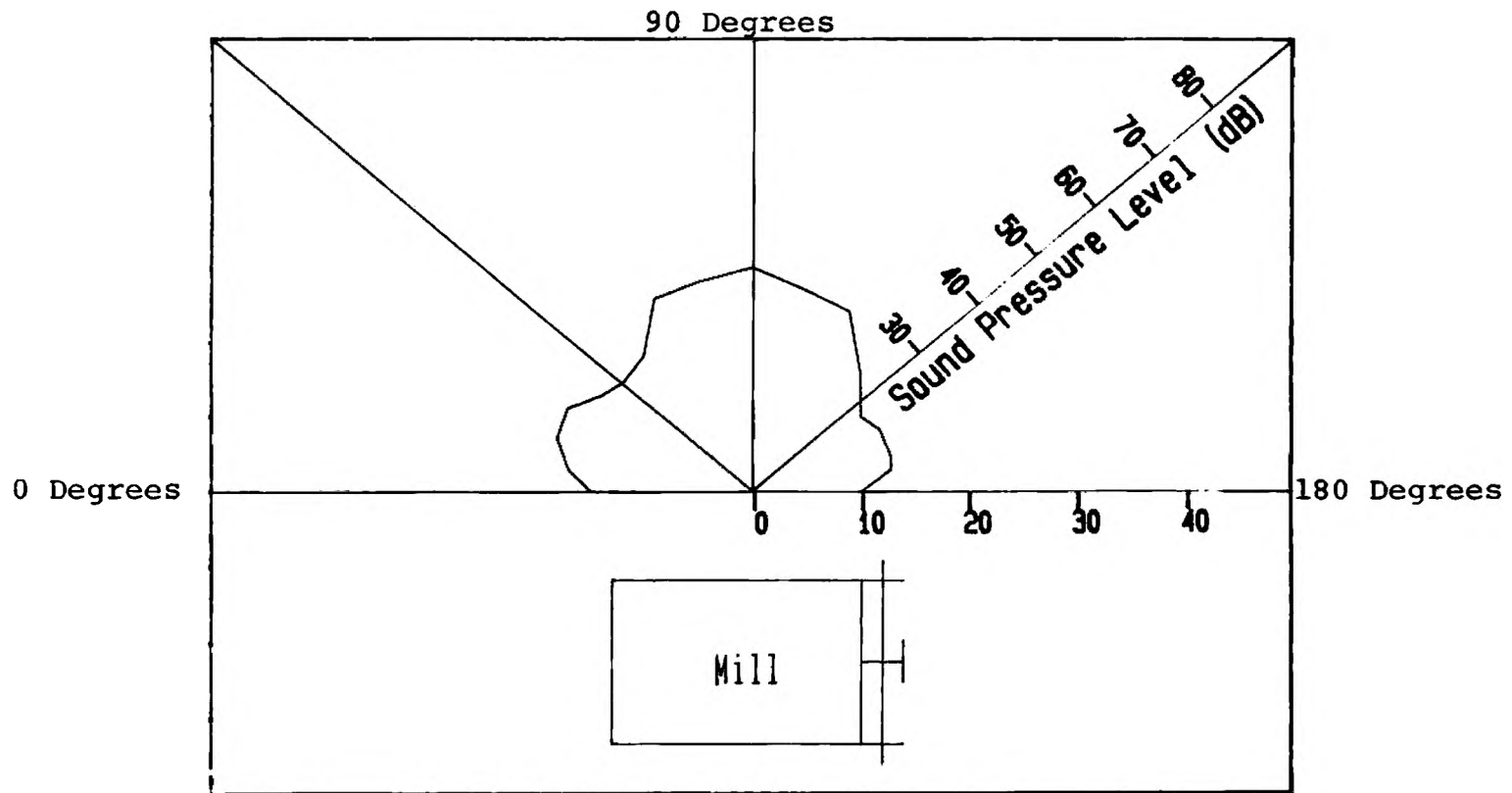


Figure 20. Angular Directivity Test Results at 3600 Hz

## A2. Discrete Frequency Analysis Results

The experimental results presented in this section were performed by the equipment detailed in section C part 1b of the Experimental Procedures.

The frequency spectrum in Figure 21 represents the resonant frequencies of the mill operating under standard conditions with no ore charge. The purpose of this determination of this spectrum was as follows:

a) To substantiate the high intensity levels of noise that were observed with the single frequency band analysis at 8 kHz in the initial work reported by Watson<sup>12</sup>;

b) To ascertain which frequency bands would best represent qualitative and quantitative changes in sound power values for further study with multiple frequency band analysis;

c) To perform tests similar to those performed with single frequency band analysis and determine if additional useful data could be obtained.

The results observed in Figure 21 indicate that the frequency spectrum of the mill operating under standard conditions with no charge is a highly complex spectrum, with numerous frequencies which represent the natural structural response of the mill. As can be seen there are several peaks present in the frequency range 7.1-8.9 kHz which represents the upper and lower cutoff frequencies of

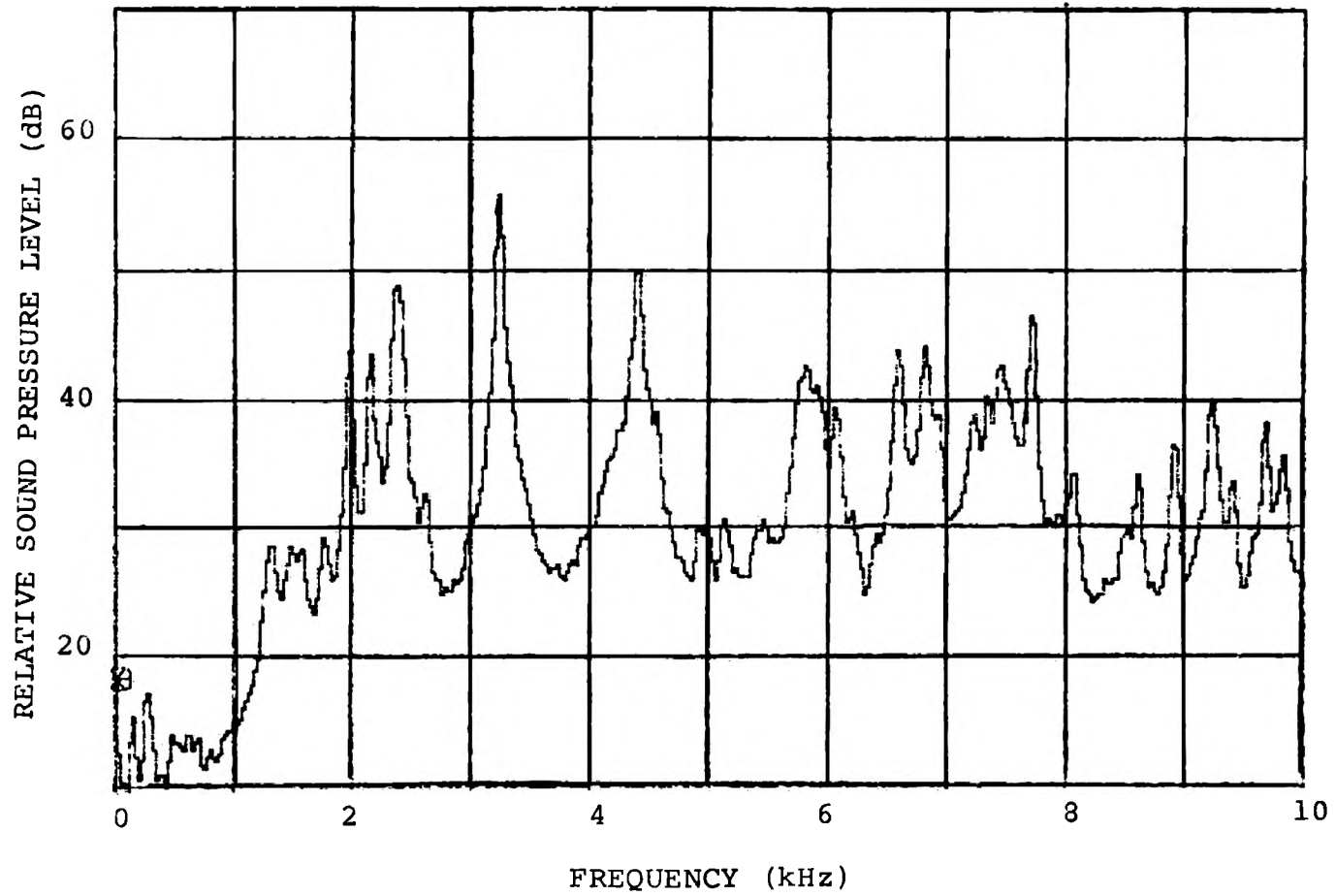


Figure 21. Sound Frequency Spectrum of Ball Mill Operating under Standard Conditions with No Charge

the 8.0 kHz 1/3 octave band. This feature is substantiating evidence for the initial work reported by Watson<sup>12</sup>, and for the continuation of this work which is presented in section B. Below approximately 1.25 kHz there is a significant decrease in the intensity levels of the frequency spectrum in Figure 21. This is also observed above approximately 7.75 kHz but to a lesser extent. The pronounced peaks between these points represent the resonant frequencies of the mill and correspond roughly to the cutoff frequencies of the 1/3 octave bands at 2-8 kHz. This feature of the discrete frequency spectrum provided the basis upon which further testing of sound levels using multiple frequency band analysis was restricted to the 2-8 kHz band range.

The results of the experiments performed to evaluate whether the additional data obtained with narrow frequency monitoring could supplement or enhance that obtained with single frequency band analysis will be discussed in conjunction with the single band frequency analysis results in the following section (B2c).

## B. SINGLE FREQUENCY BAND ANALYSIS RESULTS

The experimental results that will be discussed in this section were performed using the equipment detailed in section C part 2 of the Experimental Procedures. This section attempts to examine in further detail the initial



work reported by Watson<sup>12</sup> and include that presented in the publication by Watson and Morrison<sup>13</sup>.

### B1. Breakage Rate and Noise Energy

#### Optimization Results

It has been confirmed by various researchers<sup>37-41</sup> that the specific breakage rate constant ( $K \text{ min}^{-1}$ ) is an energy dependent grinding parameter and that this and other grinding parameters can be optimized.

The purpose of the experimental work that will be discussed here was to investigate the relationships between the noise energy parameter of ANE (absorbed noise energy) and the specific breakage rate constant. The calculation of ANE was determined by the summing the area beneath the balls only sound power value and the sound power value with grind time for the length of the grind. A large number of sound power curves were generated for the experiments in this section, therefore only the numerical relationships between ANE and  $K$  as a function of mill speed, ball loading and feed particle size will be presented.

For the grinding of a single sized feed, a semi-log plot of the fraction unbroken against time enables the calculation of  $K$  to be made. This type of plot was used throughout the experimental work for determination of the breakage rate constant. Figure 22 is a typical example of the data obtained for a dolomite charge which gave a value

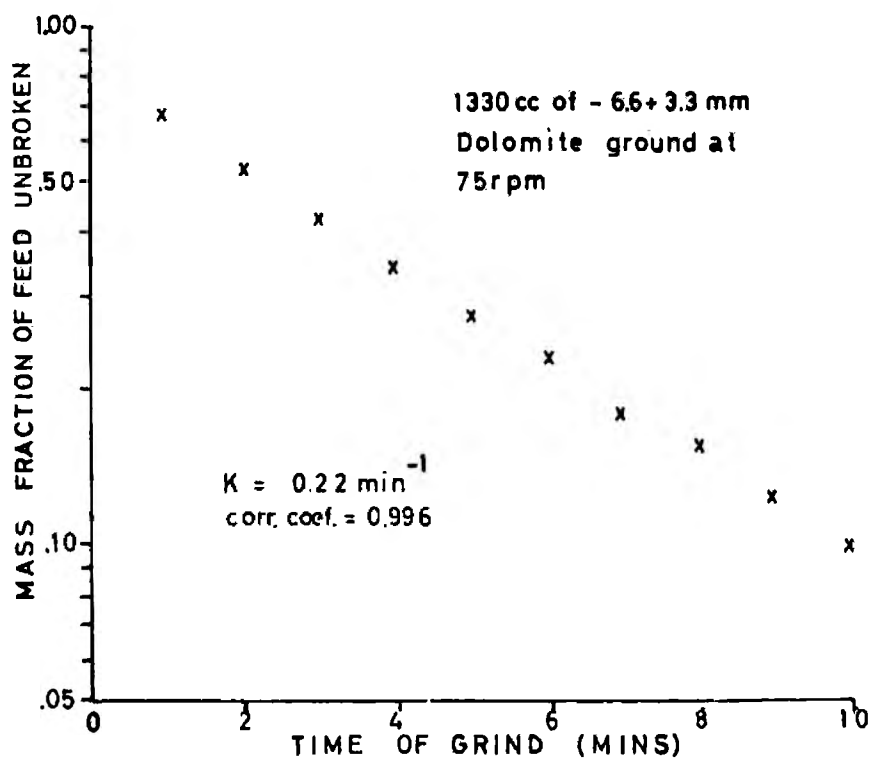


Figure 22. First Order Breakage Kinetics Plot

for K of  $0.22 \text{ min}^{-1}$ .

The relationship between K and ANE for a 10 minute grind of  $-6.6+3.3 \text{ mm}$  dolomite with a standard ball charge as a function of mill speed is presented in Figure 23. This figure illustrates results similar to that found by Herbst and Fuerstenau<sup>38</sup>. They showed that with increasing mill speed the breakage rate constant increases until a maximum is attained. In the present work ANE values for each test increase correspondingly with K until a maximum is approached. This relationship indicates that the noise energy parameter of ANE is directly related to the breakage rate of this material. This relationship is confirmed in Figure 24 where K and ANE are plotted against each other and it can be readily observed that as ANE increases the breakage rate constant also increases. This relationship suggests that absorbed noise energy could be used to evaluate batch mill performance without sizing the mill product.

Another parameter that was investigated to establish relationships between K and ANE was the effect of ball loading. The relationship between K and ANE for 1000 cc of  $-6.6+3.3 \text{ mm}$  dolomite ground for 10 minutes at 65 rpm with ball loadings ranging from 4.5 to 27.0% of the mill volume is presented in Figure 25. It is apparent from this figure that there is a relationship showing an optimum between ball load and K and that the ANE values directly reflect this relationship. For the conditions and materials

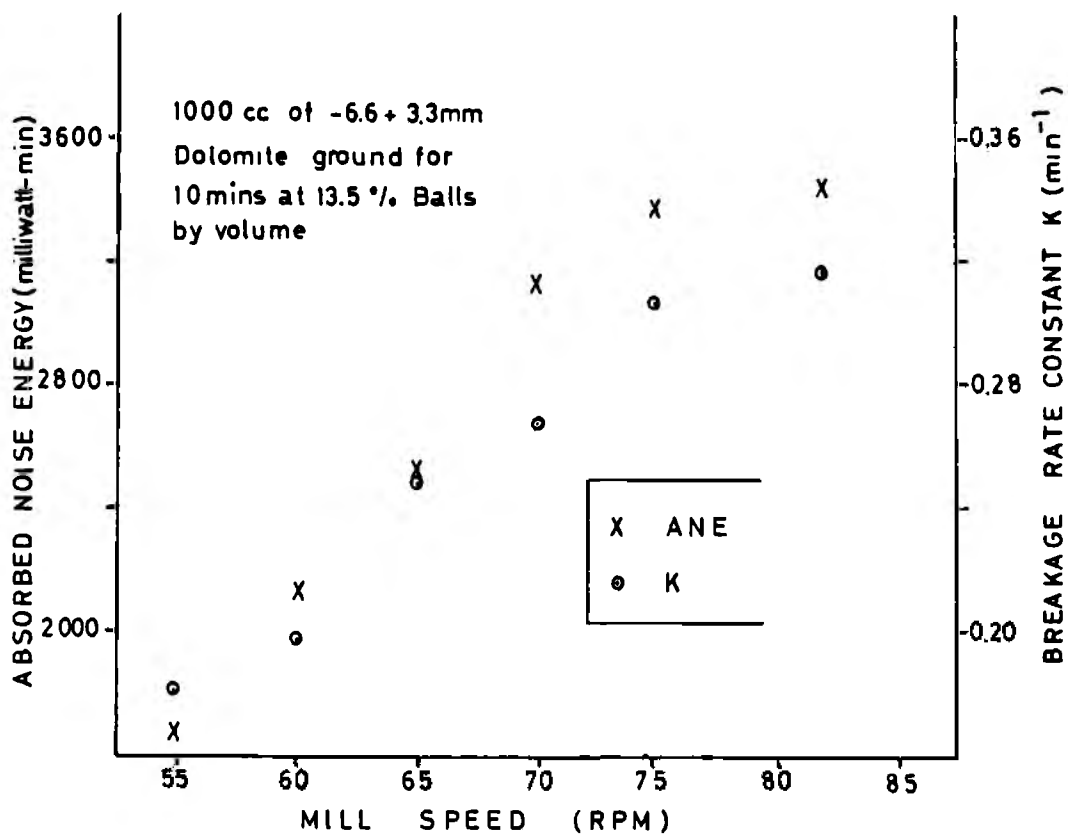


Figure 23. Absorbed Noise Energy and Breakage Rate Variation with Mill Speed for Dolomite

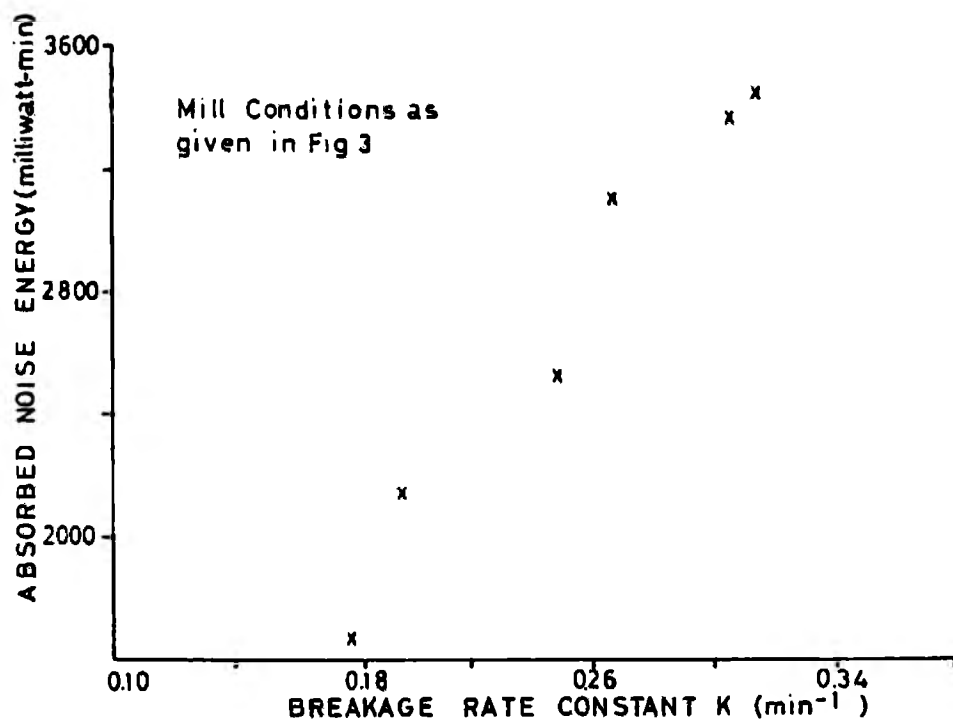


Figure 24. Absorbed Noise Energy Relationships with Breakage Rate for Dolomite (conditions as in Figure 23)

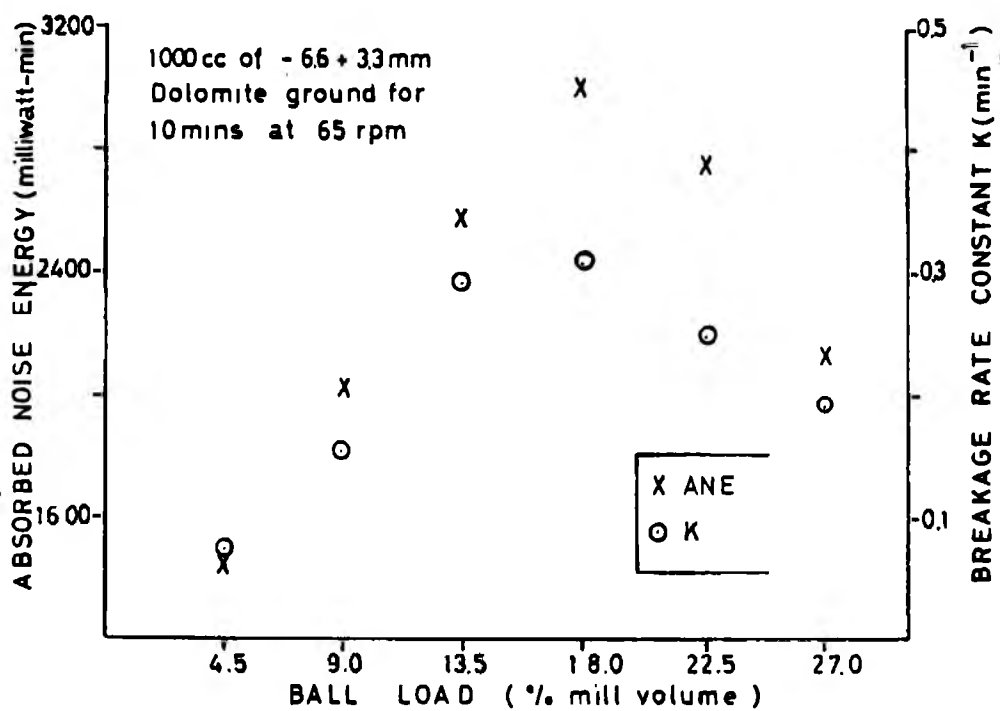


Figure 25. Absorbed Noise Energy and Breakage Rate Variations with Ball Load for Dolomite

described above, the optimum for both K and ANE was found at 18% ball loading by volume. This relationship is further evidenced in Figure 26 where K and ANE are plotted against each other.

In order to establish the effect of ore loading on the relationship between K and ANE, a series of tests were performed under standard operating conditions, using a root two series of feed sizes from 1651 microns down. The ore loading was effectively changed by varying the particle size distribution of the feed but keeping the volume constant at 1000 cc. The relationship between K and ANE for these conditions is presented in Figure 27. The relationship between K and the particle size of the feed conforms with results found by other researchers<sup>38</sup>, in that a coarser feed particle size leads to increasing breakage rates until a maximum is attained after which a decrease is observed. This relationship for the experimental work is illustrated in Figure 27 where K increases with increasing particle size to a maximum of  $0.76 \text{ min}^{-1}$  at 1168 microns and then decreases with the larger particle size. The noise energy parameter of ANE follows the same trend in Figure 27 where it also attains a maximum with the 1168 micron feed size.

In summary, the above results have shown that the ANE values for laboratory batch grinding can reflect the breakage rate parameter K, and assist in identifying the optimum milling conditions as a function of mill speed,

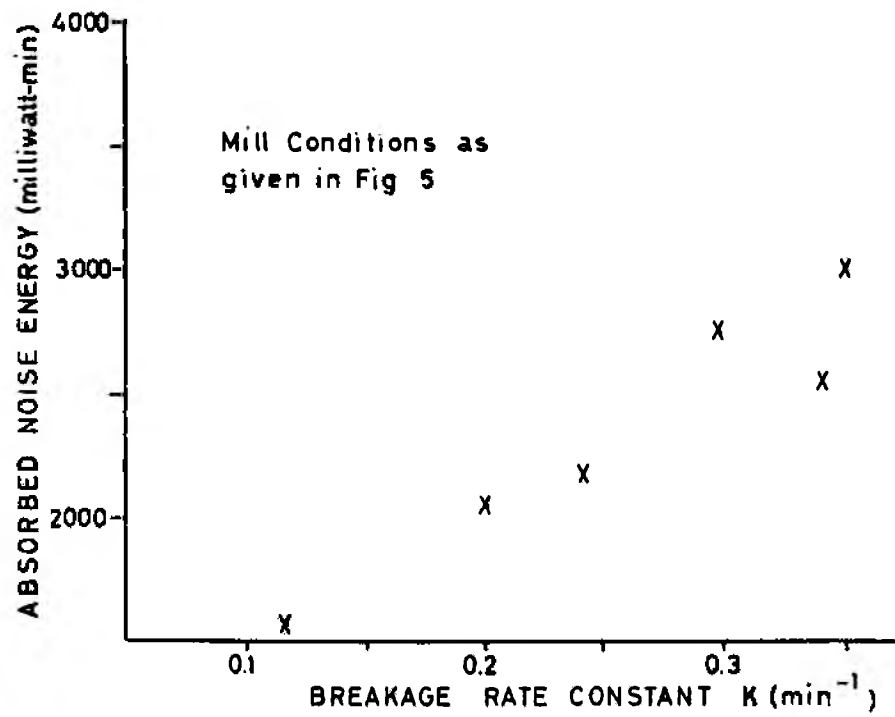


Figure 26. Absorbed Noise Energy Relationships with Breakage Rate for Dolomite (conditions as in Figure 25)



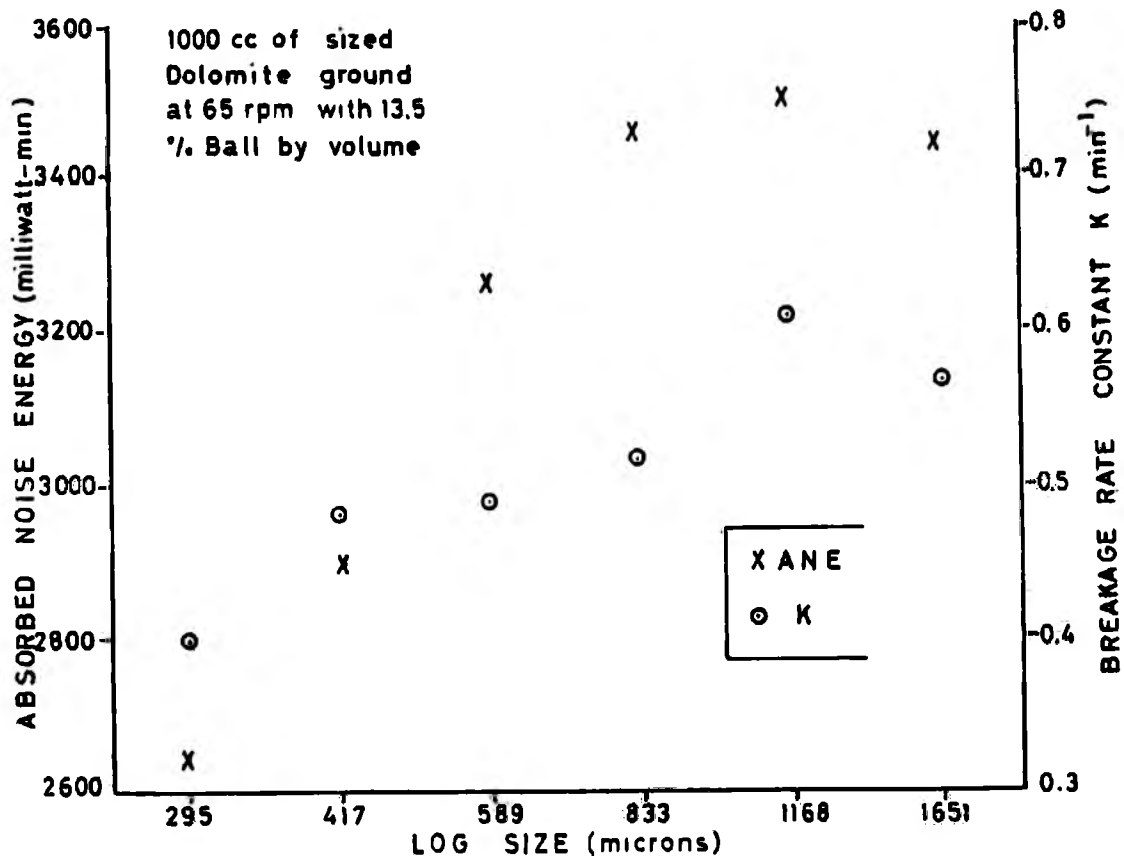


Figure 27. Absorbed Noise Energy and Breakage Variation with Feed Size for Dolomite

ball and charge loading. These relationships would suggest that mill noise parameters could be used as an on-line production parameter for a batch ball mill.

## B2. Particle Size and Noise Energy

### Variation Results

#### B2a. Single Frequency Band Testing

The work by Watson<sup>12</sup> and the experimental work described in the previous section indicate that the sound power values with grind time display an initial decrease to a minimum value and then increase with additional grind time. In order to quantify these changes in sound power values in relation to the size distribution within the mill, a series of tests under standard operating conditions were performed with a charge of -3.3+1.6 mm dolomite.

The sound power value curve and particle size distribution presented in Figure 28 were obtained by stopping the mill at 1 minute intervals and sizing the product. As can be seen in Figure 28 the middle sized particles (-417+295 microns) display a maximum value at the time interval corresponding to the minimum in sound power value. The coarse particles decrease exponentially with the initial decrease in sound power values and the fine particles continuously increase linearly. This suggests that the middle sized particles have the greatest effect on

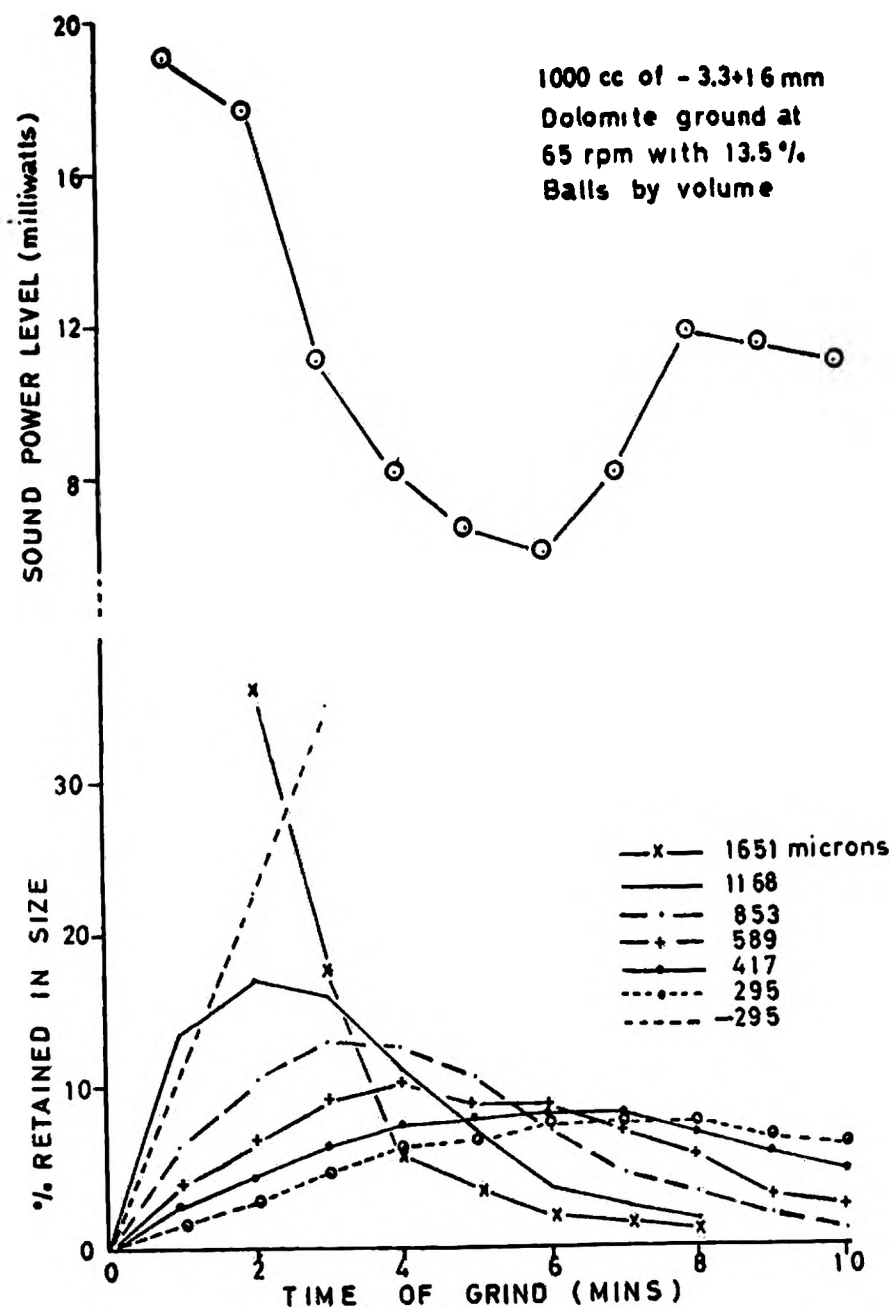


Figure 28. Sound Level and Size Variations with Grind Time for Dolomite

ball/liner collisions and hence ANE. The increase in sound power values continues after the middle sized particles are gone. This suggests that the fine particles may play an important role in absorbed noise energy from the standpoint that the rate at which these particles are produced will determine the rapidity and extent of the sound power value increase.

#### B2b. Particle Damping Tests

As discussed above, the particle size distribution of the mill charge can be related to the sound power values during grinding. The graphical representation of this was seen in Figure 28. At the minimum in sound power values which in this case was approximately 6 minutes, it is proposed that the particles in the mill are of a critical distribution, namely that the size and number of the particles present maximize the blocking of ball/liner collisions. To substantiate this conclusion a series of tests was performed to determine what the damping effects of a 2 cm layer of particles would be on the acoustic and vibrational response of the mill from the collision of a 2.5 cm ball. These experiments were performed by the equipment detailed in section C part 1c of the Experimental Procedures.

The vibrational responses of the mill in  $m/sec^2$ , for the frequency range 0-10.0 kHz for the collision of a

2.5 cm ball directly on the mill shell and through a layer of -417+295 micron particles are presented respectively in Figures 29(a) and 30(a). The acoustic sound pressure response in Pascals for the same tests are presented in the (b) section of Figures 29 and 30. Comparison of the vibrational frequency spectrum from the ball collision in Figures 29(a) and 30(a) to the acoustic spectrum for the mill operating under standard conditions in Figure 21, shows that the frequencies present and the overall spectrum shape are similar. These similarities would tend to indicate that some comparisons can be made between static vibrational and dynamic acoustical measurements. The acoustic responses derived from the particle damping tests in Figure 29(b) and 30(b) were not used as repeatability was poor and this is attributed to the very low sound levels emitted from the collisions in comparison to the more directly obtained vibrational response.

The vibrational acceleration values of the individual frequencies 1.5, 2.3, and 3.25 kHz from Table VI are plotted against the particle size of the layer of particles in Figures 31-33. Error bars are used for the presentation of this data to show the large amount of scatter for repeat tests performed. The minimum in acceleration for all three of these frequencies is attained by the collision of the ball through the layer of -417+295 micron sized particles. This corresponds with the same relationship established in Figure 28, where the minimum in sound pressure values is

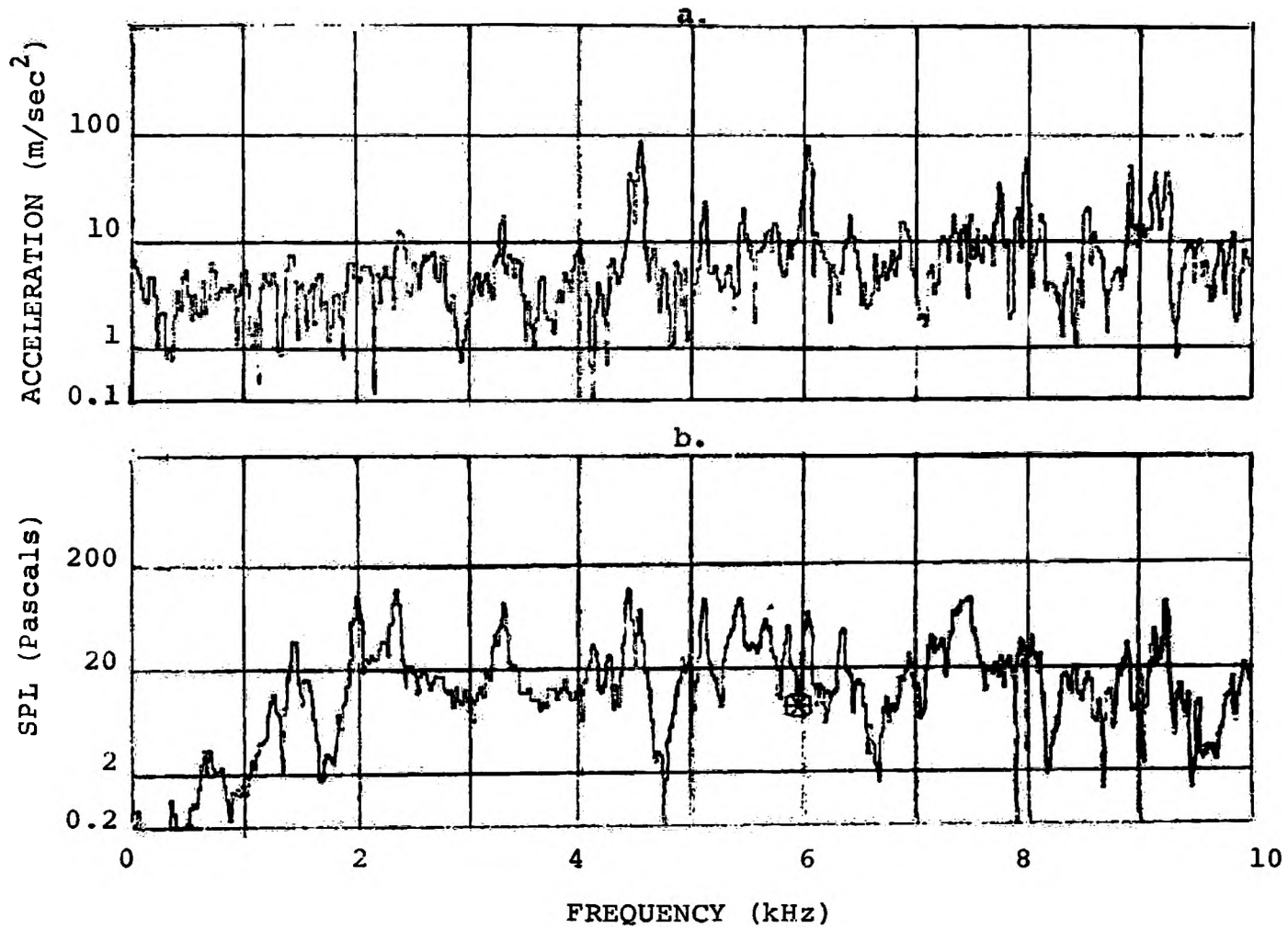


Figure 29. Sound Pressure and Acceleration Frequency Spectra for the Collision of a 2.5 cm Ball on the Mill filled with 125 Balls with No Ore Layer Present

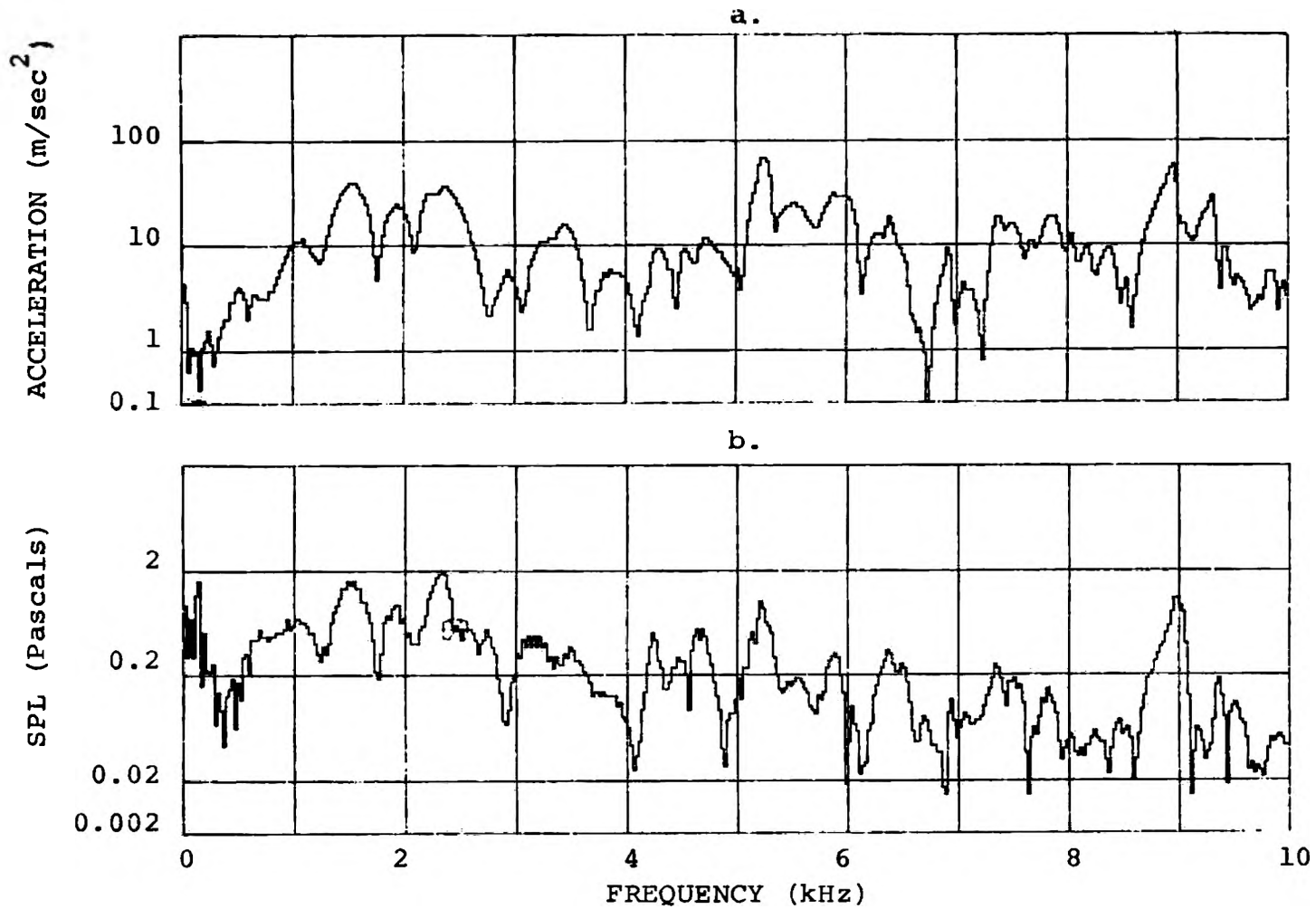


Figure 30. Sound Pressure and Acceleration Frequency Spectra for the Collision of a 2.5 cm Ball on the Mill filled with 125 Balls with a Layer of -417+295 Micron Particles Present

Table VI. Discrete Frequency Acceleration Values for the Collision of a 2.5 cm Ball through a Layer of various Sized Particles

|                                |  | <u>Acceleration (m/(secxsec))</u> |              |                  |              |                   |              |
|--------------------------------|--|-----------------------------------|--------------|------------------|--------------|-------------------|--------------|
| <u>Particle Size (microns)</u> |  | <u>-295</u>                       |              | <u>-417+295</u>  |              | <u>-589+417</u>   |              |
| <u>Frequency (kHz)</u>         |  | <u>Avg.</u>                       | <u>Range</u> | <u>Avg.</u>      | <u>Range</u> | <u>Avg.</u>       | <u>Range</u> |
| 1.5                            |  | 10.8                              | 9.0-15.0     | 1.9              | 0.9-4.0      | 2.5               | 2.0-3.0      |
| 2.3                            |  | 11.0                              | 7.0-18.0     | 2.0              | 0.8-3.0      | 2.5               | 1.0-4.0      |
| 3.25                           |  | 3.2                               | 1.5-7.0      | 1.1              | 1.0-1.5      | 1.8               | 1.5-4.0      |
| 4.3                            |  | 1.3                               | 0.8-2.0      | 0.7              | 0.4-1.5      | 2.0               | 1.5-2.5      |
| 5.75                           |  | 2.6                               | 1.0-3.5      | 2.7              | 2.0-3.5      | 4.6               | 2.0-9.0      |
| 7.5                            |  | 1.6                               | 1.0-2.0      | 1.1              | 0.6-1.5      | 2.2               | 0.6-4.0      |
| 9.0                            |  | 1.7                               | 1.0-2.0      | 2.4              | 0.4-5.0      | 3.3               | 1.5-3.5      |
| <u>Particle Size (microns)</u> |  | <u>-859+589</u>                   |              | <u>-1168+859</u> |              | <u>-1651+1168</u> |              |
| <u>Frequency (kHz)</u>         |  | <u>Avg.</u>                       | <u>Range</u> | <u>Avg.</u>      | <u>Range</u> | <u>Avg.</u>       | <u>Range</u> |
| 1.5                            |  | 3.1                               | 2.0-4.5      | 5.4              | 4.0-8.0      | 3.7               | 1.5-5.0      |
| 2.3                            |  | 3.3                               | 2.5-4.0      | 10.4             | 4.0-16.0     | 11.5              | 5.0-15.0     |
| 3.25                           |  | 2.3                               | 1.0-3.0      | 5.4              | 4.0-8.0      | 8.2               | 3.0-12.5     |
| 4.3                            |  | 3.0                               | 2.5-4.0      | 7.4              | 3.0-12.0     | 15.5              | 10.0-20.0    |
| 5.75                           |  | 4.0                               | 1.0-10.0     | 10.0             | 8.0-20.0     | 15.0              | 10.0-20.0    |
| 7.5                            |  | 1.8                               | 0.9-3.0      | 4.4              | 2.0-8.0      | 6.0               | 2.5-10.0     |
| 9.0                            |  | 2.6                               | 1.5-3.0      | 7.0              | 2.0-8.0      | 6.0               | 3.0-12.5     |
| <u>Particle Size (microns)</u> |  | <u>-3360+1651</u>                 |              | <u>No Ore</u>    |              |                   |              |
| <u>Frequency (kHz)</u>         |  | <u>Avg.</u>                       | <u>Range</u> | <u>Avg.</u>      |              |                   |              |
| 1.5                            |  | 11.4                              | 2.0-15.0     | 110              |              |                   |              |
| 2.3                            |  | 19.0                              | 15.0-20.0    | 125              |              |                   |              |
| 3.25                           |  | 14.4                              | 10.0-25.0    | 200              |              |                   |              |
| 4.3                            |  | 20.0                              | 10.0-30.0    | 800              |              |                   |              |
| 5.75                           |  | 20.2                              | 6.0-30.0     | 125              |              |                   |              |
| 7.5                            |  | 12.2                              | 6.0-20.0     | 100              |              |                   |              |
| 9.0                            |  | 10.8                              | 3.0-20.0     | 200              |              |                   |              |



attributed to presence of middle sized particles.

Additional supporting evidence for the explanation of the initial decrease, and subsequent increase in the noise levels being related to the disappearance of coarse and production of fine particle can also be found in the data from 3 frequencies plotted in Figures 31-33. This is seen by observing the decrease in the vibrational response with decreasing particle size from the top size and increasing values with the finest particle size (-295 microns). Thus, further evidence is provided that the size and number of particles present can be related to the variation in noise levels during grinding for this material.

#### B2c. Discrete Frequency Analysis

The decrease observed in the level of the discrete vibrational frequencies with decreasing particle size evaluated for the particle damping tests suggested that the study of these frequencies on a dynamic acoustical basis could possibly provide additional sound power information. In an effort to ascertain whether there was any discrete acoustic frequency that might better reflect the qualitative changes in sound levels and thus particle size distribution, a -3.3+1.6 mm dolomite charge was ground for 10 minutes under standard conditions. These tests were performed by the equipment detailed in section C part 1b of the Experimental Procedures.

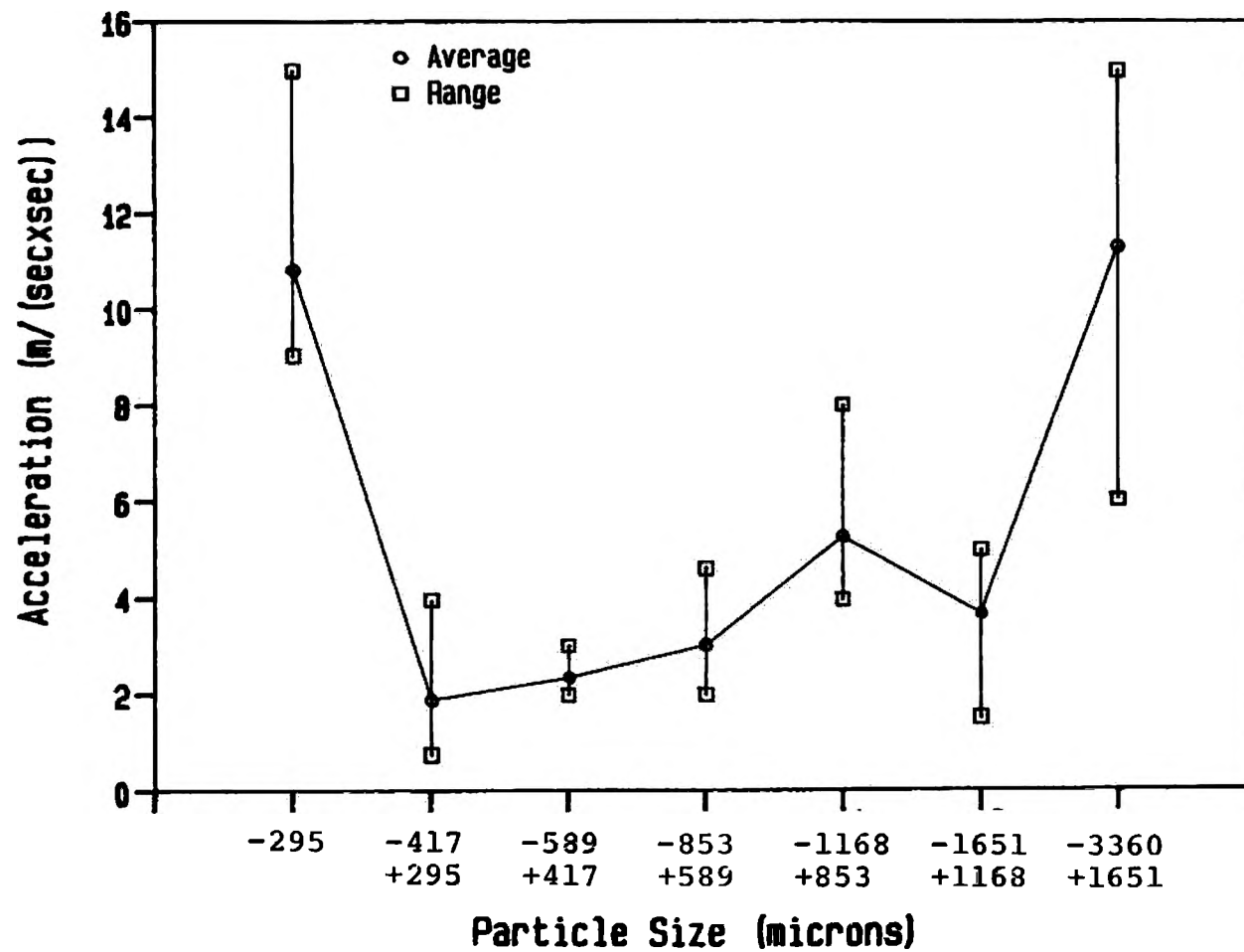


Figure 31. Acceleration Variation Relationships with Particle Size for 1.5 kHz

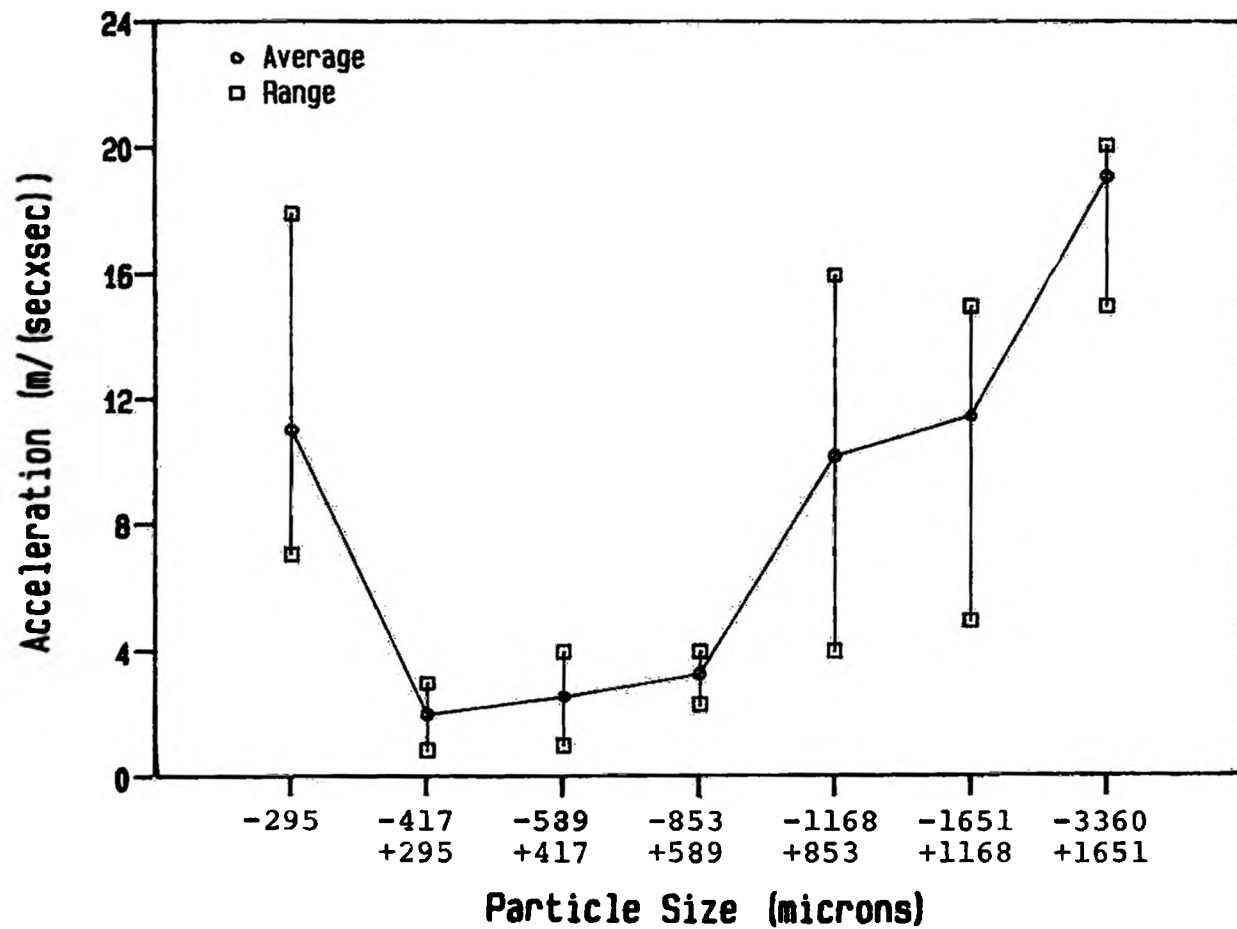


Figure 32. Acceleration Variation Relationships with Particle Size for 2.3 kHz

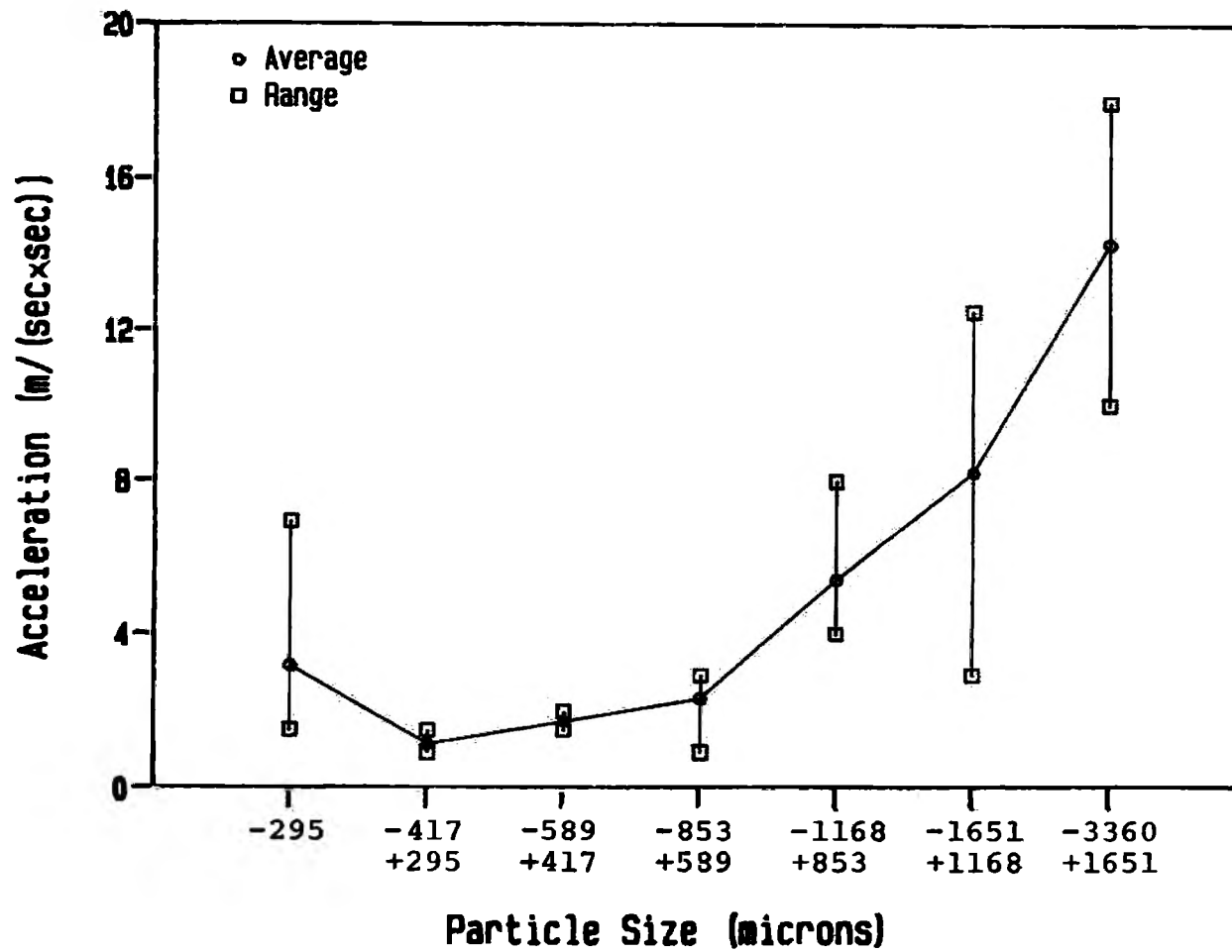


Figure 33. Acceleration Variation Relationships with Particle Size for 3.25 kHz

A spectrum of the sound pressure values was obtained at the time intervals seen in Table VII. Due to the large amount of data obtained similar to Figure 21, only individual frequencies have been presented in tabular and graphical form. As can be seen in Figures 34-35, there are some similarities with the 8 kHz frequency band sound power value with time as shown in Figure 28. A comparison of these curves reveals that for the same grinding conditions the discrete sound pressure values show a similar initial decreasing trend, but the frequency band analysis provides a better reflection of the sound levels with time using sound power. This is illustrated by the much smoother characteristics of the single frequency band sound power with grind time curve. The variability of the discrete frequency sound pressure curves was eliminated in the frequency band analysis because of the averaging with band analysis. As a result of this variability with discrete frequency analysis, further testing to try to establish relationships with grinding parameters using this method was abandoned and the analysis of frequency band sound power was considered to more adequately reflect these relationships.

### B3. Ore Character and Noise Energy

#### Variation Results

The experimental work presented in this section was

Table VII. Discrete Frequency Sound Pressure Values with Grind Time

Test Parameters

1000 cc -3.3+1.6 mm Dolomite  
 10 Minute Grind Time  
 65 RPM  
 125 2.54 cm Balls

| Freq.<br>kHz. | <u>Time</u>                                   |                |                |                |              |                |               |               |
|---------------|---|----------------|----------------|----------------|--------------|----------------|---------------|---------------|
|               | <u>30 Sec</u>                                 | <u>1.5 Min</u> | <u>3.0 Min</u> | <u>4.5 Min</u> | <u>6 Min</u> | <u>8.5 Min</u> | <u>10 Min</u> | <u>No Ore</u> |
|               | <u>R.M.S. Sound Pressure Values (Pascals)</u> |                |                |                |              |                |               |               |
| 1.3           | 0.1   | 0.11           | 0.1            | 0.09           | 0.11         | 0.16           | 0.17          | 0.5           |
| 2.0           | 0.34  | 0.3            | 0.34           | 0.29           | 0.34         | 0.29           | 0.29          | 1.4           |
| 2.25          | 0.34  | 0.38           | 0.38           | 0.23           | 0.27         | 0.34           | 0.38          | 1.2           |
| 2.4           | 0.74  | 0.65           | 0.56           | 0.47           | 0.56         | 0.65           | 0.8           | 2.8           |
| 3.25          | 0.83  | 0.83           | 0.65           | 0.74           | 0.56         | 0.74           | 0.7           | 3.0           |
| 4.3           | 0.81  | 0.65           | 0.56           | 0.45           | 0.55         | 0.58           | 0.52          | 2.3           |
| 5.0           | 0.27  | 0.24           | 0.15           | 0.11           | 0.1          | 0.16           | 0.17          | 1.0           |
| 5.1           | 0.2   | 0.15           | 0.074          | 0.074          | 0.074        | 0.09           | 0.092         | 0.84          |
| 5.8           | 0.3   | 0.43           | 0.2            | 0.2            | 0.23         | 0.2            | 0.2           | 1.2           |
| 6.6           | 0.28  | 0.2            | 0.15           | 0.11           | 0.15         | 0.09           | 0.13          | 0.5           |
| 6.8           | 0.3   | 0.2            | 0.2            | 0.18           | 0.14         | 0.13           | 0.11          | 0.65          |
| 7.5           | 0.34  | 0.3            | 0.25           | 0.16           | 0.25         | 0.25           | 0.29          | 1.85          |
| 7.8           | 0.34  | 0.43           | 0.33           | 0.25           | 0.34         | 0.38           | 0.34          | 1.2           |

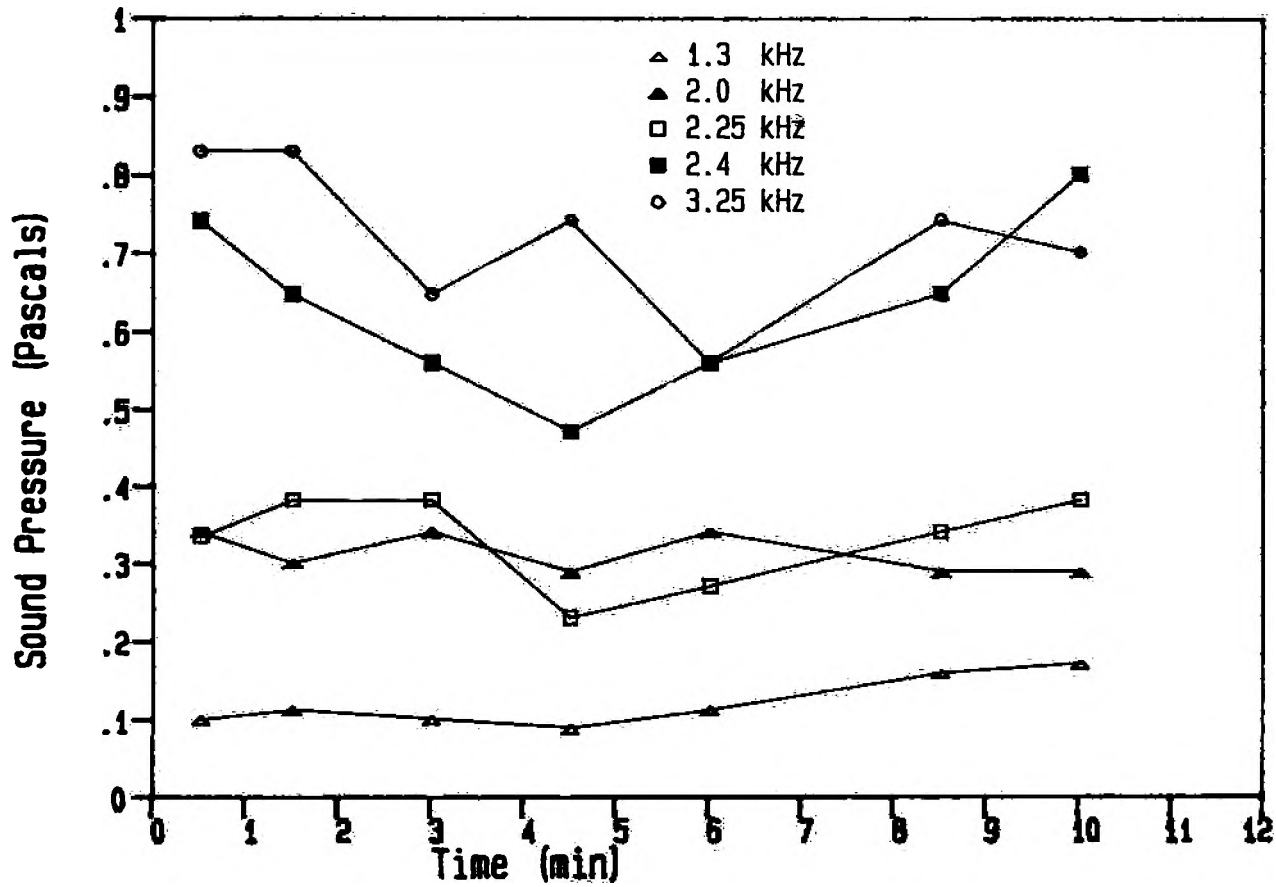


Figure 34. Sound Pressure Variation with Grind Time for various Discrete Frequencies

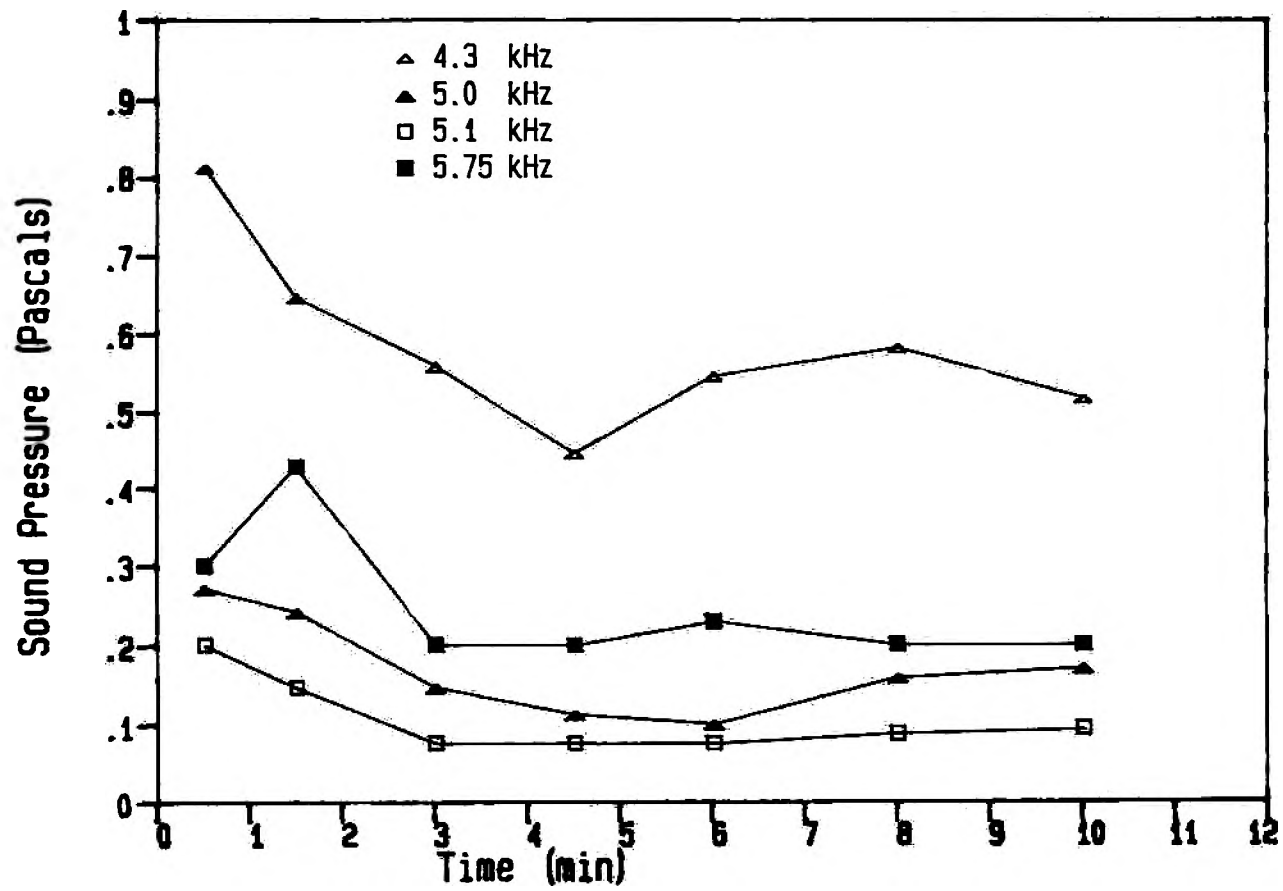


Figure 35. Sound Pressure Variation with Grind Time for various Discrete Frequencies



performed as an extension of the work reported by Watson<sup>12</sup>, which suggested that the noise produced by the mill during wet grinding varies with ore character. This previous work showed that an overall weak relationship between ANE and ore character did exist. The following discussion of further experimental work will reveal how the DANE noise energy parameter was used to better define these relationships. The evaluation of the absorbed noise energy parameter of DANE is performed similarly to ANE by summing the area between an artificial baseline (which is nearer in absolute value to the experimental sound power values) and the sound power values with grind time.

In these tests, five materials were ground dry under standard conditions and four were ground wet at 64% solids by weight at the same volume as the dry tests (1000 cc). These tests were undertaken to perform comparisons between the noise energy parameter of ANE and DANE, and the size reduction parameters of product weight % -104 micron, grams of -104 microns material produced, and theoretical size distributions.

The sound power values with grind time for the dry grinding of five materials are presented in Figure 36. With the exception of the curve for dolomite all the curves have a similar shape with the sound power values still decreasing after 10 minutes. The size distributions of the ground products of these tests on Rosin-Rammler scales are presented in Figure 37 and conform well to the mathematical

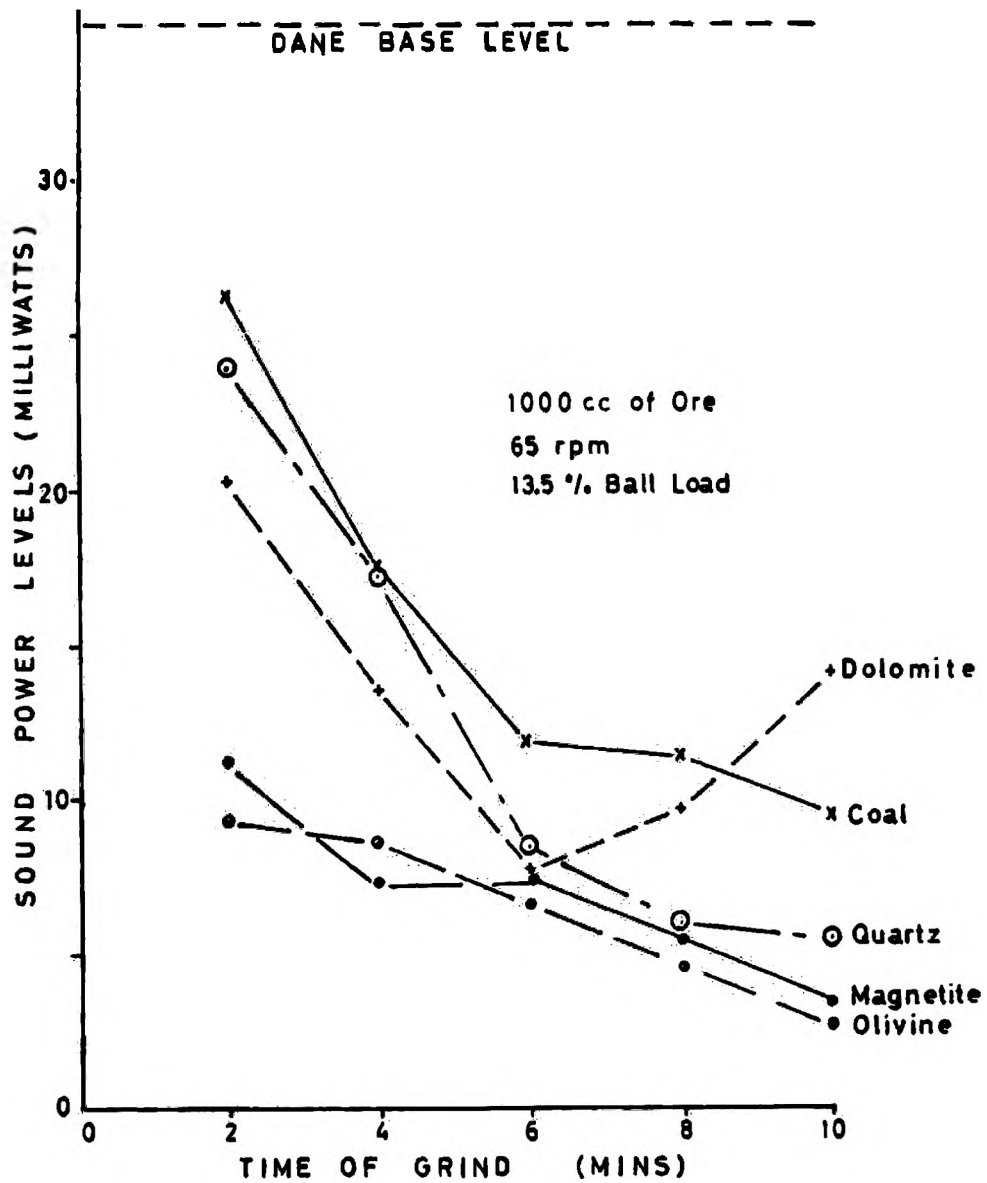


Figure 36. Sound Power Variation with Grind Time for Dry Grinding

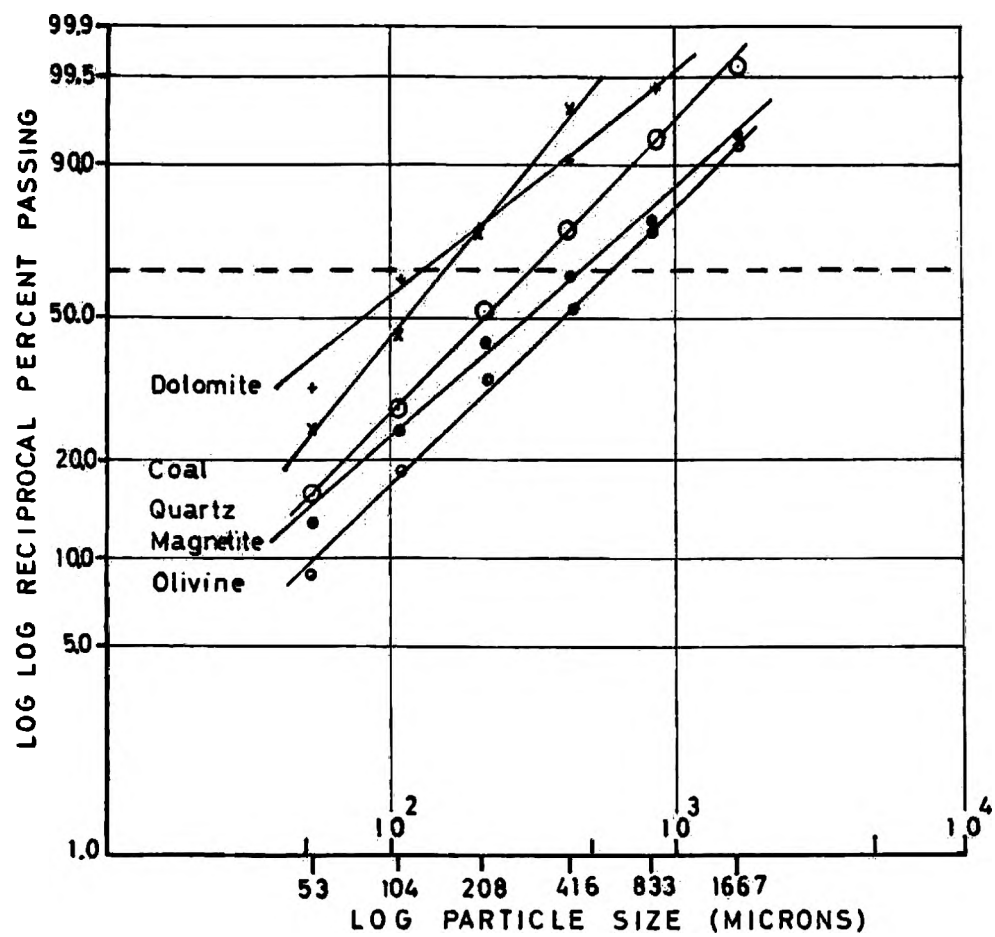


Figure 37. Rosin-Rammler Size Distribution Plots for Dry Grinding

distribution;

$$W_r = 100\exp-(X/M)^N \quad (18)$$

where  $W_r$  is the cumulative weight % retained on the screen size  $X$ ,  $M$  is the Rosin-Rammler mean, and  $N$  is the distribution modulus.

By comparing the relative positions of the five materials in Figure 36 and 37 it is evident that there are similarities between the sound power values and particle size distributions. This relationship is further identified in Table VIII which presents the data from Figures 36 and 37 in tabular form. The ANE values presented in Table VIII show no relationship with the distribution data but the DANE values do correspond in relative terms to the particle size distributions. The ANE values do not correlate well because of the extremely large area generated by the noise differences between the balls only sound power baseline and the grinding sound power values. This large area effectively overshadows the change that can be seen by the use of an artificial baseline closer in absolute value to the actual sound power values of the experimental grind.

The relationship between DANE and grinding reveals that as DANE decreases grinding increases. The olivine values show the lowest sound power values in reference to the arbitrary baseline of 35 milliwatts (and hence highest DANE) and has the coarsest distribution as can be seen in Figure 37 and according to a parameter (G) which combines the two Rosin-Rammler constants according to the equation;

Table VIII. Comparison of Sound and Size Parameters for  
Dry Grinding

|                           | Coal  | Olivine | Magnetite | Dolomite | Quartz |
|---------------------------|-------|---------|-----------|----------|--------|
| <u>Sound Data</u>         |       |         |           |          |        |
| ANE                       | 2788  | 2874    | 3000      | 3083     | 3334   |
| DANE                      | 159   | 239     | 237       | 188      | 193    |
| <u>Grind Data</u>         |       |         |           |          |        |
| Wt. % -53 micron          | 25.2  | 8.1     | 12.6      | 32.7     | 15.1   |
| Wt. % -104 micron         | 46.0  | 18.2    | 25.6      | 62.5     | 28.1   |
| Grams -104 micron         | 283   | 272     | 574       | 792      | 348    |
| <u>Rosin-Rammler Data</u> |       |         |           |          |        |
| Slope N                   | 1.21  | 0.96    | 0.86      | 0.81     | 1.01   |
| Mean M                    | 151   | 560     | 460       | 130      | 310    |
| Corr. Coef.               | 0.999 | 0.998   | 0.995     | 0.988    | 0.999  |
| Grind Parameter G         | 5.4   | 1.9     | 2.5       | 9.5      | 3.2    |

$$G = 1000/(N \times M) \quad (19)$$

The DANE parameter for magnetite and quartz show progressively decreasing values and correspondingly the particle size distribution becomes finer, which supports the suggestion that DANE and grinding are inversely related. The noise and size distribution data for the softer materials of dolomite and coal do not conform to the sequential ordering similar to that seen with the harder materials and the intersections of the sound power and size distribution curves make them difficult to separate. The dolomite sound power curve does reach a minimum value which from previous work suggests the presence of fine material and this is substantiated from the data in Table VIII.

The extreme difference in the density of coal in relation to the other material could have possibly altered the fluidity characteristics of the charge sufficiently to effect the grinding efficiency. Additionally thick coatings of the grinding medium were observed which could possibly contribute to the anomalies observed. Thus it is evident from the data in Table VIII and Figure 36 that while ANE does not reflect ore character, the DANE parameter does appear to, although the sequential ordering for the two softer materials does not conform. Therefore it is suggested that the use of absorbed noise energy in evaluating a simple batch grinding test may provide information similar to that obtained with grindability testing.

The sound power values versus grind time for the four materials subjected to wet grinding are presented in Figure 38. Similarly to the dry grinding curves the relative positions indicate that a difference in material characteristics can be detected. These curves also show that there is an increasing trend towards the end of the grind time. If the hypothesis mentioned earlier for dolomite relating the increase in sound power values to the percentage of fine material, then there should be a larger percentage of finer material in the product of wet tests versus the dry tests. By referring to the standard size distribution plot in Figure 39, it can be seen that indeed the percentages of -104 micron material are greater than those in the dry grinding.

The product of these tests did not conform to any mathematical particle size distribution so only relationships between production of fine particles and noise parameters can be made. The increase in -104 micron material is due, in part, to the decrease in mass of the ore charge for wet grinding as opposed to dry grinding with the same charge volume, but the relative positioning of the data does correlate with the previous results.

A comparison between sound and size parameters is presented in Table IX for the wet grinding tests. The dolomite and olivine results have good agreement between sound and size data with the magnetite and marble data representing intermediate values. The anomaly in the

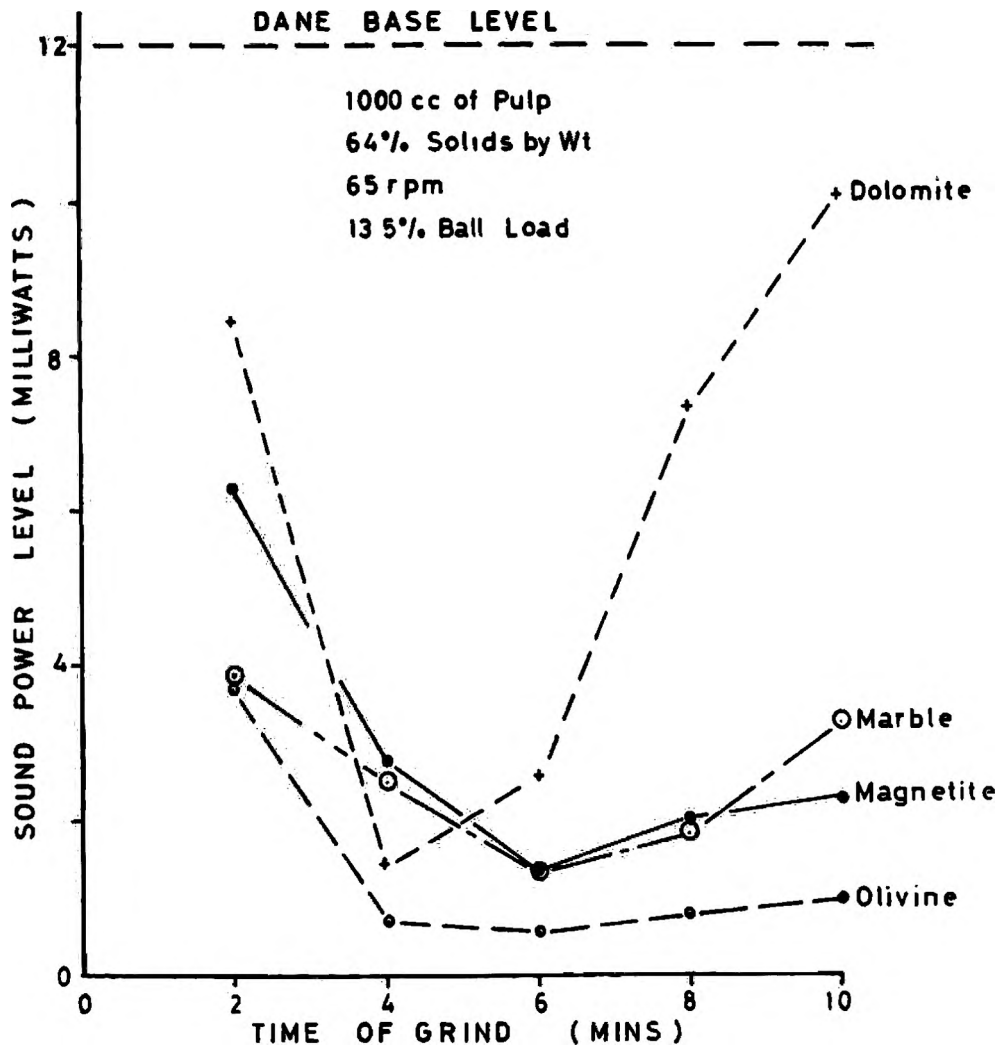


Figure 38. Sound Power Variation with Grind Time for Wet Grinding



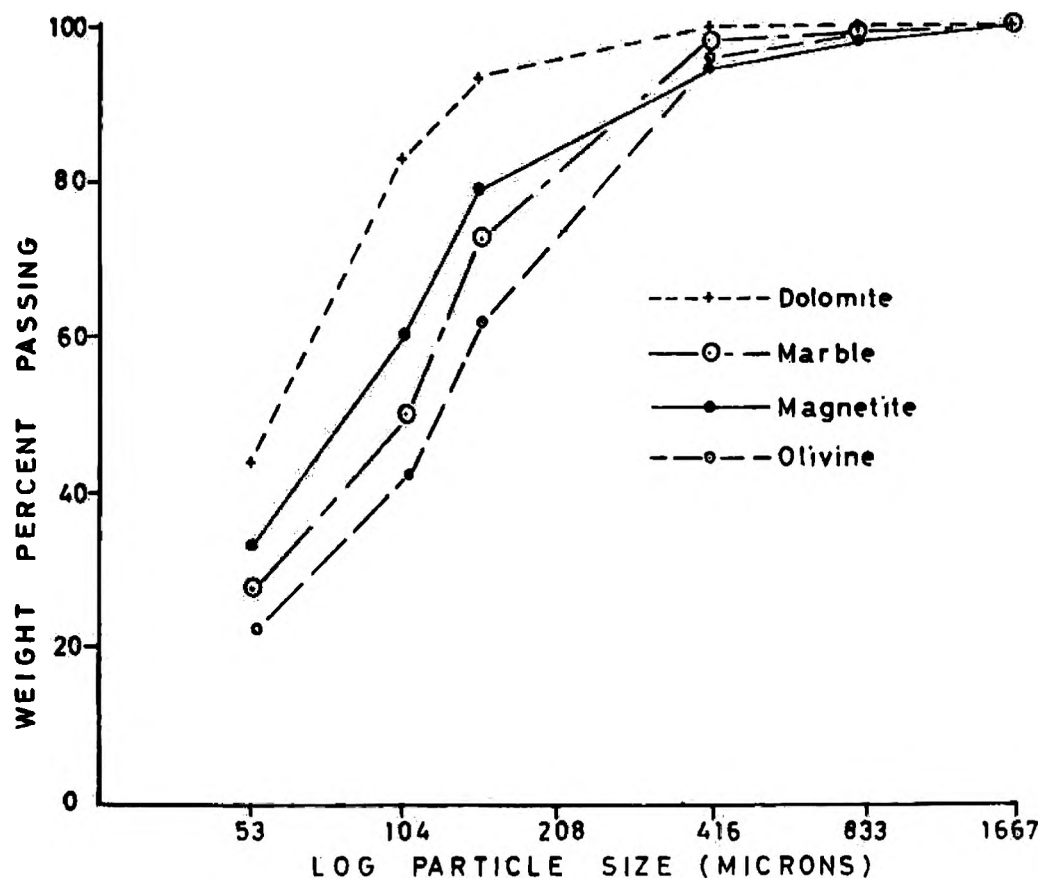


Figure 39. Product Size Distributions for Wet Grinding

Table IX. Comparison of Sound and Size Parameters for Wet Grinding

|                   | Olivine | Magnetite | Dolomite | Marble |
|-------------------|---------|-----------|----------|--------|
| <u>Sound Data</u> |         |           |          |        |
| ANE               | 776     | 742       | 703      | 878    |
| DANE              | 102     | 88        | 66       | 91     |
| <u>Grind Data</u> |         |           |          |        |
| Wt. % -53 micron  | 20.6    | 33.3      | 35.0     | 28.8   |
| Wt. % -104 micron | 42.2    | 60.0      | 78.8     | 50.2   |
| Grams -104 micron | 482     | 795       | 856      | 538    |

sequential positioning of the marble and magnetite data is attributed to the intersection of the sound power curves between 8 and 10 minutes in Figure 38. This causes the slight anomaly in the calculated DANE values for magnetite and marble and puts them in the wrong order in terms of character.

The results presented in Table X show that while reproducibility of the results is acceptable (5%), in terms of sound and size parameters, the noise measurements are performed on a logarithmic scale and errors can be magnified. Differences in sound pressure levels will transform into much larger differences in sound power and absorbed noise energy. Thus problems with reproducibility can arise especially with the measurement of ball/liner-only noise where the dB levels are in excess of 110 and an error of 0.1 dB transforms to only 0.8 milliwatts. Therefore DANE may alleviate some reproducibility problems.

### C. MULTIPLE FREQUENCY BAND ANALYSIS RESULTS

The experimental work presented in this section was performed using the equipment detailed in section C part 3 of the Experimental Procedures. The results presented here include the data from the paper by Watson and Morrison<sup>55</sup>. All experiments in this section were performed at 65 rpm with 125 2.5 cm steel balls.

Table X. Example of Reproducibility of Sound And Size Data for Magnetite Ore

| <u>Test Parameters</u>                |                   |           |               |                                   |                      |                      |                      |
|---------------------------------------|-------------------|-----------|---------------|-----------------------------------|----------------------|----------------------|----------------------|
| 1000 cc -3.3+1.6 mm Dolomite          |                   |           |               |                                   |                      |                      |                      |
| 7 Minute Grind Time                   |                   |           |               |                                   |                      |                      |                      |
| 65 RPM                                |                   |           |               |                                   |                      |                      |                      |
| 125 2.54 cm Balls                     |                   |           |               |                                   |                      |                      |                      |
| <u>Time (Min)</u>                     | <u>Sound Data</u> |           |               |                                   | <u>Size (micron)</u> | <u>Size Data</u>     |                      |
|                                       | <u>Test 1</u>     |           | <u>Test 2</u> |                                   |                      | <u>Test 1</u>        | <u>Test 2</u>        |
|                                       | <u>dB</u>         | <u>mw</u> | <u>dB</u>     | <u>mw</u>                         |                      | <u>Wt. % Ret.</u>    | <u>Wt. % Ret.</u>    |
| 1                                     | 97.1              | 5.18      | 96            | 4.07                              | 1651                 | 5.4                  | 5.1                  |
| 2                                     | 92.2              | 1.67      | 92.7          | 1.88                              | 1168                 | 2.8                  | 2.7                  |
| 3                                     | 91.6              | 1.46      | 89.9          | 0.98                              | 833                  | 1.9                  | 1.9                  |
| 4                                     | 90                | 1.01      | 88.6          | 0.72                              | 589                  | 2.4                  | 2.3                  |
| 5                                     | 88.8              | 0.76      | 91.6          | 1.46                              | 417                  | 3.3                  | 3.3                  |
| 6                                     | 90.3              | 1.07      | 88.4          | 0.94                              | 295                  | 6.5                  | 6.5                  |
| 7                                     | 87.5              | 0.56      | 87.8          | 0.6                               | -295                 | <u>77.3</u><br>100.0 | <u>77.9</u><br>100.0 |
| <u>Absorbed Noise Energy (mw-Min)</u> |                   |           |               | <u>Grinding Rate Constant (K)</u> |                      |                      |                      |
| 389.0                                 |                   |           |               | 381.0                             |                      |                      |                      |
|                                       |                   |           |               | 0.42                              |                      |                      |                      |
|                                       |                   |           |               | 0.43                              |                      |                      |                      |

## Cl. Pulp Viscosity and Grinding

### Additive Results

As mentioned earlier, the work by Klimpel et. al.<sup>46-47</sup> proposed that there is a material specific pulp density at which an optimum viscous regime is established and where grinding is the most effective. Additionally the work by various researchers<sup>44-45</sup> indicated that pulp density, which reflects viscous character, is a crucial factor in grinding efficiency. Considering that the viscous character of the mill pulp could significantly alter the ball/liner collisions, and recognizing that a change in the noise levels associated with these collisions can indicate mill conditions, experimental work was undertaken to establish whether noise measurements could detect differences in effective viscosity of the pulp.

Ores of magnetite and molybdenite were used for this experimental work. The size distribution of these feed materials is presented in Table XI. Both materials have a fairly uniform distribution with the magnetite having a finer overall distribution.

### Cl. Magnetite Ore

The cumulative average (CA) sound power values for the

Table XI. Size Distribution of Magnetite and Molybdenite Feed Ores

| Particle Size<br>(micron) | Magnetite         |                       | Molybdenite       |                       |
|---------------------------|-------------------|-----------------------|-------------------|-----------------------|
|                           | Wt. %<br>Retained | Cum. Wt. %<br>Passing | Wt. %<br>Retained | Cum. Wt. %<br>Passing |
| 1700                      | 0.0               | 100.0                 | 1.5               | 98.5                  |
| 850                       | 15.1              | 84.9                  | 28.3              | 70.2                  |
| 425                       | 19.4              | 65.5                  | 23.3              | 46.9                  |
| 212                       | 17.5              | 48.0                  | 15.1              | 31.8                  |
| 106                       | 18.0              | 30.0                  | 11.5              | 20.3                  |
| 53                        | 14.1              | 15.9                  | 9.6               | 10.7                  |
| -53                       | <u>15.9</u>       | -                     | <u>10.7</u>       | -                     |
|                           | 100.0             |                       | 100.0             |                       |

frequency bands 2-8 kHz with grind time for the magnetite ore at various pulp densities are presented in Figure 40. As detailed in previous experimental work using -6.6+3.3 mm feed, the size range of particles, that would cause the initial reduction in sound levels, is -850+425 microns. In the present work there is little in this size and therefore, the CA sound power values with grind time would be expected to increase continually with grind time, due to the relatively small percentage of the noise reducing particles and their rapid disappearance. Figure 40 shows that the CA sound power values do increase with time and that with increasing percent solids (between 60 and 72%) the CA sound power value rate of increase falls. This is explained by the increasing number of particles in the ore charge capable of blocking ball/liner collisions.

At pulp densities greater than 72% solids the CA sound power values surprisingly are higher in relation to the lower % solids. It would have been expected that the falling rate of increase of CA sound power values would have continued with increasing percent solids. The contrary observation can be attributed to a change in the rheology of the pulp resulting from the increased concentration of solids. This suggestion is supported by the fact that conditions of the grind are held constant and the only variables are orientation and dispersion of the particles in the mill.

The same increasing trends were found for 74, 76, and

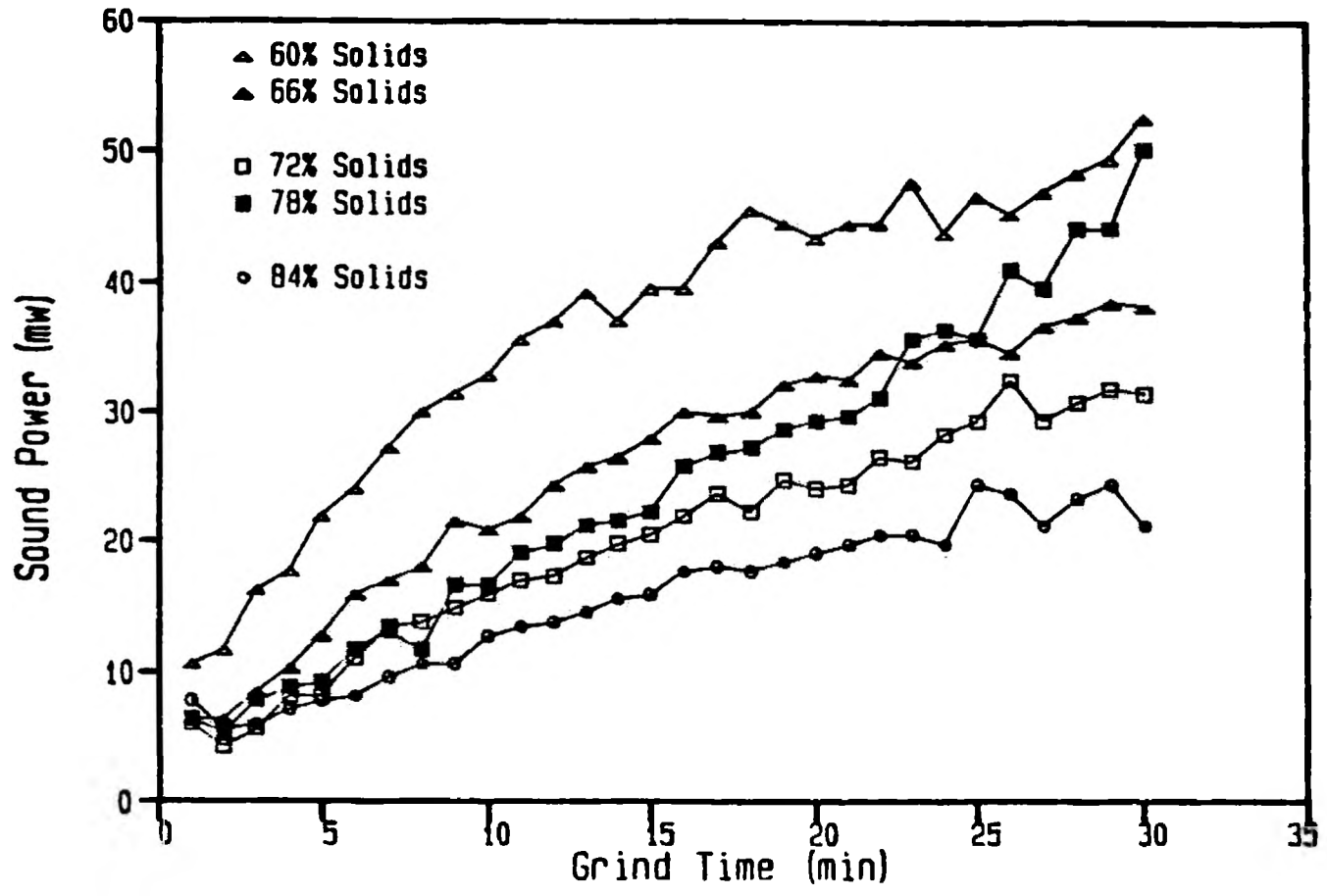


Figure 40. Sound Power Variation with Grind Time for a Magnetite Ore



80% solids. The increases in CA sound power values for 10, 20, and 25 minutes of grind time for all the percent solids tests are presented in Figure 41 which also illustrates a maximum increase in the 78-82% solids range. The increase in CA sound power values beyond 72% solids may be interpreted as a decrease in viscosity, which in altering ball/liner collisions would affect the rate of breakage of particles. As the pulp density is increased beyond 82% solids the CA sound power values start to decrease which is attributed to the pulp exhibiting yield characteristics. This was confirmed upon opening the mill at the higher % solids and finding a portion of the charge and medium stuck to the mill liner.

The variation of DANE with pulp density for the magnetite grinds are presented in Figure 42. This shows that DANE increases with pulp density until 72% solids and then falls to a minimum at 82% solids. Observation of the pulp settling behavior described by Klimpel<sup>42</sup>, and as noted in the research, suggest that the pulp commences a transition from dilatant rheology to pseudoplastic behavior at this range of pulp densities. At 82% solids the transition is complete and at higher pulp densities the pulp exhibits yield characteristics which prevent grinding due to a decrease in ball/liner collisions. These rheology changes are clearly related to the absorbed noise energy variation as presented in Figure 42, with a maximum representing the commencement of pseudoplastic rheology and

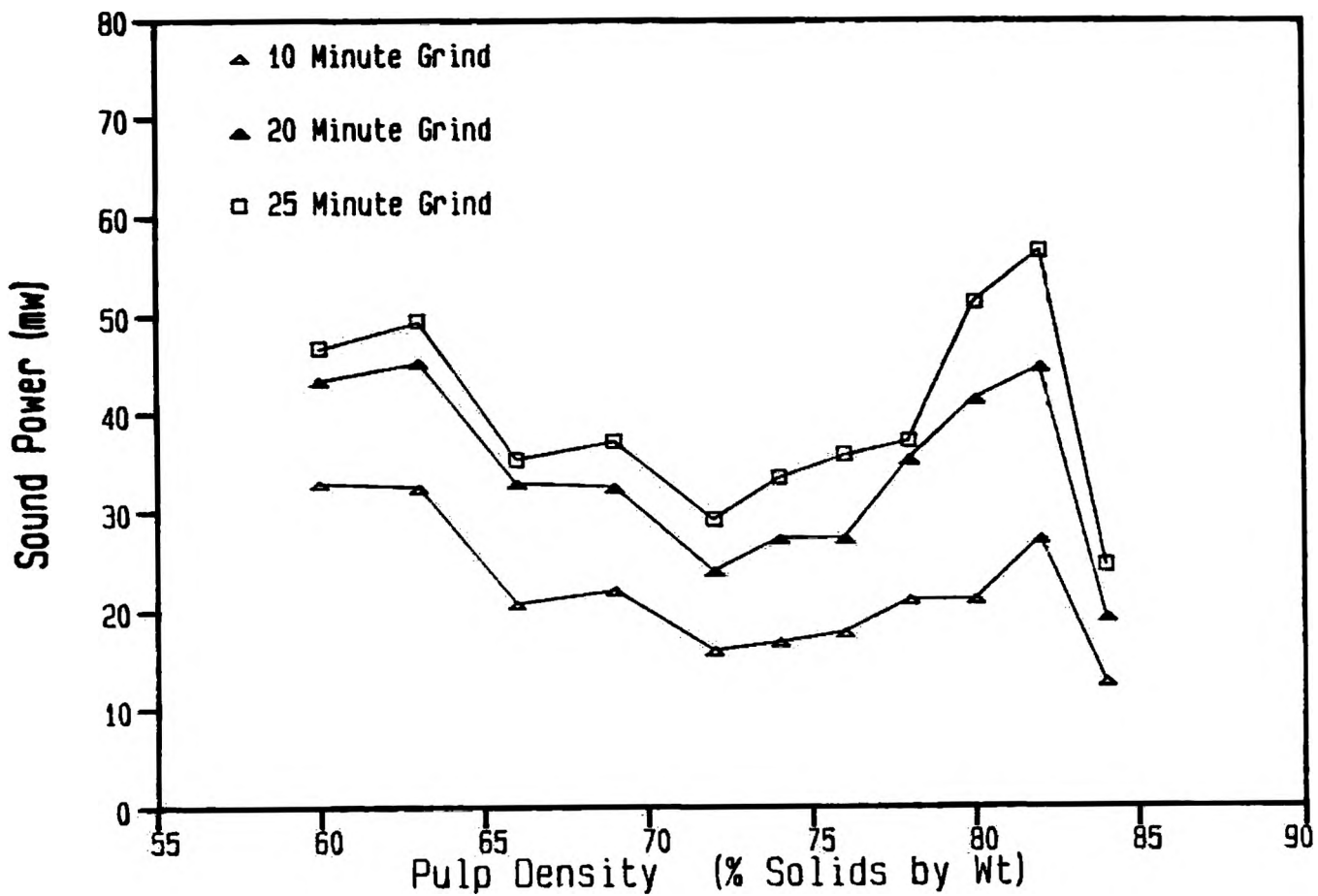


Figure 41. Sound Power Variation as a function of Grind Time and Percent Solids for Magnetite Ore

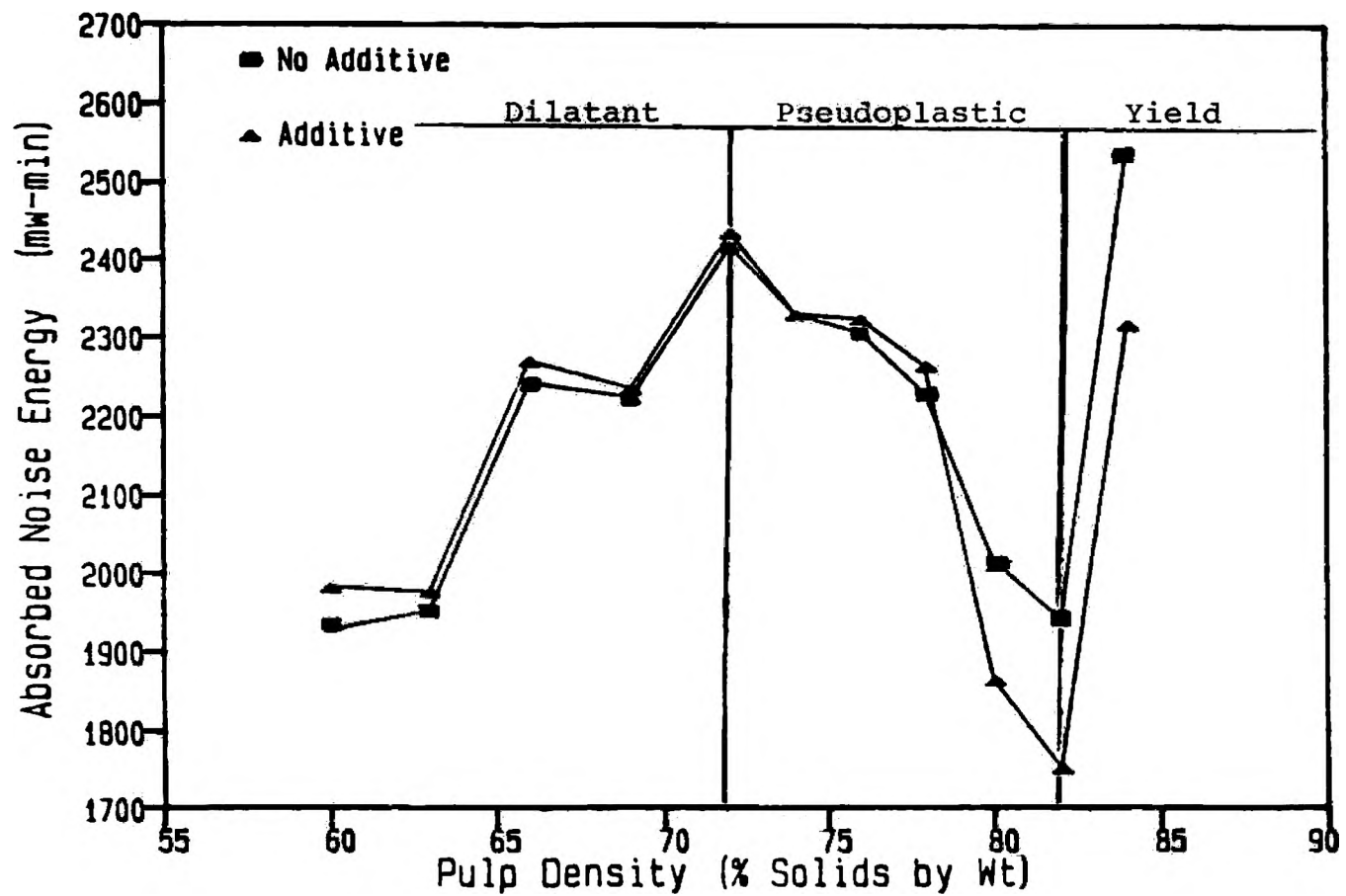


Figure 42. Absorbed Noise Energy Relationships with Pulp Density for a Magnetite with and without a Grinding Additive (NA= No Additive A= Additive)

the minimum equating to the onset of yield.

In order to correlate the rheological and absorbed noise energy relationships with grinding, a parameter similar to that used by Klimpel<sup>46</sup> was determined. Table XII(a) presents the net production of -53 micron material at the different % solids and compares these values to the DANE values. It is apparent from this data and Figure 42 that the production of -53 micron particles is not directly related to the absorbed noise energy but the transitions from dilatant to pseudoplastic to pseudoplastic with yield rheology, as identified by the noise parameter, are reflected in fine particle production. These data suggest that maximum grinding occurs in the pseudoplastic range where the mill CA sound power values are increasing. This increase in grinding can be attributed to the increased fluidity of the charge allowing more effective motion of the grinding medium in the mill and thus a greater number and extent of breakage collisions.

To establish the effect of a grinding additive on the rheological characteristics, noise energy and grinding parameters the tests described above were repeated using 1.25 kg/tonne of a low molecular weight anionic polymer grinding additive. Figures 43 and 44 illustrate the comparison between CA sound power curves from grinding tests at low and high % solids respectively with and without the additive. These plots show that at pulp densities below 80% solids the additive has little effect

Table XII. Fine Particle Production for Magnetite Ore with  
Pulp Density  
a. Without Additive  
b. With Additive

Test Parameters  
1000 cc Pulp  
30 Minute Grind Time  
65 RPM  
125 2.54 cm Balls  
1.25 kg/tonne Additive (b)

(a)

|   |      |      |      |      |      |      |      |      |      |      |      |
|---|------|------|------|------|------|------|------|------|------|------|------|
| Pulp Density                                  |      |      |      |      |      |      |      |      |      |      |      |
| <u>% Solids</u>                               | 60   | 63   | 66   | 69   | 72   | 74   | 76   | 78   | 80   | 82   | 84   |
| Net Production<br>(g) of -53<br><u>micron</u> | 594  | 664  | 619  | 675  | 722  | 719  | 686  | 684  | 696  | 706  | 561  |
| <u>DANE</u>                                   | 1929 | 1955 | 2244 | 2226 | 2416 | 2380 | 2308 | 2231 | 2018 | 1940 | 2540 |

(b)

|   |      |      |      |      |      |      |      |      |      |      |      |
|---|------|------|------|------|------|------|------|------|------|------|------|
| Pulp Density                                  |      |      |      |      |      |      |      |      |      |      |      |
| <u>% Solids</u>                               | 60   | 63   | 66   | 69   | 72   | 74   | 76   | 78   | 80   | 82   | 84   |
| Net Production<br>(g) of -53<br><u>micron</u> | 574  | 609  | 673  | 690  | 678  | 701  | 755  | 738  | 803  | 817  | 693  |
| <u>DANE</u>                                   | 1981 | 1976 | 2272 | 2238 | 2437 | 2327 | 2325 | 2266 | 1864 | 1751 | 2316 |

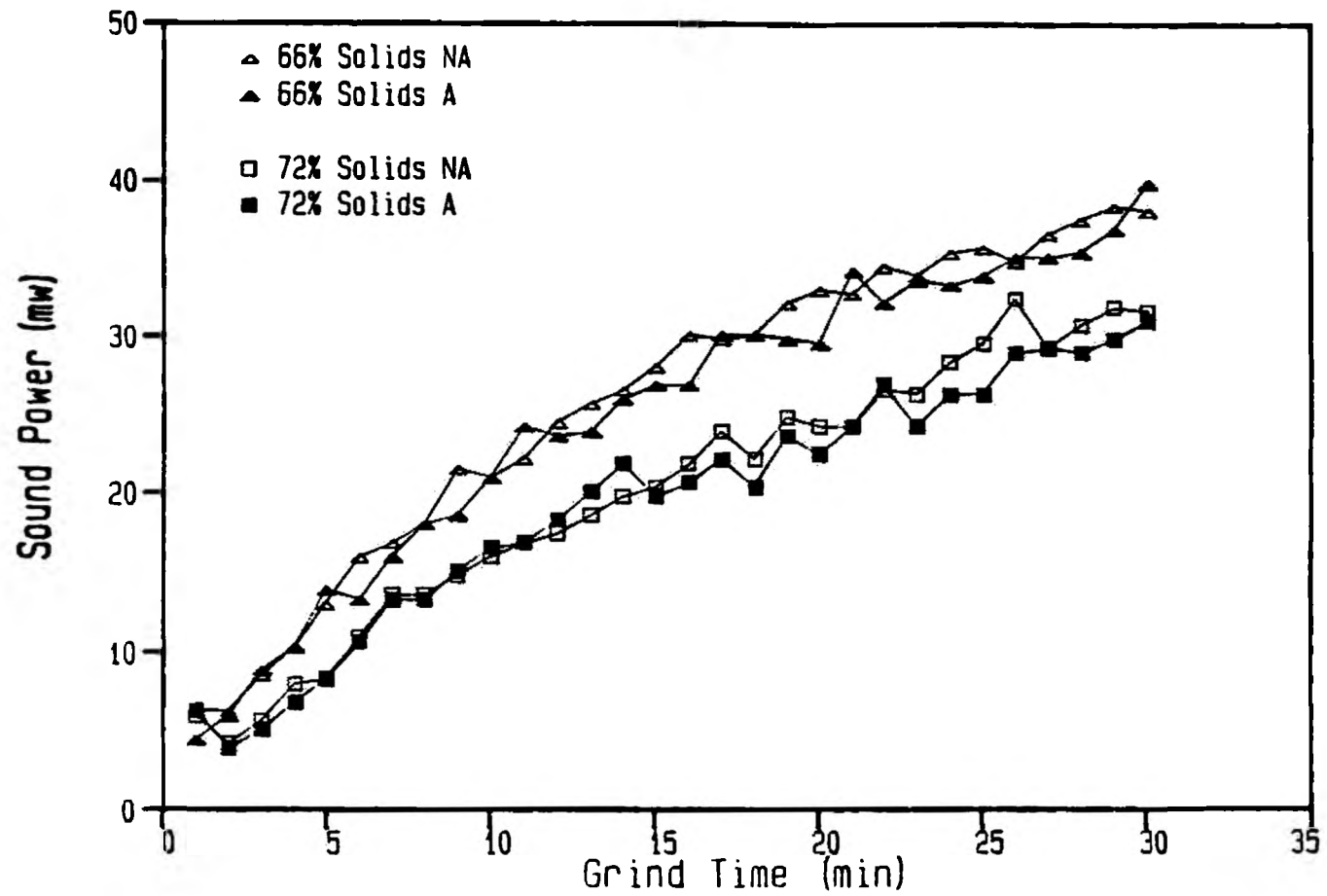


Figure 43. Sound Power Variations with Grind Time for a Magnetite Ore with and without a Grinding Additive

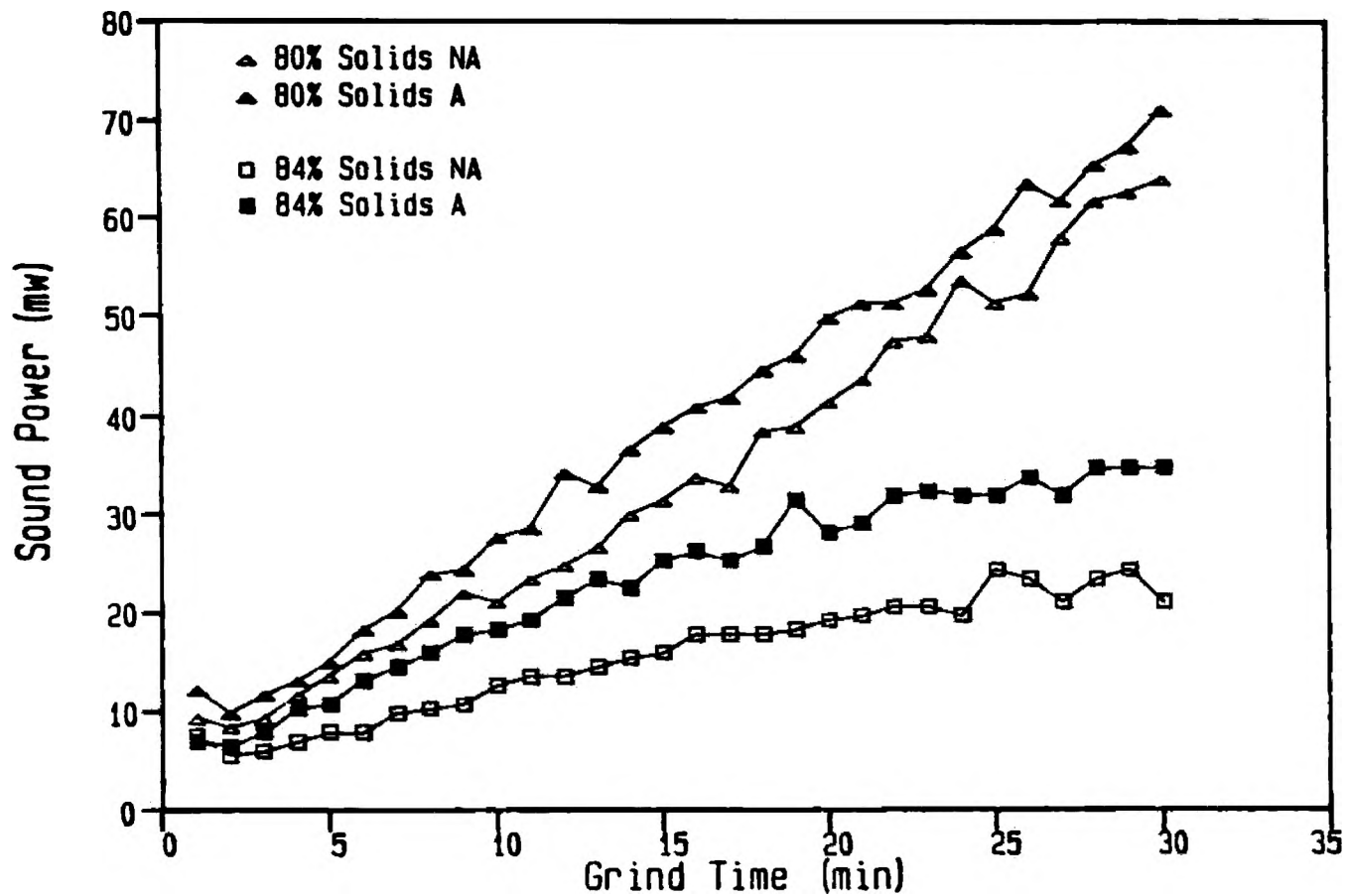


Figure 44. Sound Power Variations with Grind Time for a Magnetite Ore with and without a Grinding Additive at High Pulp Densities

but at levels 80% and greater the tests with the additive show higher CA sound power values. The increase in CA sound power values with the additive present may be explained by a change in rheology of the pulp by the adsorption of the additive on the mineral surfaces as indicated by Klimpel<sup>46</sup>.

In Figure 42 the DANE values for the additive tests show that the energies only differ significantly above 78% solids. Above this percent solids the curve is displaced to lower absorbed noise energy values, which suggests that the additive has modified the transition from dilatant to pseudoplastic and reduced still further the effective viscosity for the pseudoplastic pulp. Table XII(b) presents the net production of -53 micron particles for the additive tests as well as DANE and this shows that the additive has little effect until 76% solids where the fines production at higher pulp densities increases dramatically to a maximum at 82% solids.

The data from Figure 42 and Table XII tend to suggest that the additive has increased the grinding in the pseudoplastic range and the absorbed noise has shown a similar relative decrease. Similarly to the tests with no additive, the absorbed noise is not reflecting the production of particles but does identify the viscous regime where grinding is maximized, and shows that the effect of a grinding additive on these regimes can be detected. As opposed to the overall inverse relationship



between DANE and grinding found with narrow sized feed and single frequency band monitoring, this relationship only holds true for the pseudoplastic range of percent solids. This is because the volume of the solid charge was not held constant as in the single frequency testing.

#### Clb. Molybdenite Ore

The CA sound power curves for the molybdenite ore in Figure 45 show increasing values similar to that seen with the magnetite ore. For this material the maximum CA sound power values were found at 70% solids as shown in Figure 46 which plots CA sound power value versus pulp density for time intervals of 10, 20, and 25 minutes. The overall noise results are presented in Figure 47 where DANE is plotted against percent solids. Similarly to the magnetite DANE results, the variations in DANE for the molybdenite ore, with increasing pulp density in Figure 47, suggests that the transition from dilatant to pseudoplastic occurs at approximately 64% and yield characteristics are displayed above 70%.

The explanation of these relationships is similar to that with the magnetite ore. It is also evident that the pulp density viscous regime relationships are material specific. Table XIII(a) presents the grinding data in net production of -53 micron particles as an indication of grinding performance. Similarly to the results found with

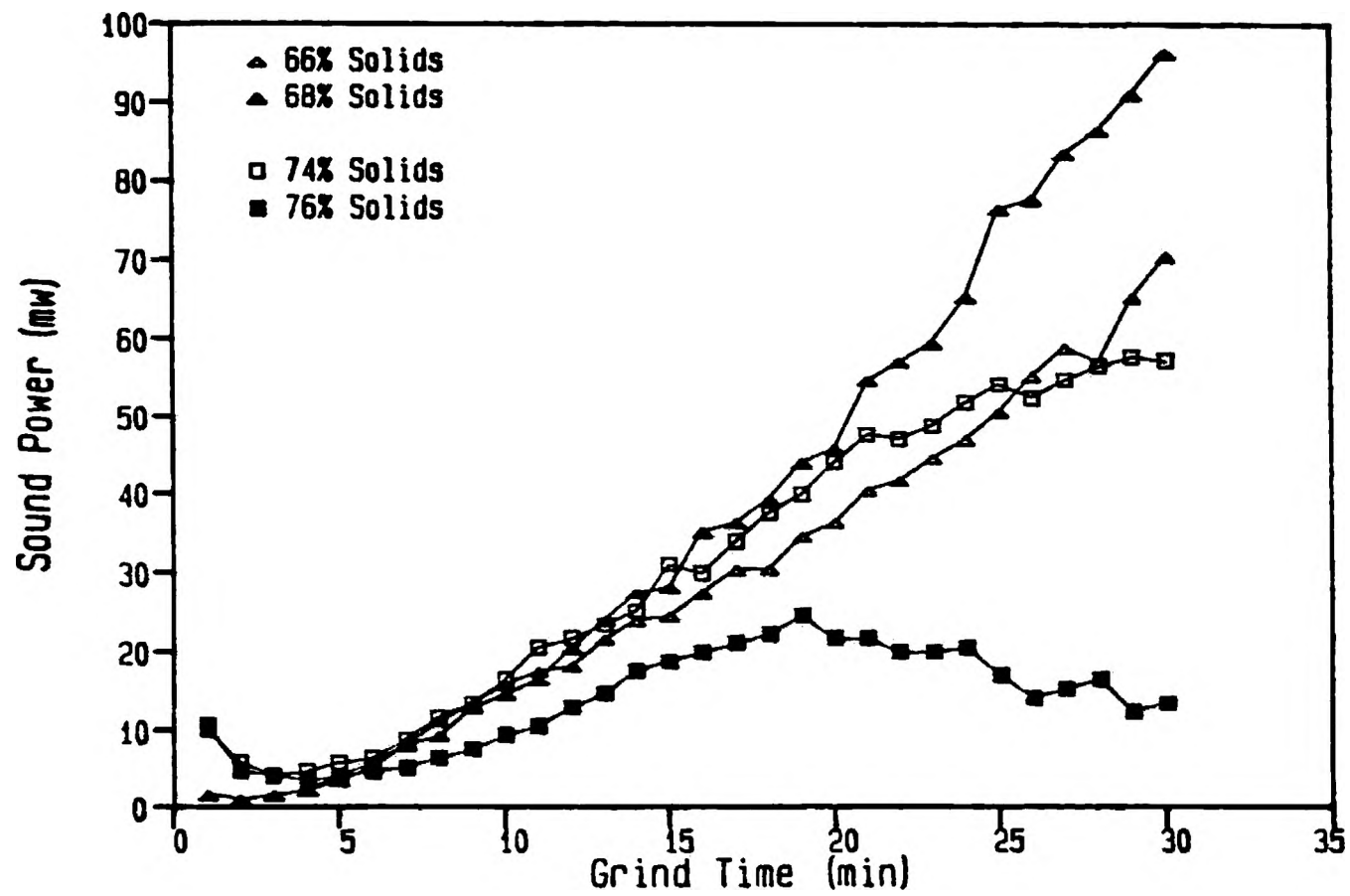


Figure 45. Sound Power Variations with Grind Time for a Molybdenite Ore

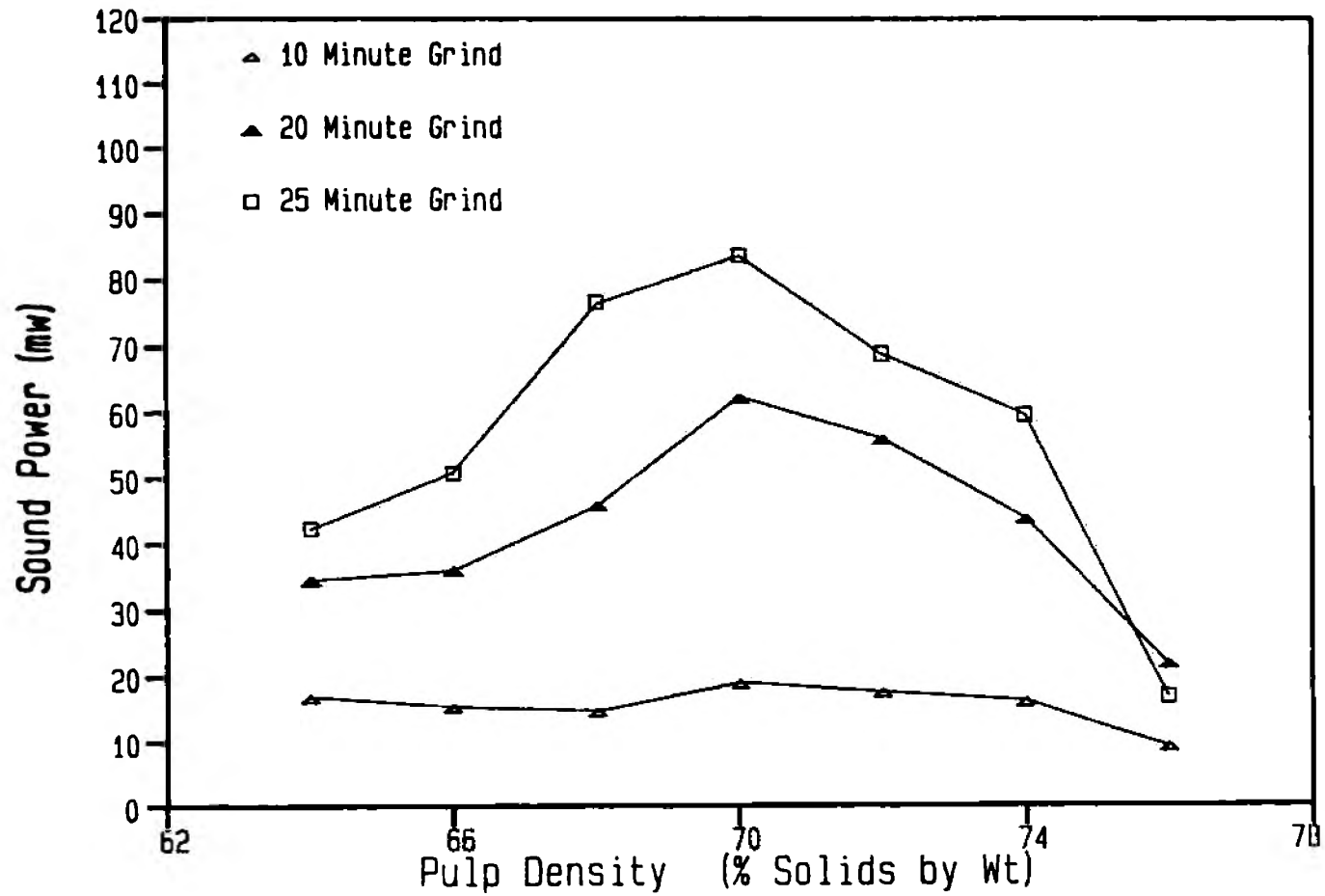


Figure 46. Sound Power Variation as a function of Grind Time and Percent Solids for a Molybdenite Ore

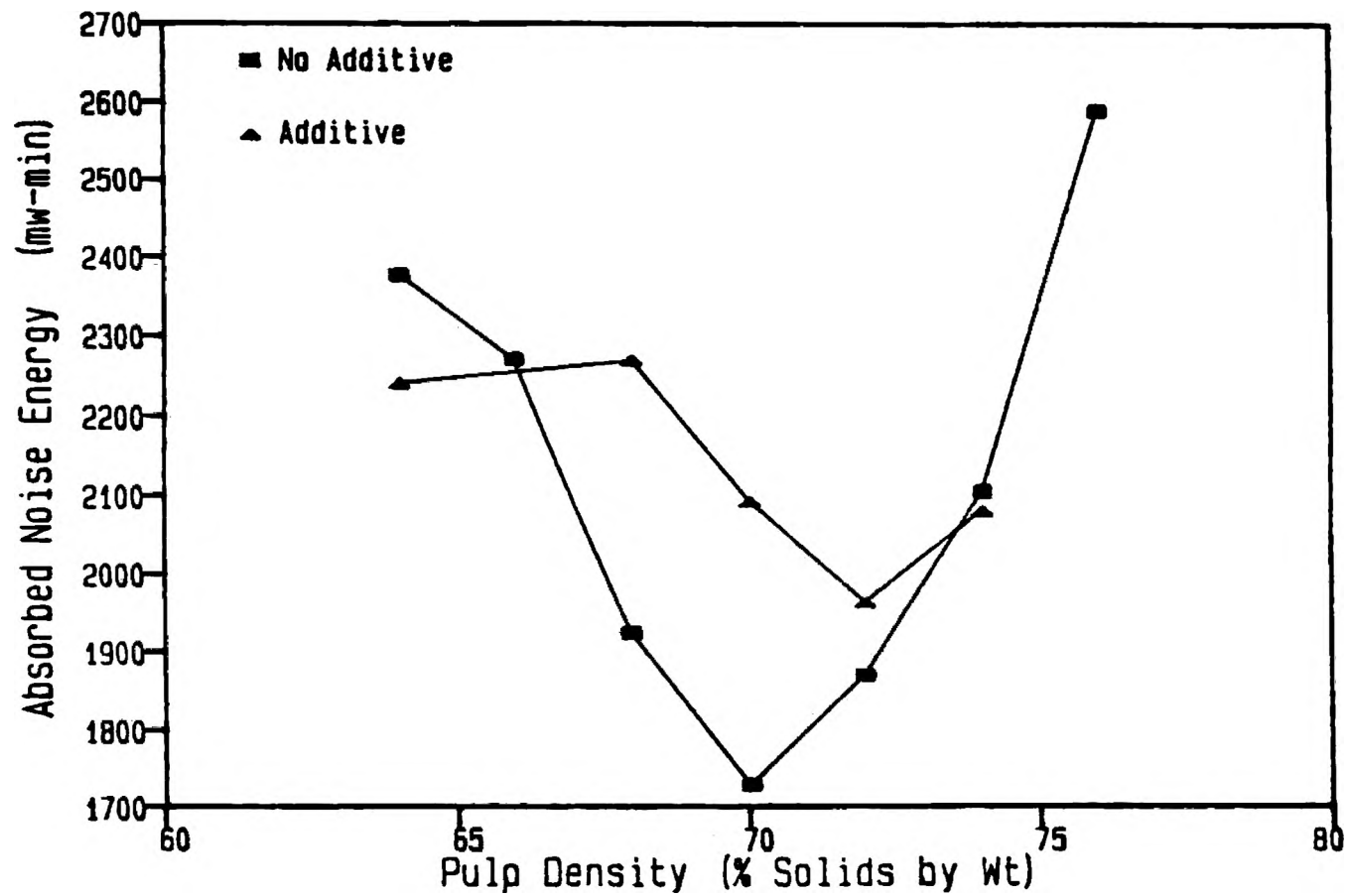


Figure 47. Absorbed Noise Energy Relationships with Pulp Density for Molybdenite Ore with and without a Grinding Additive

Table XIII. Fine Particle Production with Pulp Density for Molybdenite ore  
 a. Without Additive  
 b. With Additive

Test Parameters

1000 cc Pulp  
 30 Minute Grind Time  
 65 RPM  
 125 2.54 cm Balls  
 1.25 kg/tonne Additive (b)

(a)

| Pulp Density<br>% Solids                      | 64   | 66   | 68   | 70   | 72   | 74   | 76   |
|---|------|------|------|------|------|------|------|
| Net Production<br>(g) of -53<br><u>micron</u> | 646  | 660  | 681  | 726  | 680  | 669  | 586  |
| <u>DANE</u>                                   | 2376 | 2273 | 1921 | 1728 | 1872 | 2105 | 2571 |

(b)

| Pulp Density<br>% Solids                      | 64   | 66  | 68   | 70   | 72   | 74   |
|---|------|-----|------|------|------|------|
| Net Production<br>(g) of -53<br><u>micron</u> | 576  | 627 | 684  | 680  | 695  | 689  |
| <u>DANE</u>                                   | 2241 | N/A | 2272 | 2092 | 1965 | 2083 |

magnetite the maximum grinding occurs at the highest CA sound power values (70% solids). As indicated by Figure 47 this is in the pseudoplastic range of 64-70% solids. The CA sound power curves presented in Figure 48 show the effects of the additive on selected percent solids tests. Generally the additive has little effect on these curves and where there was a difference observed the additive caused a decrease in values as opposed to the increases seen with magnetite. This result is difficult to explain other than to postulate that the additive has not acted as a dispersant in reducing viscosity, but has had an opposite effect in effectively increasing viscosity. The DANE versus percent solids data for these tests can also be seen in Figure 47 which illustrates the higher DANE levels in the 68-75% solids range which suggests less grinding. The DANE curves show minimums at 70% solids without the additive and 72% solids with the additive which indicates that the onset of yield is slightly higher with the additive.

The results of the net production of -53 micron particles for the molybdenum ore with additive are presented in Table XIII(b). By comparing the same data for no additive in Table XIII(a) it is apparent that in general the additive has not increased grinding and has slightly decreased fine particle production. The increased DANE values reflect higher viscosity pulps and hence decreased fine particle production especially for pulps below 72% solids. The maximum grinding is again indicated by the

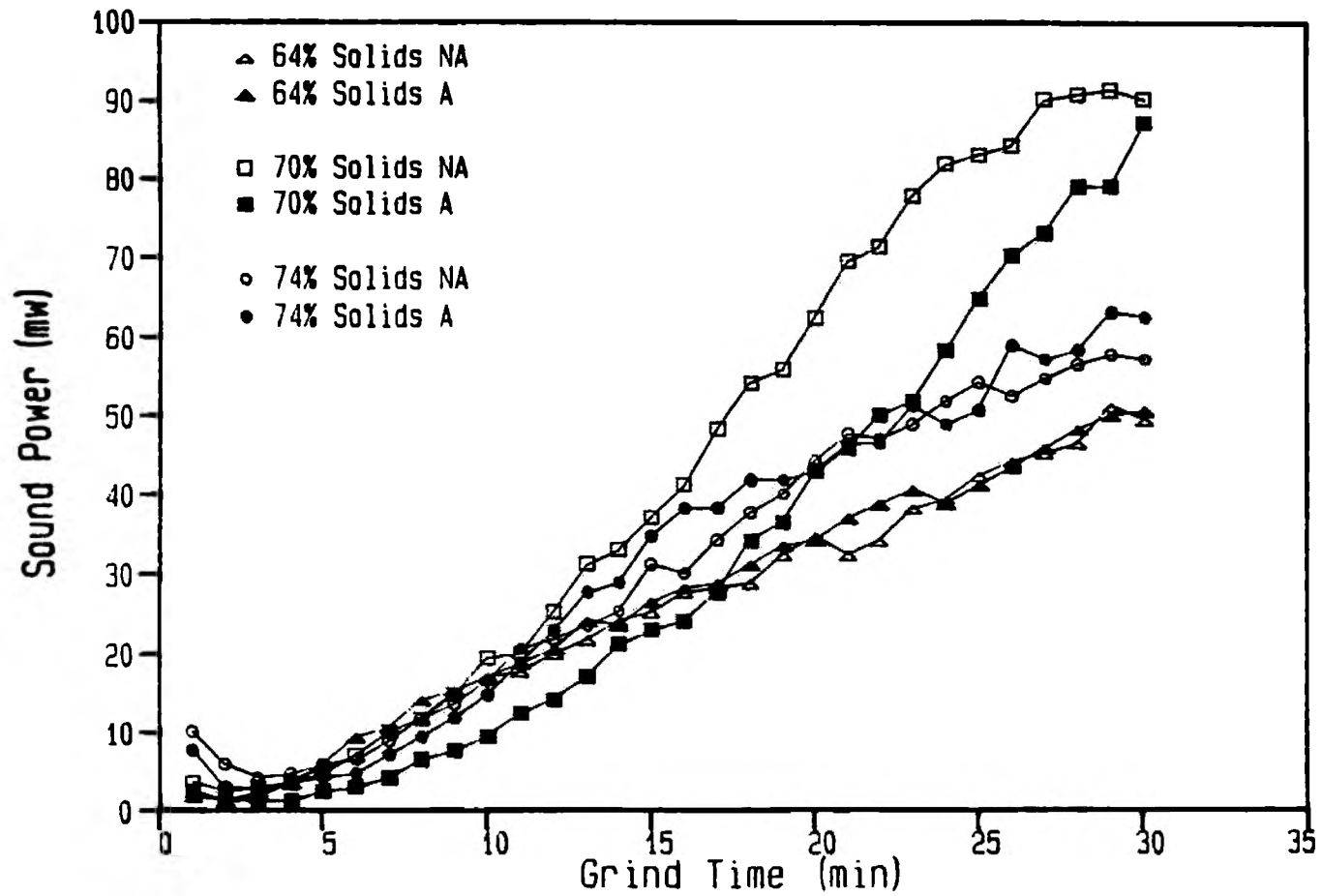


Figure 48. Sound Power Variation with Grind Time for a Molybdenite Ore with and without a Grinding Additive at Low Pulp Densities

highest CA sound power and the lowest absorbed noise energy.

In summary, the absorbed noise energy parameter of DANE can identify the viscous character of a mineral-water slurry and indicate the range of pulp densities which will provide the most effective production of fine particles. In addition, DANE can identify the the rheological changes associated with the addition of a grinding additive when they are, or are not effective.

## C2. Ore Character and Noise Energy

### Variation Results

The results of tests presented in this section were performed by the equipment described in section C part 3 of the Experimental Procedures. The purpose of the experiments performed for this part of the multiple frequency band monitoring was to extend the preliminary data obtained with single frequency monitoring at 8 kHz presented earlier in section C part 3. For these tests artificial mixtures of magnetite and traprock were subjected to grinding tests under the conditions outlined in Table XIV. The properties of the two materials and the mixtures used for this testing can also be seen in Table XIV and illustrate the extreme differences between magnetite and traprock. These two materials were chosen primarily because traprock is the major naturally occurring impurity associated with the



Table XIV. Grinding Conditions and Physical Properties of Magnetite and Traprock Feed Materials and Mixture Ratios

TR=Traprock  
MAG=Magnetite  
\*=by extrapolation

|                               | 1000 cc<br>MAG | 750 cc MAG<br>250 cc TR | 500 cc MAG<br>500 cc TR | 250 cc MAG<br>750 cc TR | 1000 cc<br>TR |
|-------------------------------|----------------|-------------------------|-------------------------|-------------------------|---------------|
| Feed Size<br>(mm)             | -3.3+1.6       | -3.3+1.6                | -3.3+1.6                | -3.3+1.6                | -3.3+1.6      |
| Grindability<br>(g/rev)       | 4.1            | 2.45*                   | 1.65*                   | 1.30*                   | 1.1           |
| Density<br>(g/cc)             | 4.2            | 3.9                     | 3.5                     | 3.2                     | 2.8           |
| Breakage Rate<br>Constant (K) | 0.25           | 0.18                    | 0.14                    | 0.12                    | 0.11          |
| Charge Volume<br>Ore (cc)     | 1000           | 1000                    | 1000                    | 1000                    | 1000          |
| Charge Volume<br>Water (cc)   | 500            | 500                     | 500                     | 500                     | 500           |
| Charge Wt.<br>Ore (g)         | 2260           | 2039                    | 1818                    | 1596                    | 1375          |
| % Solids<br>by Volume         | 66.6           | 66.6                    | 66.6                    | 66.6                    | 66.6          |
| % Solids<br>by Wt.            | 82.0           | 80.0                    | 78.4                    | 76.1                    | 73.3          |
| Grind Time<br>(Minutes)       | 30             | 30                      | 30                      | 30                      | 30            |

magnetite at the Pea Ridge Iron Ore Co., and that the study of a mixture of these materials would possibly indicate differences in ore character that may be observed in an industrial grinding operation.

The CA sound power values with grind time as a function of the artificial mixtures and pure materials is presented in Figure 49. It is clearly apparent from this figure that the mixture ratios of the charge significantly effect the sound power value variations. This is seen initially in Figure 49 by observing the CA sound power values with time for the first 6 minutes. The pure traprock charge shows the highest CA sound power values and the mixtures with increasing concentrations of magnetite show progressively lower values in order of the ratios present. The next feature of these curves that tends to reflect the character of the ore is the time of grind necessary to reach the minimum in CA sound power values. The mixtures richer in traprock show minimum values at progressively increasing times. In the later portion of the curve ( > 6 minutes) the reverse of the initial portion of the curve is noted whereby the magnetite noise levels reach higher values than the mixtures and pure traprock.

As proposed in the earlier work with the single frequency monitoring the initial sound power value decreases are related to the production of increasing numbers of coarser particles being able to block the ball/liner collisions and would reflect coarse breakage. By

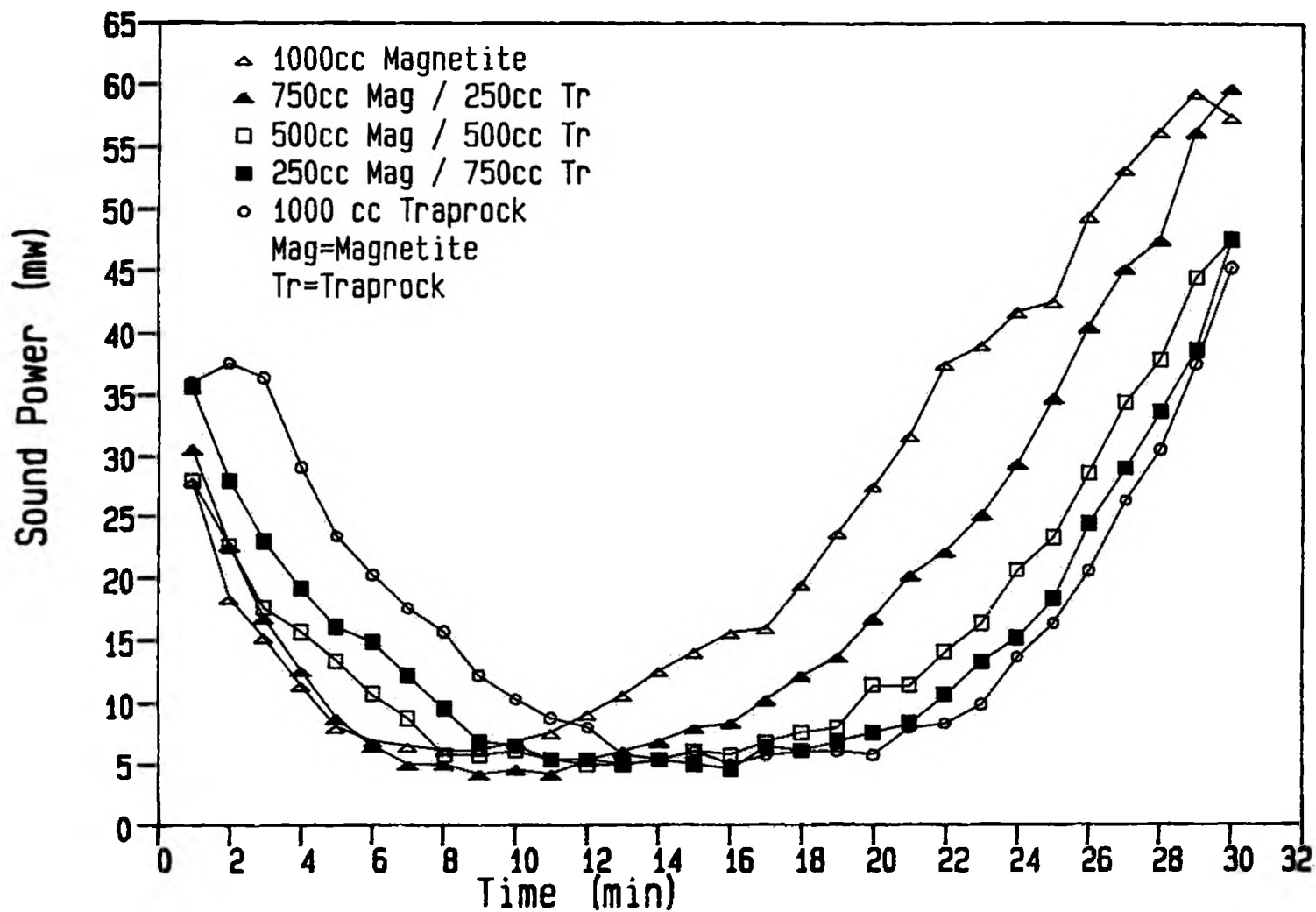


Figure 49. Sound Power Variation with Grind Time for Magnetite, Traprock, and Artificial Mixtures

referring to Table XIV and the physical characteristics of these mixtures, the gradation in values of the grinding rate constant and grindability corresponding to the mixture ratios is clearly related to the decreasing portion ( < approx. 12 minutes ) of the CA sound power value curves in an inverse manner, namely that the traprock has the lowest K and g/rev at  $0.11 \text{ min}^{-1}$  and  $1.1 \text{ g/rev}$  respectively and the highest CA sound power values. The magnetite displays the highest K and g/rev at  $0.25 \text{ min}^{-1}$  and  $4.1 \text{ g/rev}$  and the lowest CA sound power values with the mixtures having intermediate values for both noise and grinding parameters. These results provide additional supporting evidence that sound levels can indicate coarse breakage and also detect variations in ore character.

The point at which the CA sound power values reach a minimum value has been proposed to represent a critical distribution within the mill. Table XV presents the production of -75 micron particles at different times of the experimental grind. An overall relationship between the entire particle size distribution and the time taken to reach the minimum, as well as the value of the minimum, was not established, but the percentage of -75 micron particles does appear to be related to the corresponding time to reach the minimum sound power. This is shown in Table XV as underlined percentages and indicates that approximately 25-35% by weight of particles -75 microns must be present for the minimum to occur.

Table XV. Fine Particle Production with Grind Time for Magnetite, Traprock, and Mixture Ratios

Test Parameters

1000 cc Ore  
 500 cc Water  
 30 Minute Grind Time  
 125 2.54 cm Balls  
 65 RPM  
 MAG = Magnetite  
 TR = Traprock  
 u = micron

Mixture Ratios

| 1000 cc<br>MAG |               | 750 cc MAG<br>250 cc TR |               | 500 cc MAG<br>500 cc TR |               | 250 cc MAG<br>750 cc TR |               | 1000 cc<br>TR |               |
|----------------|---------------|-------------------------|---------------|-------------------------|---------------|-------------------------|---------------|---------------|---------------|
| Time<br>min    | Wt.%<br>-75 u | Time<br>min             | Wt.%<br>-75 u | Time<br>min             | Wt.%<br>-75 u | Time<br>min             | Wt.%<br>-75 u | Time<br>min   | Wt.%<br>-75 u |
| 2              | 13.4          | 2                       | 11.4          | 2                       | 9.0           | 2                       | 11.2          | 2             | 7.0           |
| 4              | 18.3          | 4                       | 14.3          | 4                       | 15.5          | 4                       | 15.7          | 4             | 11.6          |
| 7              | <u>24.1</u>   | 8                       | 26.5          | 8                       | 23.5          | 8                       | 23.4          | 8             | 16.0          |
| 10             | 31.1          | 10                      | <u>31.0</u>   | 10                      | 26.7          | 10                      | 27.4          | 10            | 20.5          |
| 12             | 34.5          | 12                      | 34.2          | 13                      | <u>34.0</u>   | 12                      | 28.6          | 12            | 25.0          |
| 16             | 42.0          | 16                      | 40.8          | 16                      | 36.1          | 15                      | <u>34.7</u>   | 15            | 28.3          |
| 20             | 47.4          | 20                      | 46.3          | 20                      | 45.0          | 20                      | 41.0          | 20            | <u>35.1</u>   |
| 25             | 54.6          | 25                      | 53.2          | 25                      | 50.4          | 25                      | 48.3          | 25            | 42.8          |
| 30             | 62.1          | 30                      | 60.0          | 30                      | 58.1          | 30                      | 56.8          | 30            | 54.6          |

The increases in sound power values beyond the minimum have been related to the production of fine particles. Figure 49 and the data in Table XV show that at the higher time intervals that the relative positioning of the CA sound power curves is directly related to the production of -75 micron particles. Magnetite shows the highest CA sound power values and produces the most -75 micron particles, the traprock the lowest, and the mixtures have intermediate values.

The above results show that certain portions of the sound power curves with time can reflect different aspects of grinding. In the previous tests relationships were established between absorbed noise energy and grinding parameters for the overall length of the grind. Table XVI presents the DANE values for different sections of the CA sound power curves in Figure 49 and these values can be seen plotted against the mixture ratios in Figure 50. These curves show that there is little correlation between the mixture ratios and DANE for the portion of the curve representing the time to the minimum, but that for the other sections plotted there is an increasing trend from pure magnetite to pure traprock with increasing concentrations of traprock.

The DANE values of these curves, the relative positioning of the initial and final portions of the CA sound power curves in Figure 49, and the values of the grinding parameters from Table XIV appear to follow

Table XVI. Absorbed Noise Energy Values for Time  
Increments with Magnetite, Traprock, and Mixture Ratios

MAG = Magnetite  
TR = Traprock  
PW = Sound Power

|                                | Mixture Ratios |                         |                         |                         |               |
|--------------------------------|----------------|-------------------------|-------------------------|-------------------------|---------------|
|                                | 1000 cc<br>MAG | 750 cc MAG<br>250 cc TR | 500 cc MAG<br>500 cc TR | 250 cc MAG<br>750 cc TR | 1000 cc<br>TR |
| Time to<br>minimum PW<br>(min) | 7              | 10                      | 12                      | 15                      | 17            |
| DANE<br>(30 min.)              | 1090           | 1241                    | 1345                    | 1354                    | 1305          |
| DANE<br>(25 min.)              | 698            | 818                     | 876                     | 827                     | 740           |
| DANE<br>(5-30 min.)            | 893            | 1053                    | 1158                    | 1190                    | 1174          |
| DANE<br>(10-30 min.)           | 626            | 783                     | 902                     | 950                     | 963           |
| DANE<br>(15-30 min.)           | 374            | 510                     | 629                     | 677                     | 701           |
| DANE<br>(20-30 min.)           | 173            | 262                     | 363                     | 408                     | 430           |
| DANE to the<br>minimum PW      | 780            | 770                     | 790                     | 680                     | 590           |

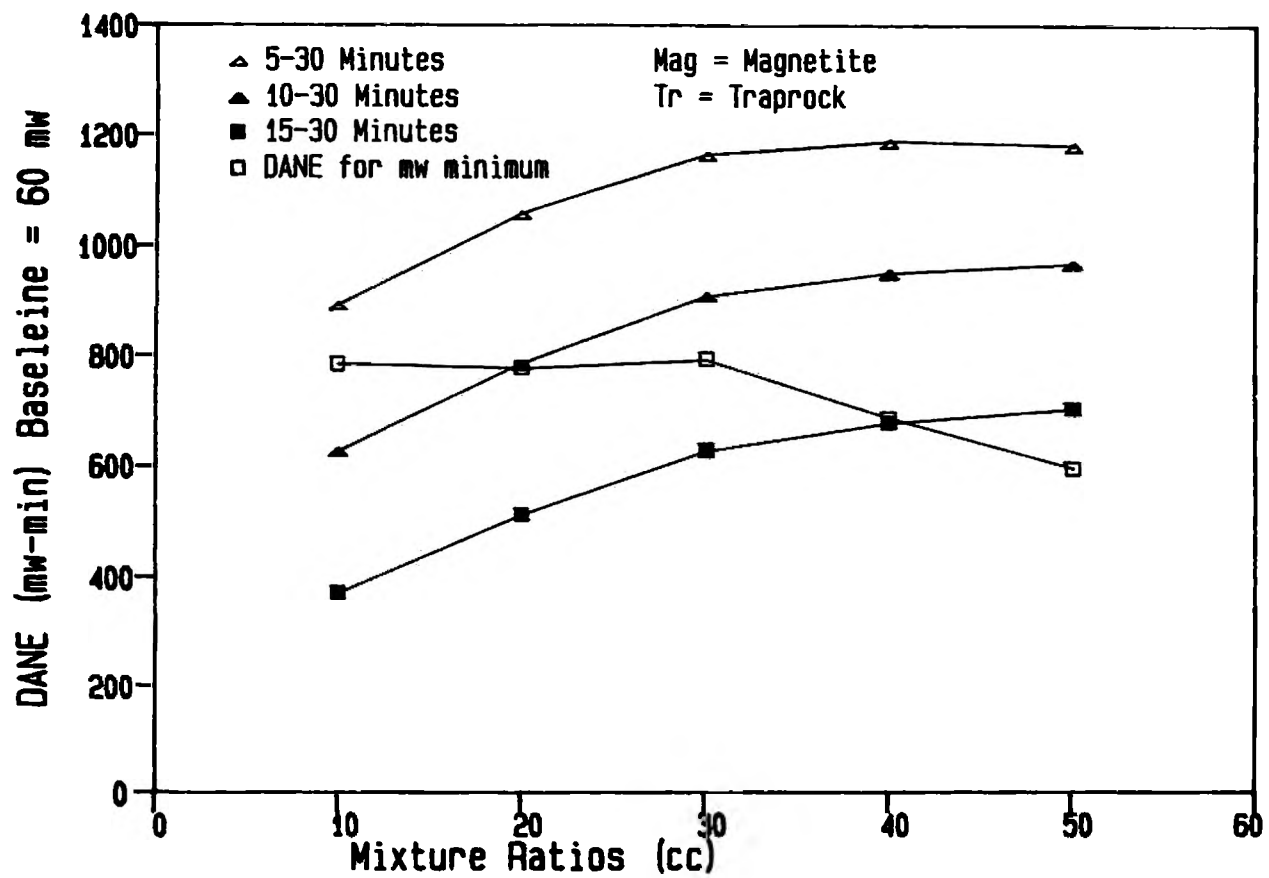


Figure 50. Absorbed Noise Energy Variations for Time Increments with Magnetite/Traprock Mixtures



logarithmic characteristics with the mixture ratios. The log-log plot in Figure 51 confirms this. The absorbed noise is therefore inversely related to the grinding parameters of K and grindability on a logarithmic basis with the mixture ratios. This relationship is similar to that found for a narrow-sized feed material with the single frequency monitoring in section B3, where DANE increased as grinding decreased. This is further evidence that noise measurements can provide useful data on the character of an ore charge both from the standpoint of coarse and fine breakage, and that the absolute value of the CA sound power value with grind time may be indicative of the production of fine particles.

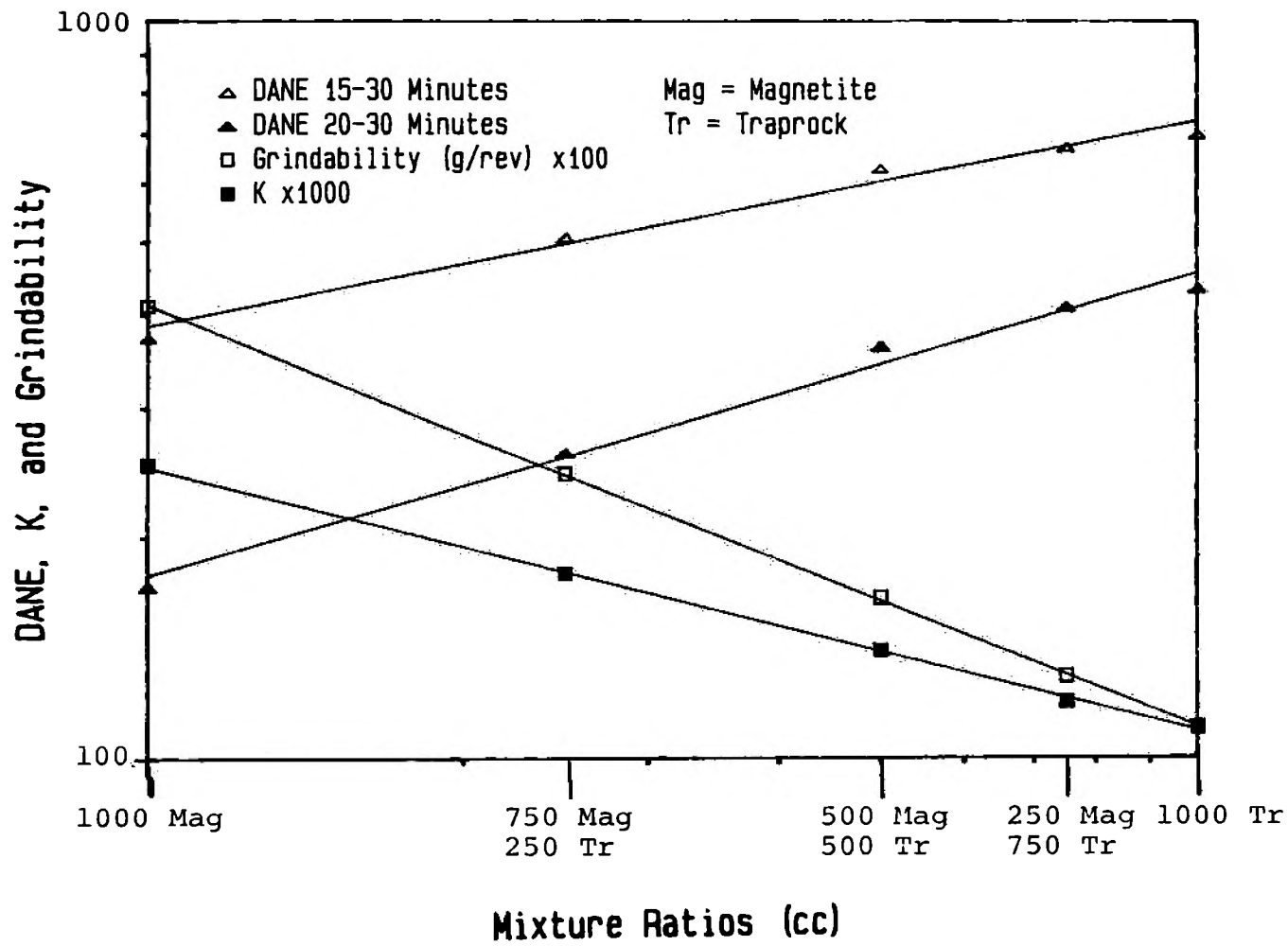


Figure 51. Logarithmic Relationships between DANE, K, and Grindability with the Magnetite/Traprock Mixtures

## V. CONCLUSIONS

1. The principal source of sound from a laboratory batch ball mill comes from ball/liner collisions. A survey of sound intensity as a function of the angle of measurement shows the sound has a lobate directional character. The best location of the microphone is along a line through the center of the mill perpendicular to the horizontal axis of the mill.

2. A discrete frequency spectrum sound pressure level analysis of an operating batch ball mill revealed that the spectrum is highly complex, but does provide useful information regarding what frequency bands may best reflect the state of the mill. Discrete frequency analysis of the vibrational characteristics of the mill also provided supporting evidence for experimental work performed with single frequency band monitoring.

3. It has been shown that the absorbed noise energy parameter (ANE) for laboratory batch grinding can reflect the breakage rate parameter  $K$ , and assist in identifying the optimum milling conditions as a function of mill speed, ball and charge loading. The relationships established would suggest that mill noise parameters could be used as an on-line production parameter for a batch ball mill.

4. The continuous variation in sound power levels with grind time is controlled by the disappearance of top size particles, and the production of middle and fine sized particles. A knowledge of the distribution of these particles, as indicated by the sound power levels with grind time, could well be a useful indicator of overall size distribution within the mill.

5. The absorbed noise energy parameter (DANE) tends to reflect ore character. The use of noise in evaluating a simple batch grinding test may provide information similar to that obtained with grindability testing.

6. The production of fine particles is not directly related to the absorbed noise energy parameter (DANE) for pulp density variations in wet grinding. However, the rheological transitions from dilatant to pseudoplastic, to pseudoplastic with yield rheology, as identified by the absorbed noise parameter, are reflected in the fine particle production.

7. It appears that mill noise reflects the mill pulp rheology with and without the presence of a grinding additive, even in the case where the additive is not effective.

8. The relationships between noise and grinding parameters

with the artificial mixture ratios of traprock and magnetite appear to be logarithmic. These relationships further substantiate the proposition that noise measurements can provide useful data regarding the grinding characteristics of an ore charge. The absolute value of the sound power level with grind time is indicative of fine particle production.

9. The relationships between sound and grinding parameters derived from laboratory scale batch grinding experiments have provided sufficient detail to enable judgements on their realistic use in industrial grinding operations to be made. For industrial batch grinding the experimental results are sufficiently encouraging to state that once the characteristic sound spectrum of an industrial mill is established, and the particle production requirements known, that mill sound levels could provide an excellent control parameter. For continuous industrial grinding the experimental results show that the currently difficult-to-control industrial grinding parameters of pulp density, viscosity, and ore character can be estimated by the use of mill sound measurements. If the relationships established for these parameters can be further identified on a continuous basis then the use of sound measurements could have a pronounced effect on the present control strategies used to measure mill performance and a strong potential to improve control.

## VI. RECOMMENDATIONS FOR FURTHER WORK

### A. LABORATORY GRINDING

Since the results discussed in Section IV were all performed on a batch basis, all recommendations are for further investigations on a laboratory continuous scale. Some possible areas are as follows:

1. Determine the frequency response of a continuous laboratory mill operating with no ore charge in an effort to establish base-line data for sound level changes with feed material present.
2. Determine the effects of changing the percent solids during wet grinding using a narrow sized and wide sized feed without recirculation of material to establish relationship between sound levels, pulp density and grinding at standard and variable operating conditions.
3. Repeat recommendation 2 using a recirculating load of classified oversized material to study the effects of recirculation on sound and grinding parameters.
4. Establish optimizing relationships between sound levels, grinding conditions, and particle production parameters and formulate mathematical model to assist in

maximizing efficiency and control.

5. Perform additional fundamental studies of the noise generating mechanism for a laboratory batch and continuous mill.

#### B. INDUSTRIAL TESTING

The relationships between sound and grinding parameters set forth for laboratory batch grinding have some direct applicability to industrial scale batch grinding. The present control strategies used are primarily stopping the mill and sizing the product to establish if further grinding is required to produce the required particle size distribution. It is recommended that a series of tests be performed on an industrial batch mill to establish sound and grinding relationships on small time intervals, which if successful would provide a control technique to alleviate recourse to the tedious and time consuming intermediate evaluations presently in use.

For continuous industrial grinding there are difficulties scaling laboratory batch experimental data directly to continuous systems and it is recommended that continuous laboratory testing be performed prior to any actual plant experimentation.

## BIBLIOGRAPHY

1. F. Milton Lewis, and James L. Coburn: "Comparitive Economics of Conventional and Semi-Autogenous Grinding", Design and Installation of Comminution Circuits , AIME, 1982
2. T.P. Harrington, P.G. Doctor, and K.A. Prisbrey: "Analysis of the Acoustic Emmission Spectra Particle Breakage in a Laboratory Cone Crusher", AIME Trans. , (270), 1980, pp. 1879-1882
3. B.A. Wills: Mineral Processing Technology , Pergamon Press, London, 1981, pp. 116-186
4. D.A. Hietman: "The Buick Concentrator", paper presented at the Arizona Conference of AIME, Dec. 1979, Tuscon, Arizona
5. E.G. Kelly, and D.J. Spottiswood: Introduction to Mineral Processing , John Wiley and Sons, New York, 1982, pp. 127-157
6. J.A. Herbst, and O.A. Bascur: "Mineral Processing Control in the 1980's - Realities and Dreams", Control '84 Mineral/Metallurgical Processing , AIME, 1984
7. H. Aurasmaa, M. Tarvainen, K. Saarhelo, and P. Uronen: "An Audiometric Control System for Wet Semi-Autogenous and Autogenous Grinding System", Dechema-Monographien , Band 79, Nr. 1549-1575, Verlag Chemie, Gmb, 1976, pp. 435-446
8. J.O. Bernt: "Automatic Control of Feed Rates to Grinding Mills in the Cement Industry", ISA Preprint # 4.1-3-64, presented at the ISA conference and exhibition Oct 1964, New York, New York
9. I.I. Belyaev: "Automation of Nephelite and Limestone Crushing", Tsvet. Metal. , (2), 1962, pp. 53-59
10. F.J. Kelly and W.A. Gow: "Comparison of Manual and Automatic Control of a Grinding Circuit", Canadian Mining Journal , March, 1966
11. H. Hardinge: "The 'Electric Ear', a Device for Automatically Controlling the Operation of Grinding Mills by their Sound", AIME Trans. , (134), 1939
12. J.L. Watson: "An Analysis of Mill Grinding Noise", Powder Tech. , (41), No.1, 1985, pp. 83-89
13. J.L. Watson and S.D. Morrison: "Indications of Grinding Mill Operation by Mill Noise Parameters", Particulate Sci. and Tech. , (3), No. 1, 1985



14. H.C. Hoover and L.H. Hoover: Translation of 'De Re Metallica' by Georgius Agricola , Dover Publications, New York, 1950
15. A.J. Lynch: Mineral Crushing and Grinding Circuits, Their Simulation, Optimisation, Design, and Control , Elsevier, Amsterdam, The Netherlands, 1977
16. R.J. Charles: "Energy-Size Reduction Relationships in Comminution", AIME Trans. , (208), 1957, pp. 80-88
17. F.C. Bond: "The Third Theory of Comminution", AIME Trans. , (193), 1967, pp. 470-484
18. E.L. Piret, J.M. Kwong, J.T. Adams, and J.F. Johnson: "Energy - New Surface Relationships in the Crushing of Solids", Chem. Eng. Progress , (45), 1949, pp. 508-708
19. J. Gross and S.R. Zimmerly: "Crushing and Grinding, III. , Relationships of Work Input to Surface Produced in Crushing Quartz", AIME Trans. , (87), 1930, pp. 35-50
20. F. Kick: "Contribution to the Knowledge of Brittle Materials", Dinglers J. , (247), 1883, pp. 1-5
21. R.P. von Rittinger: Textbook of Mineral Dressing , Ernst and Korn, 1867, Berlin
22. L.G. Austin: "A Review Introduction to the Mathematical Description of Grinding as a Rate Process", Powder Tech. , (5), 1971, pp. 1-17
23. D.F Kelsall: " A Study of Breakage in a Small Continuous Open Circuit Wet Ball Mill", Proc. 7th Int. Min. Proc, Congr. , New York, 1962
24. S.R. Broadbent and T.G. Callcott: "A Matrix Analysis of Processes Involving Particle Assemblies", Phil. Trans. R. Soc. Ser. A , (249), 1956, pp. 99-123
25. S.R. Broadbent and T.G. Callcott: "Coal Breakage Processes", J. Inst. Fuel , (29), 1956, pp. 524-539
26. G.G. Stanley: "Mechanisms in Autogenous Mills and their Mathematical Representation", J. S. Afr. IMM , (75), 1974, pp. 77-98
27. L.G. Austin: "Preliminary Results on the Modeling of Autogenous Grinding", 14th APCOM Symp. , AIME, 1977, pp. 207-226

28. L.G. Austin, V.K. Jindal, and C. Gotsis: "A Model for Continuous Grinding in a Laboratory Hammer Mill", Powder Tech. , (22), 1979, pp. 199-204
29. R.R. Klimpel: "The Use of Mathematical Modelling to Evaluate Operating Alternatives in an Industrial Comminution Facility", Proc. Int. Conf. Part. Tech. , Chicago, Illinois, 1973
30. L.G. Austin, P.T. Luckie, and D. Wightman: "Steady-State Simulation of a Cement Milling Circuit", Int. J. Miner. Process. , (2), 1975, pp. 127-150
31. L.G. Austin: "Understanding Ball Mill Sizing", Ind. Eng. Chem. Process Des. Dev. , (12), 1973, pp. 121-129
32. R.H. Snow: "Grinding Mill Simulation and Scale-Up of Ball Mills", Proc. Int. Conf. Part. Tech. , Chicago, Illinois, 1973
33. J.A. Herbst and D.W. Fuerstenau: "Scale-Up Procedures for Continuous Grinding Mill Design Using Population Balance Models", Int. J. Miner. Process. , (7), 1980, pp. 1-31
34. A.W. Cameron: " A Detailed Assesment of Concentrator Performance at Broken Hill South Ltd.", Proc. Australas. IMM , (240), 1971, pp. 53-67
35. D.F. Kelsall: "The Effects of a Change from Parallel to Series Grinding in Broken Hill South", Australas. IMM Annual Conf. , Newcastle, Aust., 1972, pp. 337-347
36. D.F. Kelsall, K.J. Reid, and P.S.B. Stewart: "The Study of Grinding Processes by Dynamic Modelling", Elec. Eng. Trans. Inst. Eng. Aust. , (1), 1969, pp. 173-186
37. P.S.B. Stewart: "The Control of Wet Grinding Circuits", Aust. Chem. Process Eng. , (23), 1970, pp. 18-21
38. J.A. Herbst and D.W. Fuerstenau: "Influence of Mill Speed and Ball Loading on the Parameters of the Batch Grinding Equation", AIME Trans. , (252), 1972, pp. 169-176
39. L.G. Austin, K. Shoji, and P.T. Luckie: "The Effect of Ball Size on Mill Performance", Powder Tech. , (14), 1976, pp. 71-79
40. D.F. Kelsall, P.S.B. Stewart, and K.R. Weller: "Continuous Grinding in a Small Wet Ball Mill. Part V. A Study of the Influence of Media Shape", Powder Tech. , (8), 1973, pp. 77-83

41. B.K. Loveday: "An Analysis of the Comminution Kinetics in Terms of Size Distribution Parameters", Journal S. A. Inst. Min. Metall. , (68), 1967
42. L.G. Austin: "Understanding Ball Mill Sizing", Ind. Eng. Chem. Process Des. Dev. , (12), 1973, pp. 121-129
43. K. Shoji, S. Lohrasb, and L.G. Austin: "The Variation of Breakage Parameters with Ball and Powder Loading in Dry Ball Milling", Powder Tech. , (25), 1980, pp. 109-114
44. W.T. Yen and T Salman: "Pulp Density of the Ball Mill and Grindability", Canadian Mining Journal , (90), 1969, pp. 63-66
45. P. Tucker: "Rheological Factors that Effect the Wet Grinding of Ores", Trans. IMM (Sect. C) , (91), 1982, pp. 117-122
46. R.R. Klimpel: "Slurry Rheology Influence on the Performance of Mineral/Coal Grinding Circuits", Mining Eng. , (34), 1982, pp. 1665-1668
47. R.R. Klimpel and L.G. Austin: "Chemical Additives for the Wet Grinding of Minerals", Powder Tech. , (31), 1982, pp. 239-252
48. J.D. Irwin and E.R. Graf: Industrial Noise and Vibration Control , Prentice Hall, New Jersey, 1979
49. M.J. Crocker and A.J. Price: Noise and Noise Control Vol. I , C.R.C. Press, Ohio, 1975
50. Journal of Sound and Vibration , Academic Press, London
51. Journal of the Acoustical Society of America
52. A.P.G. Peterson and E.E. Gross: Handbook of Noise Measurement , General Radio Co., West Concord, Mass., 1963
53. W.W. Seto: Theory and Problems of Acoustics , Schaum's Outline Series, McGraw-Hill Book Co., New York, 1971
54. C.V.R. Reddy, R.B. Bhat, and B.V.A. Rao: "A Note on the Radiated Noise from a Cement Mill by the Application of Damping Treatment", Journal of Sound and Vibration , (91), 1983, pp. 601-603

55. J.L. Watson and S.D. Morrison: "Estimation of Pulp Viscosity and Grinding Mill Performance by Means of Mill Noise Measurements", accepted by AIME/SME for publication in Mineral and Metallurgical Processing
56. A.F. Taggart: Handbook of Mineral Dressing , Sect. 6, Wiley, New York, pp. 1-60
57. F.C. Bond: "Crushing and Grinding Calculations, Parts I and II", Br. Chem. Eng. , (6), 1961, pp 378-385
58. Watson, Dr. J.L., and Cummings, Dr. A.. Personal Communication. May, 1983

## VITA

Scott Douglas Morrison was born on August 2, 1956 in New York City, New York. He received his primary education in Montville, New Jersey where he graduated from Montville Township High School in June 1974.

He entered St. Lawrence University in Canton, New York in September 1974 and received his B.S. in Geology with Honors in June 1979, after which he went to work for the Societe Generale de Surviellance in Geneva, Switzerland subsequently in Vancouver, British Columbia and Houston, Texas.

The author left the Societe Generale de Surviellance in August 1982 to attend graduate school at the University of Missouri-Rolla.

## APPENDIX A: DATA ACQUISITION PROGRAMS

## APPENDIX A1: Single Frequency Band Analysis

The following program for the Apple IIe microcomputer was used for the data acquisition of single frequency band sound pressure levels from a batch ball mill on a real time basis. The program also gives the user the ability to tabulate and plot the sound pressure and power values with time and calculate the absorbed noise energy values.

```

5  REM THIS BLOCK OF THE PROGRAM IS THE
6  REM GRINDING TEST TIME AND SAMPLING
7  REM RATE INTERVAL INPUT SECTION
10 HOME
20 PRINT : PRINT "INPUT TEST DESCRIPTION": INPUT FS
30 PRINT : PRINT "INPUT TIME OF START AND FINISH OF RUN IN MINS"
40 INPUT SR,FR:TR = FR - SR
50 PRINT : PRINT "INPUT SAMPLE PERIOD(SEC)": INPUT SP
60 PRINT : PRINT "INPUT TIME BETWEEN SAMPLES(SEC)": INPUT TB
70 DIM X(50),Y(50),MWA(50)
80 DIM NL(500),AN(500),DB(500),WA(100),AD(100)
81 REM THIS BLOCK OF THE PROGRAM SENDS A
82 REM SIGNAL TO A RELAY SYSTEM TO TURN
83 REM THE MILL ON AND OFF. IT ALSO ACCEPTS
84 REM AN ANALOG SIGNAL FROM THE MICRO-
85 REM PHONE TO BE CONVERTED TO A DIGITAL
86 REM SIGNAL AND SUBSEQUENTLY CONVERTED
87 REM TO ACTUAL SOUND PRESSURE LEVELS.
99 & BOUT,(DV) = 65535,(AM) = 128: & PAUSE = 2
100 C = C
110 I = 0:TN = 0
120 & TIME TO HR,MN,SC
130 TO = HR * 60 * 60 + MN * 60 + SC: IF N = 0 THEN TZ = TO
140 I = I + 1
150 & AIN,(TV) = NL(I),(C#) = 6
160 TN = TN + NL(I)
170 & TIME TO HR,MN,SC
180 TI = HR * 60 * 60 + MN * 60 + SC
190 IF TI > TR * 60 + TZ - 5 THEN GOTO 310
200 IF TI - TO < SP THEN GOTO 140
210 N = N + 1
220 AN(N) = TN / I
230 DB(N) = 70 + NL(I) / 50.75
235 SDB = SDB + DB(N)
240 PRINT N,DB(N)
250 PRINT I
260 & TIME TO HR,MN,SC
270 TI = HR * 60 * 60 + MN * 60 + SC
280 IF TI > TR * 60 + TZ - 3 THEN GOTO 310
290 IF TI > = TO + TB THEN GOTO 100
300 GOTO 260
310 HOME : PRINT : PRINT

```

```

312 MDB = INT (SDB * 10 / N) / 10
314 FOR I = 1 TO N
315 SS = SS + (DB(I) - MDB) ^ 2
316 NEXT I
318 ST = INT (SS * 100 / (N - 1)) / 100
320 & BOUT,(DV) = 0,(AM) = 128
330 D$ = ""
331 REM THIS BLOCK IS THE PRINT STATEMENT
332 REM WHICH PRINTS THE DATA FOR SPL ON
333 REM 1/4 MIN INTERVALS AND CONVERTED
334 REM PWL ON A 1 MIN BASIS. STATISTICAL
335 IN FOR M AT I ON ISALSOCALCUL AT ED AND
336 PRINT ED
340 PRINT D$;"PR#1"
350 PRINT "NOISE ANALYSIS"
360 PRINT : PRINT "TEST ";F$
370 L = 1
380 M = L + 3
390 K = 0
400 PRINT
410 PRINT : PRINT "TIME";
415 TQ = INT (TB * 100 / 60) / 100
420 FOR I = L TO M
430 K = K + 1
440 PRINT TAB( K * 10);SR + I * TQ;
450 NEXT I
460 PRINT : PRINT
470 PRINT "NOISE";
480 K = 0
490 FOR I = L TO M
500 DB(I) = INT (DB(I) * 10) / 10
510 K = K + 1
520 PRINT TAB( K * 10);DB(I);
530 NEXT I
540 L = L + 4
550 IF L < = TR * 60 / TB THEN GOTO 380
560 MI = 60 / TB
570 FOR I = 1 TO N
580 TDB = TDB + DB(I)
590 IC = IC + 1
600 IF TR < 1 THEN MI = TR / TB * 60
610 IF IC = MI THEN GOTO 640
620 C = C
630 NEXT I
640 TDB = TDB / IC

```



```

650 IM = IM + 1
660 MWA(IM) = 10 2 (TDB / 10) * 10 2 ( - 9)
670 MWA(IM) = INT (MWA(IM) * 100) / 100
680 TDB = INT (TDB * 10) / 10:AD(IM) = TDB
690 IC = 0:TDB = 0
700 IF I = N THEN GOTO 720
710 GOTO 630
720 PRINT : PRINT : PRINT "SUMMARY": PRINT : PRINT "TIME(MIN)";
    "DECIBELS"; TAB( 40);"MILLIWATS"
730 FOR L = 1 TO IM: PRINT
740 PRINT SR + L / IM * TR; TAB( 20);AD(L); TAB( 40);MWA(L)
750 NEXT L
760 PRINT : PRINT
763 MMW = 10 2 (MDB / 10) * 10 2 ( - 9)
764 MMW = INT (MMW * 10) / 10
765 PRINT : PRINT : PRINT "MEAN DB LEVEL= ";MDB;" (" ;MMW;"

766 PRINT "STANDARD DEVIATION= ";ST
770 PRINT D$;"PR#0"
780 HOME : PRINT : PRINT : PRINT
790 X = FRE (0)
830 PRINT : PRINT "INPUT MILL NOISE FOR BALLS ONLY"
835 INPUT BO
837 PRINT D$;"PR#1"
840 PRINT : PRINT "BALLS ONLY MILLIWATTS= ";BO
841 FOR I = 1 TO IM
842 X(I) = I * 20
843 Y(I) = BO - MWA(I)
844 CA = CA + (Y(I) + Y(I - 1)) / 2
845 NEXT I
846 PRINT "MILLIWAT-MIN= ";CA: PR# 0
847 PRINT " TO PLOT AND PRINT THE MW-TIME CURVE-INPUT 1"
848 INPUT PP
849 IF PP < > 1 THEN GOTO 1030
850 REM THIS BLOCK ALLOWS THE USER TO PLOT
851 REM AND PRINT THE PWL WITH GRIND TIME
855 HGR2 : HCOLOR= 7
860 HPLOT 0,159 TO 279,159
870 HPLOT 0,0 TO 0,159
880 FOR I = 1 TO IM
910 X = X(I)
920 Y = (140 - 0.5 * Y(I)) * 4
930 HPLOT X - 2,Y TO X + 2,Y
940 HPLOT X,Y - 2 TO X,Y + 2

```

```
960 NEXT I
970 A = A
990 PR# 1
1000 PRINT CHR$(9);"G2"
1010 TEXT
1030 PR# 0
1040 TEXT
1045 PR# 0
1050 END
```

## APPENDIX A2: Multiple Frequency Band Analysis

The following program was used for the data acquisition of multiple frequency band sound pressure levels from a batch ball mill. The program stores the analog data in a digital form for the 30 frequency bands on real-time intervals of 20 seconds on magnetic discs.

```

50 DIM R(500),X(50),Z(50),Y(100,30)
55 DIM FR(30)
60 READ N
62 DATA 30
64 FOR J = 1 TO N
66 READ FR(J)
68 DATA 25,31.5,40,50,63,80,100,125,160,200,250,315,400,500,630,
    1.25,1.6,2.0,2.5,3.15,4.0,5.0,6.3,8.0,10.0,12.5,16,20
95 NEXT J
100 INPUT "INPUT INTEGRATION TIME SEC";Z
200 INPUT "INPUT TEST DESCRIPTION";F$
220 REM THIS BLOCK IS FOR THE INPUT OF
221 REM THE TEST TIME INTERVAL
250 PRINT : PRINT "INPUT TIME OF START AND FINISH OF RUN IN MIN"
300 INPUT SR,FR:TR = FR - SR
330 REM THIS BLOCK SENDS A SIGNAL TO A
331 REM RELAY SYSTEM TO TURN THE MILL
332 REM ON AND OFF.
350 & BOUT,(DV) = 65535,(AM) = 128: & PAUSE = 2
375 & TIME TO HR,MN,SC
380 TS = HR * 60 * 60 + MN * 60 + SC
400 I = 1:J = 1
410 & TIME TO HR,MN,SC
420 TZ = 60 * 60 * HR + 60 * MN + SC
450 N = 40 + 20 * J
500 & LOOK FOR AIN,(TV) = Q,(TH) = N,(C#) = 4: GOTO 550
550 & AIN,(TV) = Y(I,J),(C#) = 7
600 IF J = 17 THEN PRINT Y(I,J); SPC( 2)
610 IF J = 26 THEN PRINT Y(I,J)
650 J = J + 1
700 IF J > 30 THEN GOTO 800
750 GOTO 450
800 J = 1:I = I + 1
850 & TIME TO HR,MN,SC
900 TI = HR * 3600 + MN * 60 + SC
925 IF TI - TZ < 20 THEN GOTO 850
950 IF TI - TS < TR * 60 THEN GOTO 450

```

```

952 DI = I - 1
953 TB = 20
954 & BOUT,(DV) = 0,(AM) = 128
955 REM THIS STATEMENT SENDS THE PROGRAM
956 REM TO THE DATA STORAGE SECTION
957 GOSUB 1060
958 PRINT "FOR HARD COPY INPUT 1           ": INPUT HC
959 REM THIS BLOCK PRINTS THE FREQUENCY PWL
960 IF HC < > 1 THEN GOTO 1055
962 TB = 20
965 D$ = ""
970 PRINT D$: PR# 1
975 PRINT "NOISE ANALYSIS"
980 PRINT : PRINT "TEST=";F$
985 PRINT : PRINT SPC( 30)"TIME"
990 PRINT "NOISE IN BITS"
1009 L = 1
1010 I = 0
1012 R = 0
1013 TQ = INT (TB * 100 / 60) / 100
1014 I = 1
1015 R = R + 1
1016 POKE 36,6:Z = SR + I * TQ: PRINT Z;
1017 POKE 36,12:Z = Z + SR + I * TQ: PRINT Z;
1018 POKE 36,18:Z = Z + SR + I * TQ: PRINT Z;
1019 POKE 36,24:Z = Z + SR + I * TQ: PRINT Z;
1020 POKE 36,30:Z = Z + SR + I * TQ: PRINT Z;
1021 POKE 36,36:Z = Z + SR + I * TQ: PRINT Z;
1022 POKE 36,42:Z = Z + SR + I * TQ: PRINT Z;
1023 POKE 36,48:Z = Z + SR + I * TQ: PRINT Z;
1024 POKE 36,54:Z = Z + SR + I * TQ: PRINT Z
1027 PRINT : PRINT
1028 R = 0
1029 J = L
1030 FOR K = 1 TO 30
1031 PRINT FR(K);
1032 R = R + 1
1033 POKE 36,6: PRINT Y(J,K);
1034 POKE 36,12: PRINT Y(J + 1,K);
1035 POKE 36,18: PRINT Y(J + 2,K);
1036 POKE 36,24: PRINT Y(J + 3,K);
1037 POKE 36,30: PRINT Y(J + 4,K);
1038 POKE 36,36: PRINT Y(J + 5,K);
1039 POKE 36,42: PRINT Y(J + 6,K);
1040 POKE 36,48: PRINT Y(J + 7,K);
1041 POKE 36,54: PRINT Y(J + 8,K)
1043 NEXT K
1045 Z = 0

```

```
1048 SR = SR + 3
1049 L = L + 9
1050 IF SR < TR * 6 / TB THEN GOTO 1012
1052 PR# 0
1055 END
1057 REM THIS BLOCK STORES PWL DATA
1060 D$ = ""
1065 PRINT "INPUT FILE NAME"
1070 INPUT F$
1090 PRINT D$;"OPEN";F$;" ,D2"
1100 PRINT D$;"WRITE";F$
1110 PRINT DI
1111 PRINT TB
1112 PRINT TR
1120 FOR K = 1 TO DI
1130 FOR J = 1 TO 30
1140 PRINT Y(K,J)
1150 NEXT J
1160 NEXT K
1170 PRINT D$;"CLOSE";F$
1175 PRINT D$;"CATALOG,D1"
1180 RETURN
```

## APPENDIX B: SOUND DATA ANALYSIS PROGRAM

## APPENDIX B1: Absorbed Noise Energy Program

The following program calculates the absorbed noise energy in mw-min for the experimental sound power values with grind time. It sums the area beneath an input baseline and the actual sound power with grind time.

```
10 DIM X(40),Y(40)
12 HOME
15 PRINT
16 REM THIS BLOCK ALLOWS THE USER TO INPUT
17 REM THE ARTIFICIAL OR BALL ONLY PWL,
18 REM GRIND TIME, AND INDIVIDUAL PWL AT
19 REM 1 MIN INTERVALS
20 INPUT "INPUT MW FOR BALLS/WATER ONLY";BO
25 PRINT
30 INPUT "INPUT LENGHT OF GRIND IN MIN";N
35 PRINT
40 FOR I = 1 TO N
45 INPUT "INPUT MW VALUE FOR EACH MIN OF TEST";X(I)
50 NEXT I
51 REM THIS BLOCK CALCULATE THE ABSORBED
52 REM NOISE ENERGY AND PRINTS IT TO
53 REM THE SCREEN
55 FOR I = 1 TO N
60 Y(I) = BO - X(I)
65 CA = CA + (Y(I) + Y(I - 1)) / 2
70 NEXT I
75 PRINT
77 CA = INT (CA * 100) / 100
80 PRINT "DANE=";CA
```



## APPENDIX B2: Cumulative Frequency Analysis

The following program was used to manipulate the stored digital data from multiple frequency band sound pressure level measurements during grinding. It enables the user to convert the digital data representing sound pressure levels for the 30 frequency bands into actual sound pressure values and then sound power values and finally to an overall cumulative average sound power for the frequency bands 2-8 kHz. In addition it will print the individual frequency sound power values with grind time and the cumulative average sound power values with grind time.

```

10 DIM Y(90,30),FR(30),SUM(90),DB(90,30)
64 FOR J = 1 TO 30
66 READ FR(J)
68 DATA 25,31.5,40,50,63,80,100,125,160,200,250,315,400,500,630,
      1.25,1.6,2.0,2.5,3.15,4.0,5.0,6.3,8.0,10.0,12.5,16,20
69 NEXT J
70 REM THIS BLOCK IS THE DATA RECOVERY SECTION
72 GOSUB 1060
73 REM THIS BLOCK CONVERTS DIGITAL DATA TO
74 REM TO SPL THEN PWL WITH TIME AND FREQ. BAND
75 REM AND CALCULATES CA PWL
76 FOR J = 1 TO SS
80 FOR K = 15 TO 30
85 DB(J,K) = 76.904 + (.08299 * Y(J,K))
90 NEXT K
95 NEXT J
100 FOR J = 1 TO SS
110 FOR K = 15 TO 30
115 DB(J,K) = 102 (DB(J,K) / 10) * 102 ( - 9)
120 NEXT K
121 NEXT J
122 N = 0
126 FOR J = 1 TO SS STEP 3
127 N = N + 1
128 FOR K = 20 TO 26
130 SUM1 = 0
132 FOR M = J TO J + 2
134 SUM1 = SUM1 + DB(M,K)
136 NEXT M
138 AVG = SUM1 / 3
140 SUM(N) = SUM(N) + AVG
142 NEXT K
143 PRINT SUM(N)
144 NEXT J
146 FOR J = 1 TO TR
148 SUM(J) = INT (SUM(J) * 10) / 10
150 NEXT J
151 REM THIS BLOCK PRINTS CA PWL FOR 2-8KHZ
153 PR# 1
154 PRINT F$
155 PRINT "TIME(MIN)"; SPC( 4);"CUM FREQ"
157 FOR J = 1 TO TR
159 PRINT SPC( 2);J; SPC( 10);SUM(J)

```

```
161 NEXT J
163 PR# 0
165 REM THIS BLOCK PRINTS THE PWL WITH TIME
166 REM AND FREQUENCY BAND
958 PRINT "FOR A HARD COPY OF MW INPUT 1"
959 INPUT HC
960 IF HC < > 1 THEN GOTO 1052
970 PR# 1
975 PRINT "NOISE ANALYSIS"
980 PRINT : PRINT "TEST=";F$
985 PRINT : PRINT SPC( 30)"TIME"
990 PRINT "NOISE IN BITS"
991 FOR J = 1 TO SS
992 FOR K = 15 TO 30
993 Y(J,K) = INT (DB(J,K) * 100) / 100
994 NEXT K
995 NEXT J
1000 SR = 1
1009 L = 1
1010 I = 0
1012 R = 0
1013 TQ = INT (TB * 100 / 60) / 100
1015 PRINT : PRINT
1016 POKE 36,10:Z = SR * TQ: PRINT Z;
1017 POKE 36,16:SR = SR + 1:Z = SR * TQ: PRINT Z;
1018 POKE 36,22:SR = SR + 1:Z = SR * TQ: PRINT Z;
1019 POKE 36,28:SR = SR + 1:Z = SR * TQ: PRINT Z;
1020 POKE 36,34:SR = SR + 1:Z = SR * TQ: PRINT Z;
1021 POKE 36,40:SR = SR + 1:Z = SR * TQ: PRINT Z;
1022 POKE 36,46:SR = SR + 1:Z = SR * TQ: PRINT Z;
1023 POKE 36,52:SR = SR + 1:Z = SR * TQ: PRINT Z;
1024 POKE 36,58:SR = SR + 1:Z = SR * TQ: PRINT Z;
1025 POKE 36,64:SR = SR + 1:Z = SR * TQ: PRINT Z
1027 PRINT : PRINT
1028 R = 0
1029 J = L
1030 FOR K = 15 TO 30
1031 PRINT SPC( 4);FR(K);
1033 POKE 36,10: PRINT Y(J,K);
1034 POKE 36,16: PRINT Y(J + 1,K);
1035 POKE 36,22: PRINT Y(J + 2,K);
1036 POKE 36,28: PRINT Y(J + 3,K);
1037 POKE 36,34: PRINT Y(J + 4,K);
1038 POKE 36,40: PRINT Y(J + 5,K);
1039 POKE 36,46: PRINT Y(J + 6,K);
1040 POKE 36,52: PRINT Y(J + 7,K);
1041 POKE 36,58: PRINT Y(J + 8,K);
1042 POKE 36,64: PRINT Y(J + 9,K)
1043 NEXT K
1047 SR = SR + 1
1048 SZ = SZ + 3.33
1049 L = L + 10
```

```
1050 IF SZ < TZ THEN GOTO 1012
1052 PR# 0
1055 END
1060 D$ = ""
1065 PRINT "INPUT FILE NAME FOR TEST WITH ORE"
1070 INPUT F$
1090 PRINT D$;"OPEN";F$
1100 PRINT D$;"READ";F$
1110 INPUT DI
1111 INPUT TB
1112 INPUT TR
1120 FOR K = 1 TO DI
1130 FOR J = 1 TO 30
1140 INPUT Y(K,J)
1150 NEXT J
1160 NEXT K
1165 SS = DI:TZ = TR:TT = TB
1170 PRINT D$;"CLOSE";F$
1470 RETURN
```

**APPENDIX C: SCREEN SIZE ANALYSIS PROGRAM**

The following program was used to calculate size distributions and grinding rate constants for experimental screening data. It enables the user to plot to the computer screen the size distribution data or print in tabular form the same in addition to the grinding rate constant value.

```

2 HOME
10 DIM S(20),WT(20),WPR(20),CPP(20)
15 REM THIS BLOCK IS THE INPUT SECTION
19 PRINT : PRINT
20 INPUT "INPUT LENGTH OF GRIND                IN MIN";MIN
30 INPUT "INPUT SAMPLE NAME";E$
80 PRINT : PRINT : PRINT : PRINT
110 GOSUB 1000
115 REM THIS BLOCK CALCULATES WEIGHT %
116 REM RET., CUMULATIVE % PASSING, AND
117 REM THE GRINDING RATE CONSTANT
120 FOR I = 1 TO N
130 SUMM = SUMM + WT(I)
135 DIR = 1000 - SUMM
140 NEXT I
150 FOR I = 1 TO N
160 WPR(I) = (WT(I) / SUMM) * 100
165 WR = WR + WPR(I)
170 NEXT I
180 CPP(0) = 100
190 FOR I = 1 TO N
200 CPP(I) = CPP(I - 1) - WPR(I)
210 NEXT I
216 KM = LOG (100 / WPR(1)) / MIN
220 HOME
225 REM THIS BLOCK PRINTS SIZE DISTRIBUTION
226 REM DATA AND THE GRINDING RATE CONSTANT
230 PRINT "TO TABULATE DATA ON PRINTER TYPE 2 IF NOT TYPE 0"
240 INPUT Y
250 IF Y = 2 THEN PR# 1
260 PRINT SPC( 10)"SIZE DISTRIBUTION DATA"
270 PRINT SPC( 10)"*****"
280 PRINT
290 PRINT "SIZE(MICRON)"; SPC( 1)"WT(G)"; SPC( 2)"WT%RET"; SPC( 2);
    PASS"
300 PRINT "-----"
310 FOR I = 1 TO N
320 CPP(I) = INT (CPP(I) * 10) / 10
330 WPR(I) = INT (WPR(I) * 10) / 10
340 PRINT S(I); TAB( 15);WT(I); TAB( 22);WPR(I); TAB( 30);CPP(I)
350 NEXT I
351 PRINT "-----"
352 PRINT "TOTAL"; TAB( 15);SUMM; TAB( 22);WR
353 PRINT
354 PRINT "GRINDING RATE CONSTANT=";KM

```

```
356 PRINT "TIME OF GRIND(MIN)=";MIN
358 PRINT : PRINT
360 PR# 0
361 VTAB 24
365 REM THISBLOCK PLOTS THE SIZE DISTRIBUTION
370 PRINT "TO GRAPH DATA TYPE 1"
380 INPUT Z
390 IF Z = 1 GOTO 410
400 GOTO 950
410 HGR
420 HCOLOR= 7
430 HPLOT 0,0 TO 0,150
440 HPLOT 0,150 TO 260,150
480 FOR I = 1 TO N - 1
490 P = (S(I) + 200) / 15
500 Z = 150 - WPR(I)
510 A = 150 - CPP(I)
520 P1 = (S(I + 1) + 200) / 15
530 Z1 = 150 - WPR(I + 1)
540 A1 = 150 - CPP(I + 1)
550 HPLOT P,Z TO P1,Z1
560 HPLOT P,A TO P1,A1
570 NEXT I
600 VTAB (22)
610 PRINT "TO END PROGRAM INPUT 1"
620 INPUT ZZ
630 TEXT
640 HOME
950 END
975 REM THIS BLOCK IS AN INPUT SECTION
1000 PRINT "NO OF SIZES"
1100 INPUT N
1200 FOR I = 1 TO N
1300 PRINT "SIZE(MICRON),WT(G)"
1400 INPUT S(I),WT(I)
1500 NEXT I
1600 RETURN
```

**APPENDIX D: MILL CHARGE DETERMINATION PROGRAM**

The following program calculates ore and water charge quantities for wet batch ball milling experiments where different percent solids are desired. The values calculated are performed on a constant ball void filling basis in an effort to approximate industrial conditions.



```
5 HOME
7 DIM X(40),Y(40),W(40),SS(40),VV(40),PS(40)
20 PRINT
22 REM THIS BLOCK IS THE INPUT SECTION
25 INPUT "INPUT MATERIAL TYPE";MT$
27 PRINT
30 INPUT "INPUT VOID VOLUME TO BE OCCUPIED BY PULP(CC)";VV
35 PRINT
40 INPUT "INPUT DENSITY OF ORE TO BE USED (G/CC)";SG
45 PRINT
50 INPUT "INPUT NO. OF CALCULATIONS TO BE PERFORMED";N
55 PRINT
60 FOR I = 1 TO N
70 INPUT "INPUT % SOLIDS DESIRED";PS(I)
75 NEXT I
76 REM THIS BLOCK CALCULATES ORE/WATER
77 REM CHARGE QUANTITIES AND %SOLIDS BY VOL.
78 FOR I = 1 TO N
80 SS(I) = PS(I) / 100
85 VV(I) = SS(I) * VV
90 X(I) = VV(I) / (1 - SS(I) + (SS(I) / SG))
100 Y(I) = VV - (X(I) / SG)
102 X(I) = INT (X(I) * 100 / 100):Y(I) = INT (Y(I) * 100 / 100)
103 W(I) = INT (W(I) * 100 / 100)
105 W(I) = (X(I) / SG) / (Y(I) + (X(I) / SG)) * 100
108 W(I) = INT (W(I) * 100 / 100)
110 NEXT I
115 HOME
117 REM THIS BLOCK PRINTS CHARGE QUANTITIES
120 GOTO 130
125 C = 1: PR# 1
130 PRINT "BALL MILL CHARGE QUANTITIES"
135 PRINT "MATERIAL=";MT$
140 PRINT "DENSITY (G/CC)=";SG
150 PRINT "MILL VOID VOLUME(CC)=";VV
160 PRINT : PRINT
180 PRINT "% SOLIDS"; SPC( 4);"% SOLIDS"; SPC( 4);"ORE CHARGE";
    WATER CHARGE"
185 PRINT "BY WT."; SPC( 7);"BY VOL."; SPC( 4);"GM."; SPC( 11);"CC."
```

```
186 PRINT "*****"
187 PRINT
190 FOR I = 1 TO N
200 PRINT TAB( 2);PS(I);; TAB( 16);W(I); TAB( 27);X(I); TAB( 40);Y
205 PRINT
210 NEXT I
212 PR# 0
215 IF C = 1 THEN GOTO 240
218 PRINT : PRINT
220 INPUT "INPUT 1 TO PRINT RESULTS";ZZ
230 IF ZZ = 1 THEN GOTO 125
235 GOTO 270
240 C = 0
250 INPUT "INPUT 2 FOR FURTHER CALCS";YY
260 IF YY = 2 THEN GOTO 5
270 END
```